THE INFLUENCE OF METAL CRYSTALLITE SIZE OF THE COBALT FISCHER-TROPSCH CATALYST ON THE RE-OXIDATION OF COBALT WITH WATER

By
Erna Antoinette van Schalkwyk
B-Eng. (Chem. Eng.) (PU for CHE)

Submitted to the University of Cape Town in fulfilment of the requirement
for the degree of
MASTER OF SCIENCE IN ENGINEERING

Department of Chemical Engineering
University of Cape Town
Rondebosch
Cape Town
South Africa

September 1998

ACKNOWLEDGEMENTS

I would like to thank the following:
My supervisor, Dr. Eric van Steen, for his help and guidance during the masters project, and helping me see it through.

Professor Cyril O'Connor, the Head of Chemical Engineering as well as the Catalysis Research Unit for his constructive criticism and for giving me the opportunity to study at UCT.

Dr. Klaus Möller for his help and willingness to help at any time.

Professor Mark Dry for his valuable input during seminars.

Michael Claeys for explaining to me all the small details about the Fischer-Tropsch synthesis.

Audry, Suzana and Gary for the atomic absorption analyses and H_2 chemisorption measurements that were so essential to my project. Joachen Macke and Peter Dobias for always helping me and fixing the problems I had with my rig.

Rein Weber for letting me use his precious glass rig. Leslie Petrik for her help and letting for me use her reduction rig. Paul Galatolo for showing me the set-up for catalyst preparation. Pam Link for ordering all the chemicals and equipment and Lorna van Besouw for organising transport to conferences.

Dee Bradshaw for her kindness and inspiration.

SASOL, without whose funding this research would not have been possible.

Bill Randall and Granville de la Cruz for doing the electric wiring on my rig. Craig Balfour and Bill for keeping me connected to the outside world (e-mail and internet

connection) and for keeping the network up and working. Maria, Jackie, Nellie, Martin and James for ensuring that the department was always clean and neat and making it a pleasure to work there.

Colin and Pierre for exploring the mountains with me. Warwick, for his great company, coffee breaks and for correcting my English grammar. Zonke for being such comforting friend and showing me to what level a woman can rise. Imraan, for being such a cool friend, working late hours at night and for teaching me more about computers. Erik for being a great sport and keeping me company in Afrikaans.

Frank, Soovi and Peter for the entertainment in the office up the corridor. Uwe and Heiko for great evenings in and out; all I can say is: "Eet Kreef". Richard and Andreas for working with me on the Fischer-Tropsch synthesis. Quiriene and Mark for being friends in need.

Britt-Helen, one of the most amazing people that I have met. I would like to thank her for the time we shared, the mountains, and the wine. Kevin for being the best housemate ever.

Fash, St.John and Chappie for filling the time in Chem. Eng. with fun and laughter. Chris, Klaus and Holger, for the best time in my life, many late nights and no sleep. Shaun for the best humour around. Ansgar for showing me the best places in Cape Town. Edwa, Marié and Gavin for eternal friendship and for standing by me throughout the masters. Peter Roeger and Boz, my gurus: thanks for teaching me the ways of the sea, surfing with me and for being such great friends

I want to thank my parents, Charlotte and Peet, for standing by me in every possible way and for partially funding my masters. I can only express my deepest gratitude. Thanks to my sisters, Lida, Willemien and Suretha for caring so much.

God for making the sea and mountains and giving me the time to enjoy them.

SYNOPSIS

Catalyst productivity and selectivity to C_{5+} hydrocarbons are an important criteria in choice of Fischer-Tropsch catalyst. Cobalt-based catalysts appear to provide the best compromise between performance and cost for the synthesis of hydrocarbons [Iglesia, 1997]. The cobalt-based catalysts can be best applied in slurry reactor technology because of the high activity and the good heat transfer of the slurry reactor. Due to the nature of the slurry reactor, high partial pressures of water are generated when operated at high conversions. In addition, the back-mixing in the slurry reactors gives a homogenous concentration profile throughout the reactor with high water and low reactants concentrations.

The cobalt catalyst is more expensive than the iron catalyst and to make the cobalt catalyst economically viable, the lifetime of the catalyst has to be stretched to 2-3 years. Possible deactivation by water thus becomes of major concern. Although the deactivation of bulk cobalt with water is not thermodynamically feasible, the re-oxidation of the metal surface might be possible. The surface atoms of a solid are exposed to a different environment than the atoms in the bulk of the solid. They have fewer neighbours than the bulk atoms do. The neighbours of each surface atom may be distributed anisotropically. Therefore the thermodynamic properties associated with the surface region are defined separately from the bulk thermodynamic properties. Studies of small particles have shown that these exhibit properties different from those of the bulk phase especially when dispersion approaches unity [Somorjai, 1994]. Significant surface oxidation is found when the Co/Al_2O_3 is treated with low H_2O/H_2 ratio [Schanke *et. al.* 1996].

In the present study the role of the cobalt crystallite size on the re-oxidation of a 5%(wt) Co/SiO_2 catalyst has been investigated with TPR, TPO, H_2 chemisorption, TEM and Fischer-Tropsch synthesis. The supported catalysts used in this study were prepared by impregnating a silica support with an aqueous solution of cobalt nitrate, using the

incipient wetness technique. Impregnation was followed by drying and activation of the cobalt precursor. Different cobalt crystallite sizes were obtained by changing the activation method. Calcining at higher temperatures before reduction resulted in larger cobalt crystallites (21-28 nm) whereas direct reduction of the cobalt precursor resulted in smaller cobalt crystallites (16-18 nm). After reduction, the catalysts were opened up in the atmosphere, which caused a surface oxidation to take place. The catalysts were then re-reduced *in situ* before H_2 chemisorption measurements, TPO and Fischer-Tropsch synthesis were done.

The deactivation of supported cobalt catalysts was studied in a fixed-bed reactor under non-reacting conditions, using a H_2/H_2O mixture with ratio of 4:1. The water treatment procedure simulated the hydrothermal conditions that develop under Fischer-Tropsch synthesis conditions for comparison purposes. The catalysts and their water-treated counterparts were then tested in a fixed-bed reactor under Fischer-Tropsch conditions. Hydrothermal treatment at 200°C led to a catalyst with lower reducibility. The decrease in degree of reduction is attributed to the formation of both reducible and non-reducible (<900°C) cobalt silicates.

The change in the oxidation state of cobalt during re-oxidation was characterised by TPR and TPO. Small shifts in the low temperature peak maximum to higher temperatures were observed in the TPR spectra. This indicates an enhanced formation of metal support interaction due to water treatment. TPO showed the degree of reduction to decrease for each catalyst after water treatment.

H_2 chemisorption is a good indication of metal surface sites accessible for Fischer-Tropsch synthesis. According to hydrogen chemisorption measurement, the extent catalyst deactivation by water treatment is inversely proportional to the cobalt crystallite size, i.e. smaller crystallite size gave a higher degree of deactivation.

Transmission electron micrographs showed a non-homogenous dispersion of cobalt particles on the support. In some cases large clusters of smaller cobalt particles were

visible, that made it difficult to estimate the actual cobalt crystallite size from the photographs. It was however observed that the water treatment had no effect on the cobalt particle or cluster size.

The hydrocarbon yield decreased with increase in particle size, which is consistent with H_2 chemisorption data that show an inverse correlation of the number of accessible sites with particle size. Calcining the catalyst at higher temperatures caused the cobalt particles to agglomerate and fewer sites were then available for Fischer-Tropsch synthesis. The α-olefin selectivity increased and chain growth probability decreased with decrease in site density because less α-olefin re-adsorption takes place at lower site densities.

The total hydrocarbon yield decreased after water treatment. The increase in α-olefin selectivity observed after water treatment indicates fewer sites available for α-olefins to re- adsorb and re-enter the chain growth system and to produce more paraffinic products of higher molecular weight.

It was concluded that the observed deactivation after water treatment was caused by the re-oxidation of cobalt that initiated the formation of a metal-support compound. The metal support interaction is a significant deactivation pathway for Co catalysts as it leads to irreversible loss in active sites. The postulated effect of the crystallite size on the cobalt re-oxidation with water is as follow: as the particle size decreases, the dispersion increases and more cobalt particles are then in contact with the support, giving the opportunity for larger amount metal support interaction to form. The deactivation due to water continues until all possible cobalt-silicates are formed. Thus smaller particles result in a larger deactivation due to the increase in contact between support and metal. The dependence of the deactivation due to water on the cobalt crystallite size was confirmed by the larger decrease in H_2 volume uptake after water treatment for the catalyst with a smaller average cobalt particle diameter.

TABLE OF CONTENTS

APPENDICES

LIST OF FIGURES

LIST OF TABLES

NOMENCLATURE

A	area (m^2)
AAS	atomic adsorption spectroscopy
A_g	free gas (H_2 chemisorption)
AM	adsorbed gas (H_2 chemisorption)
A_S	metal surface area (m^2/g_{cat})
A^s	surface work content
a_m	surface area occupied by and atom m
C_n	paraffin/olefin with n carbons
C_n^*	adsorbed surface species with n carbons
-cx	calcined at x00°C
CFB	circulating fluidised bed
D	dispersion (%)
d	desorption steps
d_{avg}	average particle diameter
d_i	particle size
d_{LN}	length-number mean diameter (nm)
d_{VA}	volume-area diameter (nm)
E	total energy of the solid
EIA	Energy Information Administration
E^o	energy of the solid per atom
E^s	specific surface energy
FFB	fixed fluidised bed
FI	flow indicator
FIC	flow indicator and controller
FTS	Fischer-Tropsch synthesis
G	total free energy of the system
ΔG	change in Gibbs free energy
g	growth steps
g_i	gibbs energy per mole

G^o	free energy per atom
G^s	surface free energy
HC	hydrocarbon
H^s	specific surface enthalpy
IEA	International Energy Agency
k_a,	rate constant for adsorption
k_d	rate constant for desorption.
l_m	molar density
M	atomic mass (g/gmole)
m	the mass of the sample (g)
$M_{(s)}$	metal (solid)
$M_xO_{y(s)}$	metal oxide (solid)
N	number of atoms in the solid
(N)	catalyst prepared from nitrate precursor
N_A	Avogadro's constant $6.022*10^{23}$ atoms per mole
N_{CO}	total number of exposed atoms (H_2 chemisorption)
N_D	number of deactivated sites
N_S	total number of metal atoms present on the surface
n_s	mean number of atoms
N_{sites}	total number of sites
N_T	total number of metal atoms in the surface and bulk
P	pressure (kPa)
PI	pressure indicator
PIC	pressure indicator and controller
Pr_x	Fischer-Tropsch product with x carbons in chain
R	ideal gas constant (8.314 kPa*m^3/kgmole/K)
SMSI	strong metal support interaction
-s-	slow heating rate during pre-treatment or activation
S_n	carbon selectivity for chains with n carbon atoms
S_P	specific surface area
Sp_x	surface species containing x carbon atoms
S^s	entropy per unit area of surface created
STP	standard temperature and pressure (273.15K and 101.3kPa)
T	temperature (K)

T_{high}	TPR high temperature peak maximum
T_{low}	TPR low temperature peak maximum
T_{max}	maximum peak temperature (TPR)
T_{melt}^{bulk}	melting temperature (K) of a solid
T_{Tam}	Tamman temperature (K) = 0.5 T_{melt}^{bulk}
T_{Hut}	Hüttig temperature: (K) = 0.333T_{melt}^{bulk}
TCD	thermal conductivity detector
TEM	transmission electron microscopy
TIC	temperature indicator and controller
TPO	temperature programmed oxidation
TPR	temperature programmed reduction
UHV	ultra high vacuum
V	volume (m^3)
V_{H2}	volume hydrogen chemisorbed (cm^3)
V_{ma}	volume occupied by an atom m
V_m, ν_m	volume of the monolayer (ml/g_{cat})
-w	water treated catalyst
WHSV	weight hourly space velocity (hr^{-1})
wt%	weight percentage
Y_{HC}	total yield of hydrocarbons
ZPC`	point of zero charge.

Greek symbols

α_n	chain growth probability of species with n carbons
β_n	termination probability of species with n carbons
ρ	density of the material
$\wp$	the surface area
Φ_{sites}	deactivation parameter
$\Phi_{ads, H2}$	deactivation parameter according to hydrogen chemisorption data
Φ_{FT}	deactivation parameter according to hydrocarbon yield
θ	fractional coverage of the surface (H_2 chemisorption)

CHAPTER 1

Introduction

1. INTRODUCTION

1.1 The Fischer-Tropsch Synthesis

The Fischer-Tropsch synthesis is a process that converts coal into gasoline, diesel oil, wax and alcohols. Coal is gasified to provide hydrogen and carbon monoxide. Carbon monoxide is then hydrogenated over a metal catalyst, under Fischer-Tropsch reaction conditions, to produce higher hydrocarbon chains.

1.1.1 A Historical Sketch and Reactor Technology

The Fischer-Tropsch reaction was developed in the early 1920's - 30's in Germany. Franz Fischer and Hans Tropsch discovered that carbon monoxide and hydrogen react at high pressure in the presence of iron, nickel and cobalt catalysts yielding higher hydrocarbons [Pines, 1981].

The original German industrial reactor was a fixed bed reactor with the cobalt catalyst packed between perpendicular metal plates. Because of the highly exothermic character of the reaction, heat transfer plays an essential part in the reactor development. Cooling of the fixed bed reactor took place by regulating the steam pressure in a water-filled pipe system, (indirect heat exchange). These reactors are similar to a heat exchanger unit, with plates perpendicular to the water pipes. The heat removal was not sufficient and resulted in localised overheating [Dry, 1981].

In 1934, the Ruhrchemie erected a pilot plant, using the Ni-MnO-Al_2O_3-kieselguhr catalyst. The difficulties that they encountered were (a) the short lifetime of the catalyst (4-6 weeks), (b) expensive design of the converters, (c) loss of catalyst metals and promoters during catalyst regeneration, and (d) expensive conversion of oil to marketable products [Storch *et al.*, 1951].

Fischer and Meyers developed Ni-ThO_2-kieselguhr and Co-ThO_2-kieselguhr catalysts that can operate at low to medium pressure. The initial studies were on Ni because of the short supply of Co; however, the CH_4 selectivity with the Ni catalyst was too high. Ruhrchemie AG tested

the Co catalysts on a pilot plant in 1933-1939. In 1935 FTS was operated commercially in Germany, using the Co catalyst. Fischer continued the research with Pichler and discovered that Fe gave satisfactory results in the middle pressure range, 5-20 atm. The synthesis on Fe was greatly improved by operating in this range. Alkalised Fe in this pressure range became a possible replacement for Co in the German commercial plants.

The employment of gas recycle tubular reactors followed. The heat of reaction was removed as sensible heat in the reaction gas. High linear gas velocities through the catalyst bed ensured removal of the heat of reaction along the length of the tubes, resulting in a near-isothermal reactor [Dry, 1981].

Fears of an impending shortage of petroleum in the United States led to a large research and development program in coal-to-oil processes. The American petroleum and related industries initiated studies on the FTS on Fe in fluidised and entrained reactors. Ten years later an abundance of petroleum in the world and its availability at very low prices caused the decrease and termination of most research programs in America [Anderson, 1984].

The slurry process was introduced during the period 1945-1958. The synthesis gas was bubbled through a suspension of finely divided catalyst in a liquid. In FTS, the liquid is usually a cut from the product spectrum e.g. high boiling wax. Heat removal took place by circulating the slurry through a heat exchanger [Dry, 1981]. The advantage of the slurry bed reactor is the flexibility in temperature control. Because of the nature of the slurry reactor, the slurry is well mixed and results in an isothermal reactor. The pressure drop over the reactor is lower than the fixed bed reactor. Online catalyst removal and additions reduce capital costs [Jager *et al.*, 1994].

The SASOL FTS plant using coal as a resource was started in 1955 in South Africa. An alkalised Fe catalyst was used in two types of reactors: fixed-bed with recycle unit and in 1985 an entrained-solids reactor.

Following the successful utilisation of fluidised beds in catalytic cracking, this technique found its way to the Fischer-Tropsch synthesis. Basically, there are two types of units:

- FFB: fixed fluidised bed, where the catalyst remains in a fixed area with the gas passing upward through the bed.
- CFB: circulating fluidised bed in which the catalyst is entrained in a fast moving gas stream.

The heat of reaction is removed by heat exchangers. The fluidised bed has good temperature control which enables operating at high conversions [Dry, 1981].

As a result of sharply rising crude oil prices in the 1970's SASOL decided to build SASOL II and SASOL III. The new plants were similar to the initial plant, but this time the FTS fixed-bed reactors were not included. SASOL developed the synthol process based on the circulating fluidised bed that was employed in SASOL II and III. SASOL II and III came online in 1980 and 1982 respectively [Dry, 1996]. For the production of gasoline, the entrained iron process of SASOL seems to be the best choice. To obtain a wider distribution of products, including wax, the slurry reactor and fixed bed units seem appropriate [Anderson, 1984].

The oil embargo by the Organisation of Petroleum Exporting Countries in 1973, followed by a fourfold increase in the price of petroleum, again accelerated the research on coal-to oil processes [Anderson, 1984].

The world-wide recessions in 1982 sharply decreased demand for petroleum. OPEC was unable to control the price of oil among its members. The relatively low cost and abundance of petroleum has discouraged new coal-to-oil ventures [Anderson, 1984]

In 1985 a synfuel plant came on stream in New Zealand. The technology was based on Mobil's MGT process where syngas produced from CH_4 is first converted to methanol and then to gasoline using Mobil's ZSM-5 catalyst [Wender, 1995].

In 1992, the Mossgas FT complex came on stream in South Africa. Syngas is produced from off-shore natural gas and SASOL circulating fluidised bed FT reactors were used. The

apparent limited reserves of natural gas in the area is a concern for the future of the plant [Dry, 1996]. The plant produces mainly diesel fuel and gasoline.

In 1993, Shell commissioned a fixed bed Fischer-Tropsch operation in Malaysia, using a cobalt based catalyst. Syngas is produced by partial oxidation of methane (non-catalytic). Waxes and high quality diesel fuel are the main products [Dry, 1996].

In 1993, SASOL commissioned a commercial slurry reactor to operate with a cobalt based catalyst [Jager and Espinoza, 1995].

Oil accounts for 40 percent of the total primary energy demand. Oil availability in the future will be a major factor in the world's economic condition. The International Energy Agency (IEA) and the Energy Information Administration (EIA) projected that the world oil production will have to be increased by about one-third in the next 15 years to rapidly rising demand [Riva, 1995]. With the Gulf war in the 1990's (20 years after the Arab oil embargo), research on the Fischer-Tropsch process is worth continuing. The objectives of the Fischer-Tropsch synthesis might change with time according to the economic viability and market demands.

1.1.2 Fischer-Tropsch Product Spectrum

To have an overall process efficiency, a catalyst with high volumetric productivity, high C_5 + yields and low selectivity light hydrocarbons, especially methane, is required [Iglesia *et al.*, 1992].

The major products in the Fischer-Tropsch synthesis are linear hydrocarbons and some branched hydrocarbons. The linear hydrocarbon fraction contains mainly olefins and paraffins. Oxygenates are formed as a side product i.e. alcohols, aldehydes and ketones. In high temperature Fischer-Tropsch synthesis some minor quantities of naphthenes and aromatics are formed.

The generic equations for straight chain alkanes are:

$$(2n+1)\ H_2 + n\ CO \rightarrow C_nH_{(2n+2)} + n\ H_2O$$

with heat of reaction of -231kJ/mol, and:

$$(n+1)\ H_2 + 2n\ CO \rightarrow C_nH_{(2n+2)} + n\ CO_2$$

of which heat of reaction is -228kJ/mol.

The straight chain alkenes formation are described as:

$$2n\ H_2 + n\ CO \rightarrow C_nH_{2n} + n\ H_2O$$

The reactions that lead to alcohol formation are:

$$2n\ H_2 + n\ CO \rightarrow C_nH_{(2n+1)}OH + (n-1)\ H_2O$$

and

$$(n+1)\ H_2 + (2n-1)\ CO \rightarrow C_nH_{(2n+1)}OH + (n-1)\ CO_2$$

The exact product distribution depends on the reaction conditions and catalyst composition [Quyoum *et al.*, 1998].

To understand the chemistry of syngas conversion, one must take a closer look at the events occurring at the surface of the catalyst.

The products can be divided into primary products and secondary products. A primary product forms during a single sojourn of a reactive intermediate on a FTS site. All the products formed by desorption without subsequent re-adsorption are primary products (see Figure 1-1) [Iglesia *et al.*, 1993].

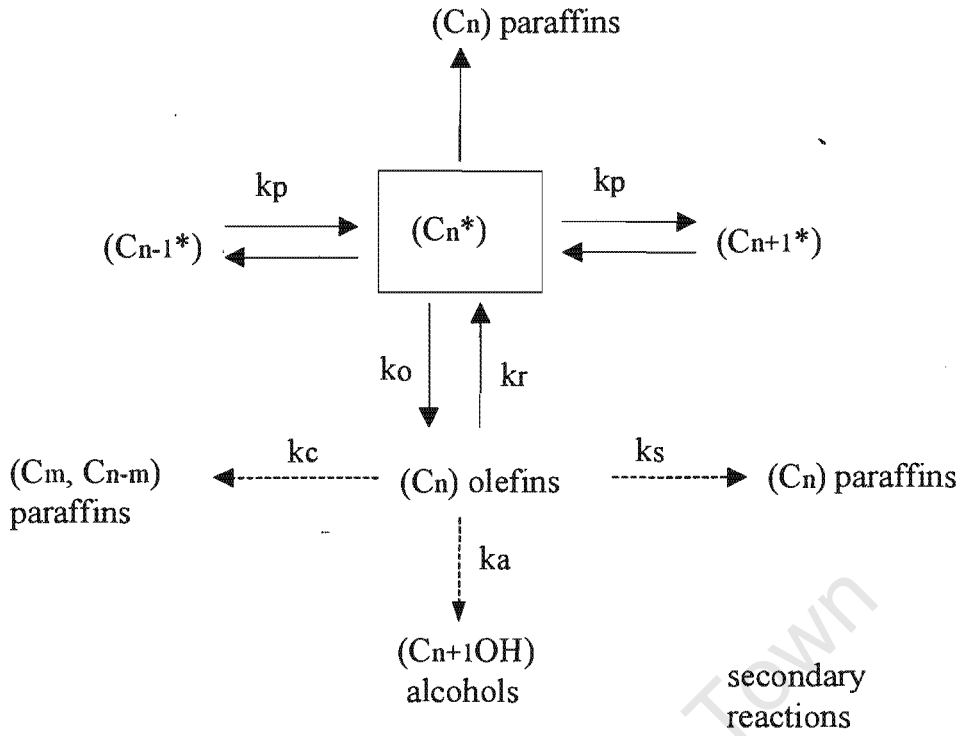

Figure 1-1: The chain growth and termination and secondary reactions in FTS on the cobalt catalyst.

Cn* : is the adsorbed surface species with n carbon atoms. kp: is the rate constant for chain termination, ko: is the rate constant for olefin formation, kr: is the rate constant for readsorption, kc, ka and ks are rates of formation of secondary products.

Secondary reactions can alter the FTS selectivity by chemical transforming the primary product on a second catalytic function.

1.1.3 The Mechanism of the Fischer-Tropsch Synthesis

Since the discovery of the Fischer-Tropsch synthesis, scientists have been trying to explain how chain growth takes place on the catalyst surface. Gaining this knowledge could help achieve higher selectivity to useful compounds. Three separate proposals for the FTS mechanism have received dominant consideration. The three differ in the manner in which C-C bonds of the product are proposed to be formed.

Fischer and Tropsch (1926) proposed the first mechanism in 1926, the so-called carbide mechanism. The assumption on which their theory rests, is that CO adsorbs dissociatively on

the catalyst surface, to form a surface carbide. Later development suggested that the C-C bonds of the product are produced via polymerisation of CH_2 on the metal surface.

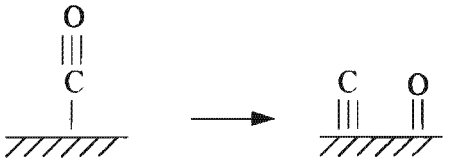

Figure 1-2: The dissociative adsorption of CO

The surface carbide is then partially hydrogenated forming carbene species.

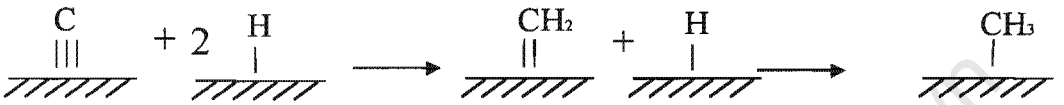

Figure 1-3: The hydrogenation of the surface carbide

The methylene group can undergo further reaction with hydrogen to form a methyl group on the catalyst surface. This methyl group then has the option of either desorbing by hydrogen addition or starting a new chain.

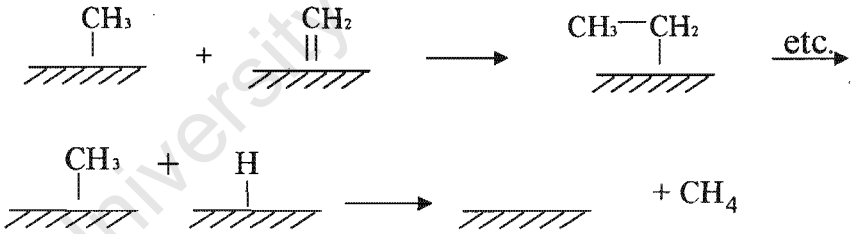

Figure 1-4: The methylene group undergoing chain growth

The second mechanism advanced by Anderson and Emmett and their co-workers is the following: the C-C bonds are made through a condensation reaction. Two hydroxy methylene surface intermediates react by forming water and surface oxy species [Anderson, 1975].

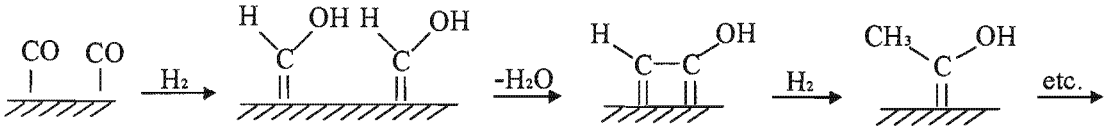

Figure 1-5: The self-condensation of surface hydroxycarbene intermediates

The third alternative method, proposed by Pichler and Schulz, involves C-C bond formation in the propagation via insertion of CO into a metal-alkyl bond [Pichler and Schulz, 1970].

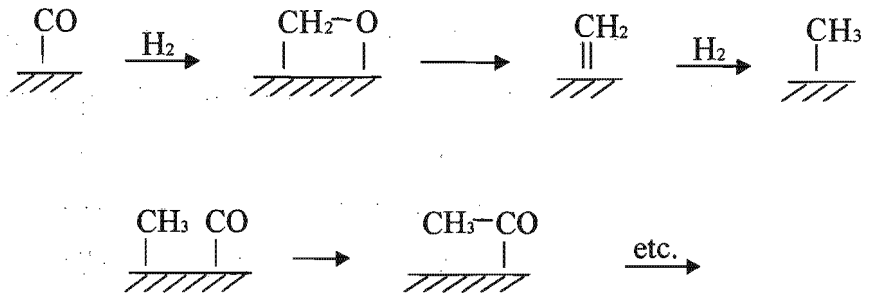

Figure 1-6: Chain growth by the insertion of CO

The CO insertion method is based on knowledge obtained in the hydro reactions from homogenous organometallic chemistry. In the main chain-growth scheme, oxygen from CO is removed before chain growth. The intermediate is a hydrocarbon radical [Anderson, 1984].

It is possible that methanation and the formation of higher hydrocarbons can proceed via various mechanisms running in parallel. The search for the main chain growth mechanism in the Fischer-Tropsch synthesis has been going on for a long time. There have been several investigations on which intermediates initiate chain growth, and how chain growth takes place. By co-feeding ^{13}C atoms as part of the syngas, and analysing for ^{13}C in the products, some indication can be found of the mechanism by which chain growth takes place [Krishna and Bell, 1993].

The labelled molecule may either initiate chain growth, build into the growing chain by adding repeatedly or react in other ways.

Araki and Ponec (1976) tested the CO insertion model vs. the carbide model by using a nickel catalyst. Nickel is a metal that does not form bulk carbides as easily as iron and does not produce much C_{2+} hydrocarbons either. This made the analyses of the results easier. The nickel surface was partially covered by carbon-13 ($^{13}C_c$) by disproportionation of carbon monoxide:

$$2\,^{13}CO \rightarrow {}^{13}C_c + {}^{13}CO_2$$

from CO and H_2. The species has two options, to grow or to desorp as methane (termination).

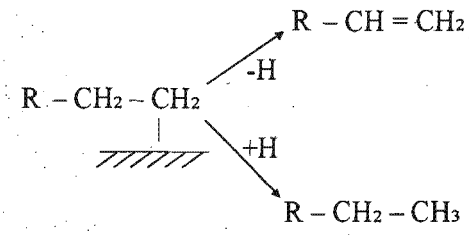

Figure 1-8: The kinetic scheme of primary formation of olefins and paraffins via dissociative and associative chemidesorption during FTS [Schulz *et al.*, 1988]

When no branching and formation of only one type of product are assumed, the distribution of products can be described with the probability of chain prolongation, α_n. The sum of the probabilites for a surface species Sp_n, to grow further or to desorp equals 1 [Schulz *et al.*, 1988]

$$\alpha_n + \beta_n = 1$$

where β_n is the probability of termination.

1.1.4 Olefin and α-Olefin Selectivity

Desorption of a formed surface species leads to three kinds of product compounds (see Figure 1-7): paraffins, olefins and oxygenates (alcohols and aldehydes). In most actual cases the primary olefins are partially converted into paraffins through secondary hydrogenation reactions. The primary selectivity is thus obscured.

The Fischer-Tropsch process forms liquid products that fill the pores of the support on which the active catalyst sites are found. Because olefins have a greater solubility in the synthesis liquids [van't Blik and Niemandsverdriet, 1984], it might lead to an increase in the extent of readsorption. The reabsorbed olefins cannot be distinguished from those formed

Methane formation is thermodynamically favoured above the formation of higher hydrocarbons. The inhibition of methane formation is what makes the Fischer-Tropsch synthesis so unique.

1.1.5 The Product Distribution

After the main mechanism of the Fischer-Tropsch process was identified, Schulz et al. (1988) described the process as a non-trivial surface polymerisation reaction. This summarises the unique character of the system in which one step of chain growth (on CH_2 unit) is performed through a set of reactions of hydrogen transfer, elimination of oxygen and formation of a new C/C bond.

A mathematical model has been developed to describe the polymerisation processes in the Fischer-Tropsch synthesis. The Flory-carbon-number-distribution :

$$S_n = n \bullet (1-\alpha)^2 \bullet \alpha^{n-1}$$

where S_n is the carbon selectivity for chains with n carbon atoms and α is growth probability. A plot of (S_n/n) vs. n gives a straight line when α is independant of chain size n.

In most cases the chain growth probability increases with chain size that leads to a curvature in Flory-carbon-number-distribution plots of FTS products. It is difficult to detect these deviations when the measurements are limited to a narrow molecular range [Iglesia *et al.*, 1993].

1.2 Catalyst for Fischer-Tropsch Synthesis

The transition metals in group VIII have the ability to dissociatively adsorb carbon monoxide and hydrogen. Therefore, this group of metals is suitable for the Fischer-Tropsch synthesis. The metals are arranged according to the average molecular weight of the organic products, i.e. in descending chain length:

Ru > Fe > Co > Rh > Ni > Ir > Pt > Pd

The metals in order of increasing specific activity:

Ru > Fe > Ni > Co > Rh > Pd > Pt > Ir

[Vannice, 1975].

These activity measurements were done at not done between 240 and 280°C at atmospheric pressure and not at optimum temperature and pressure for each catalyst, e.g. cobalt was tested at 240°C with a H_2/CO ratio = 3.

Of the platinum group, ruthenium was shown to be the most active. The other Pt-group catalysts and those of Re and W had a low activity, with methane as the major product. Supported Mo has modest activity and modest tendency to produce higher hydrocarbons [Anderson, 1984], but its nitride and carbide show excellent alkene synthesis rate [Adesina, 1996].

The discovery of the Fischer-Tropsch synthesis was on the iron catalyst. Shortly after, cobalt and nickel were found to produce higher hydrocarbons under similar conditions. Of the three metal catalysts, cobalt has the greatest tendency to produce hydrocarbons with more than one carbon atom per molecule [Pines, 1981]. Ni is essentially a methanation catalyst [Adensina, 1996].

The stability and catalyst lifetime depend on its resistance against carbonyl and carbide formation. Co and Ni form carbonyls more readily than Ru. Carbides of Ru are not known to be formed under FTS conditions [Adensina, 1996]. Volatile carbonyl formation often limits the operating pressure for Ni. Cobalt and nickel can also be converted to the carbides of the metals: Co_2C and Ni_3C, which have a low activity compared with the metals [Anderson, 1984] but the formation of Co and Ni carbide is thermodynamically not favoured under Fischer-Tropsch conditions. [Adensina, 1996]. Fe has a stronger tendency than Co and Ni to produce elemental carbon that deactivates the catalyst. In fact, of all the metals, only iron and cobalt are used in industry [van Steen, 1993].

In the FTS, carbides and oxides of Fe can be formed. Carbides, nitrides and carbonitides of Fe can be used as catalysts [Anderson, 1984]. The main differences between cobalt and iron as a catalyst is that the methane selectivity is generally higher for cobalt and readsorption of reactive product compounds is stronger for cobalt. With iron branching takes place as a primary branching reaction, while with cobalt, branching is mainly due to a secondary branching reaction [van Steen, 1993]. Co-based catalysts were later preferred to the iron

catalyst simply because cobalt required considerably milder operating pressures [Adesina, 1996] and has a higher intrinsic activity.

Promoters are applied to improve the selectivity and activity of the catalyst [van Steen, 1993]. Adding alkali metals to the transition metal surfaces changes the binding energy of the reactive molecule. Potassium is a well known Fe promoter, which improves the olefin-to-paraffin ratio. Light transition metal oxides (Mn, V, Ti) can be added. These compounds facilitate CO dissociation at the adlineation sites (the metal/promoter interface). The addition of rare earth oxides decreases the support acidity and promotes CO dissociation [Adesina, 1996].

Pd, Ir, Pt do not dissociate CO easily enough to be a good catalyst for Fischer-Tropsch synthesis. Fe, Co, Ni, Ru, and Rh, dissociate CO at slightly elevated temperatures, and the oxides of these metals can be reduced by syngas at temperatures around 470K. These metals are the most suitable for the Fischer-Tropsch synthesis [Moulijn *et al.*, 1993]

1.3 Cobalt as Fischer-Tropsch Catalyst

A cobalt-based catalyst appears to provide the best compromise between performance and cost for the synthesis of hydrocarbons [Iglesia, 1997]. The Fischer-Tropsch synthesis temperature for cobalt range from 190°C to 210°C. Olefins, particularly α olefins, seem to be a primary product of FTS. [Anderson, 1984].

Although cobalt is the most active catalyst for the Fischer-Tropsch synthesis, it is not always used, because of several complications that the catalyst exhibits. The cobalt catalyst is re-oxidised by water, is solvent sensitive and undergoes to large extent sulphur poisoning. The catalyst is more expensive than iron. The catalyst thus needs to be supported and to be highly dispersed to get optimal use of the catalyst. Every possible particle should be activated and in contact with the synthesis gas.

The high activity of cobalt causes a large initial temperature increase, when the catalyst is operated at high conversions in a fixed bed reactor. With recent development of the slurry reactor, the temperature in the reactor can be controlled much better. When the cobalt catalyst is used in a slurry reactor, deactivation is observed. A possible cause could be the

water formed as by product in the Fischer-Tropsch synthesis. The slurry reactor has back mixing that ensures a homogenous concentration throughout the reactor, thus a high concentration of water to reactants can accumulate in the reactor.

Turnover rates increase when small amounts of Ru (Ru/Co < 0.008 at.) are added to Co [Iglesia, 1997]. Supported cobalt catalyst promoted by a second metal (Pt, Re, and Ru [Belambe *et al.*, 1997].) has been shown to be a good FTS catalyst [Hanssen *et al.*, 1997]. The aim of bimetallic catalysts is to take advantage of possible synergetic effects between the 2 metals, and thus produce a higher active, selective and stable catalyst [Adesina, 1996]. The promoter enhances the reducibility of the cobalt oxides and improves the dispersion of the active metal. In some cases the second metal helps keeping the surface clean and increases the coverage of reactive intermediates [Hanssen *et al.*, 1997]. This increases the number of surface exposed cobalt atoms and results in an increase in CO hydrogenation rate [Iglesia *et al.*, 1993].

The true turnover frequency of cobalt always stays the same, regardless of the second metal. This enhanced reducibility could form a spillover of hydrogen. Hydrogen may adsorb on the reduced noble metal, dissociate and spill over to cobalt. Formation of bimetallic particles for Pt, Ru, Ir, and Rh has been proposed by other authors [Iglesia *et al.*, 1993], but Hilmen *et al.* (1996) showed that direct contact between cobalt and the noble metal is not required for obtaining the promoting effect.

1.3.1 The Influence of Cobalt Dispersion on the Fischer-Tropsch Synthesis

The structure of supported metals varies with dispersion. CO hydrogenation on metals originally appeared to be structure sensitive [Reuel and Bartholomew, 1984].

Specific activity changes with metal loading and dispersion which might be related to primary structure sensitivity, secondary structure sensitivity and metal-support interaction.

- Primary structure sensitivity is planar (high co-ordination) surface sites and is intrinsically more active than edge and corner (low co-ordination) sites.

- Secondary structure sensitivity results from self-poisoning mechanisms. CO hydrogenation is not favoured on low co-ordination sites.
- Metal-support interactions are more pronounced in highly dispersed catalysts.

Primary structure sensitivity does not affect CO hydrogenation. Secondary structure sensitivity effects due to carbon deposition do not affect the activity. Metal-support interaction might have an influence on the activity and selectivity of the Fischer-Tropsch catalysts [Johnson *et al.*, 1991].

Early studies of the structure sensitivity of the Fischer-Tropsch synthesis on the cobalt catalyst suggested that the cobalt crystallite size and the type of support have a strong influence on the selectivity and rate of the reaction [Reuel and Bartholomew, 1984]. These authors concluded that CO hydrogenation on Co/Al_2O_3 is very sensitive to the structure of the meal crystallites, even though the dispersion range was very narrow and the concentration of surface atoms with unique co-ordination is not influenced strongly by crystallite size [Iglesia *et al.*, 1993]. The structure sensitivity was explained by the need or sites that co-ordinate CO strongly. These authors also proposed that the density of strong binding sites and the natures of the reactive CO species depend strongly on the crystallite size of the cobalt.

Recent reports by the same authors showed that the synthesis of light hydrocarbons on the cobalt catalyst is structure insensitive [Johnson *et al.*, 1991]. They concluded that the strong structure sensitivity reported previously reflects marked differences in the extent of reduction. Changes in dispersion modify the reduction properties of cobalt precursors and can lead to their incomplete reduction during catalyst activation or to partial reoxidation during catalysis. The residual presence of cobalt oxide species strongly influence CO hydrogenation rates [Iglesia *et al.*, 1993].

Iglesia *et al.* (1992) investigated the structure sensitivity of CO hydrogenation on Ru and Co supported on titania, silica and alumina and observed it to increase linearly with cobalt metal dispersion, irrespective of the chemical identity of the underlying support.

Surface science studies by Geerlings and co-workers [Geerlings *et al.*, 1991] suggested that CO hydrogenation on the transition Group VIII metals is structure insensitive. For example Co/W have highly different geometries, but have similar activity. The activities match the activity of highly active Co/alumina [Johnson *et al.*, 1991].

Iglesia *et al.* (1992) obtained results supporting the findings of Johnson *et al.* (1991). They showed at normal CO partial pressures, on fully reduced Co surfaces, the Fischer-Tropsch synthesis to be insensitive to dispersion and support effects. The many reports that state influence of support and dispersion, Iglesia *et al.* (1992) explained by the operating conditions that alter the structural requirements of the rate limiting step i.e. transport effects. The observed change in selectivity is due to differences in readsorption, site density and support pore structure, which controls the rate removal of reactive olefins from catalyst pellets. Cobalt-time yield increases linearly with increasing dispersion of cobalt crystallites supported on silica. Site time yield (turnover rates) does not strongly depend on metal dispersion [Iglesia, 1997]

The rate of CO hydrogenation on well-reduced cobalt surfaces, is independent of dispersion [Johnson *et al.*, 1991], and metal-support interaction [Iglesia *et al.*, 1992]. CO hydrogenation rates are proportional to the number of exposed Co and Ru surface atoms [Iglesia *et al.*, 1992].

The intrinsic surface chemistry is thus not strongly affected by surface modifications like change in metal crystallite size or by metal-support interaction.

Catalysts tested under Fischer-Tropsch conditions for 120h showed a rapid decrease in conversion, during the first five hours. The decrease thereafter was moderate and related to dispersion. The higher the dispersion, the higher the rate of decrease. [Niemelä and Krause, 1996]. This can be ascribed to re-oxidation of metallic cobalt particles.

1.3.2 The Effect of Water on FT- Co Catalyst

Deactivation is seen as losing a fraction of activity (active sites). Deactivation can be caused by coke formation, poisoning by impurities that diffuse from the support (in case of a

supported metal catalyst) or form internal metal, or form the feed. Impurities can come form the metallic compounds of the practical reactor system as well [Ertl *et al.*, 1997].
A common cause of deactivation is loss of specific surface area. All high surface area supports have meta-stable structures. Given time, the thermodynamic drive to minimise surface free energy will lead to losses of texture, a deactivation called sintering. Another case of deactivation is loss of active component (metal) in the solution or gas phase [Ertl *et al.*, 1997]. Although the re-oxidation of bulk cobalt with water is not thermodynamically favoured many authors have investigated the possibility of the Fischer-Tropsch synthesis product, water, causing deactivation of the cobalt catalyst [Schulz *et al.*, 1995a, Rothaemel *et al.*, 1997, Hanssen *et al.*, 1997, Iglesia, 1997, Schanke *et al.*, 1996].

Water is known to deactivate iron. Water vapour in the FTS on nitrided Fe was shown to be an inhibitor, but the rate promptly regained its previous value when the addition of water was stopped [Anderson, 1984]. Since the iron catalyst deactivates fast and is relatively cheap, deactivation by water is of no concern. The cobalt catalyst is more expensive than the iron catalyst and to make the cobalt catalyst economically viable, the lifetime of the catalyst has to be stretched to 2-3 years. Possible deactivation by water thus becomes a major concern. The re-oxidation of cobalt with water is not yet fully understood.

Several influences of water on the selectivity of the cobalt catalyst have been reported [Schulz *et al.*, 1995a, Rothaemel *et al.*, 1997, Hanssen *et al.*, 1997]. Water increases FTS reaction rates and the selectivity to olefins and C_{5+} hydrocarbons at low reactant pressures or conversions. These water effects depend on the identity of the support [Iglesia, 1997]. Since the specific site activity does not change, a moderate increase of olefin formation was observed by Rothaemel *et al.* (1997), which was explained by inhibition of secondary hydrogenation reactions of olefins due to water addition. They concluded that the surface of the metal is oxidised by water, and thus the number of sites available for methane formation has been decreased.

Water did not have an influence on the chain length distribution of the Re promoted Co/Al_2O_3 catalyst. For unpromoted cobalt catalyst, water treatment showed a shift towards higher selectivity to C_3-C_6 compounds [Hanssen *et al.*, 1997]. Water treatment prior to reaction, decreases the olefin to paraffin ratio. A decrease in methane selectivity and degree of CO

conversion is observed when water is added in the feed stream. The change in selectivity is because of the decrease in active sites due to the surface oxidation of cobalt.

The promoted catalyst showed a similar deactivation to the unpromoted catalyst. Rhenium supports the reduction of cobalt, but after the water treatment the active material is re-oxidised, particularly the fraction of the cobalt metal that is reduced when rhenium is present [Rothaemel *et al.*, 1997].

Since cobalt and silica are mobile at elevated temperatures and under hydrothermal conditions [Kogelbauer *et al.,* 1995], it is possible for re-oxidised metal surfaces to move into contact with the support and to form a metal support bond. It is then expected that the higher the dispersion, the higher deactivation will be. The active atoms can migrate into the support structure forming cobalt silicates and thus become inactive.
Cobalt silicate is not detectable in XRD, suggesting a highly dispersed phase [Kogelbauer *et al.*, 1995]. Coulter and Sault (1995) showed formation of highly dispersed surface silicates (XPS). They also suggested the migration of Co^{2+} into the silica framework at elevated temperatures. The formation of cobalt silicate from cobalt oxide and water reaches equilibrium round about 800 K (high temperature). The concentration of Co^{2+} ions migrating into the silica framework depends on the cobalt dispersion and on the number of available tetrahedral defect sites near the surface for incorporation of Co^{2+} ions. The formation of cobalt silicates reduces the amount of easily reducible metal.

Kogelbauer *et al.* (1995) showed that treating the silica-supported cobalt catalyst with water in the presence of air, inhibits the formation of non-reducible cobalt silicates.

Rothaemel *et al.* (1997) doped a Co/Al_2O_3 catalyst with Re, and found that Re enhanced the dispersion of Co, and thus the activity for syngas conversion. The same deactivation (70% decrease in CO conversion) was found for the Co/Al_2O_3 catalyst and the Re-doped catalyst, when exposed to water vapour.

According to Iglesia (1997), 5-6 nm cobalt crystallite diameters are difficult to achieve during synthesis. They appear to re-oxidise and deactivate rapidly in the presence of water.

1.4 Supported Metal Catalysts

To reduce the cost of the catalyst, a high contact area of the metal with the syngas is desirable. A high surface area of the active metal compound can be obtained by supporting the catalyst on a high surface inert material. Inorganic oxides such as alumina, silica, titania, zirconia and magnesia are typical high surface carriers [Sewell, 1996]. The coalescence is prevented due to the separation of the metal crystals by the support component. In order to obtain this, the support must have a higher resistance to sintering than the catalytic species. The preferred preparation procedure of such catalysts is by impregnation on a high surface carrier, because of the simplicity of the process [Anderson, 1975].

Supported catalysts are widely applied in heterogeneous catalysed reactions. [Perego and Villa, 1997].

1.4.1 Choice of Support

The support must have certain desirable characteristics. Generally they are:

- inertness
- strong mechanical properties
- stability under reaction conditions
- high surface area
- porosity; and
- low cost

Alumina, silica and activated carbon display the above qualities, of which alumina is the most widely used in industry [Anderson, 1975].

1.4.1.1 Silica as a Support

Silica is a high surface carrier with an amorphous structure. It is prepared by the polymerisation of silicic acid. Silanol groups are condensated (-Si-OH) to form siloxane groups (-Si-O-Si-). If the condensation is carried far enough it yields a silica hydrosol. The sol particles consist of a non-ordered arrangement of SiO_4 tetrahedral. These particles can aggregate into chains and networks. Siloxane linkage is formed between the particles. The surface of the silica particle is well hydrated. The concentration of the surface chemical bound

hydroxyl groups is about 5 OH per nm^2. Surface siloxane groups are also found on the surface reaching a concentration of 2 per nm^2 [Anderson, 1975].

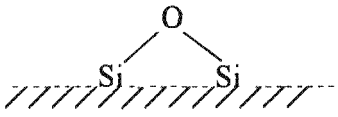

Figure 1-10: The surface siloxane group

At 390K only physically adsorbed water is removed. Heating above this temperature results in a loss of chemically bound hydroxil groups. The process is rapidly reversible by re-hydration with water or water vapour at room temperature. If the temperature exceeds 770K, rehydration takes place slowly in liquid water or strong base at room temperature [Anderson, 1975].

SiO_2 is considered as an inert support, but with Co supported on high surface silicas ($\geq$ 200 m^2/g) indication of the formation on cobalt silicate surface species are found [Rosynek and Polansky, 1991]. Silicate formation takes place more easily with the higher surface silica's [Puskas *et. al.*, 1992, Ming and Baker, 1995].

For high metal dispersion, a high surface silica is needed. The size of the pores decreases with increase in surface area. If the pores would get too small the removal of liquid products formed during FTS would be transport limited.

A high dispersion of metal on a silica support with large pores, would be the optimum catalyst.

1.4.2 Preparation of Supported Metal Catalyst

The preparation of a supported catalyst consists of depositing a catalytic active compound on a high surface support. The main objective is to achieve optimal dispersion of the active compound and the catalyst to be stable against sintering. The two main steps in catalyst preparation is:

1. depositing active compound precursor on the support; and
2. transforming the precursor into the required active component. It can be in the oxide, sulphide or metal state, depending on the reaction.

A large majority of deposition methods use aqueous solutions and involve liquid-solid interface. In some cases, the gas phase is used and that involves gas-solid interfaces. When using aqueous solutions to achieve deposition of active material, ion exchange and impregnation are amongst the popular methods, along with anchoring, grafting, spreading and wetting. When the support is put into the active compound solution, ion exchange, impregnation, dissolution of the support and formation of surface compounds all take place.

Carefully controlling the right parameters, will help the desired deposition method to take place. Variables in supported catalyst preparation are: temperature, pH, catalyst precursor, type of solvent, and activation of catalyst precursor. These variables have an influence on the final state of the catalyst and the surface characteristics of the active metal [Ertl *et al.*, 1997].

1.4.2.1 The Influence of the pH of the Impregnation Solution

The pH controls the surface charge of the support in the solution and thus the introduction of active component with the surface. When an oxide surface is brought into contact with water, the surface is generally covered with hydroxyl groups (-OH). When the support S-OH, with S as Al, Si, Ti, Fe, is put into water, a surface charge forms.

$$S-OH = S-O^- + H^+$$

$$S-OH + H^+ = S-OH_2^+$$

The resulting surface charge arises from the excess of one type of charge site over the other. The pH of the solution determines the net surface charge [Ertl *et al.*, 1997] and has an influence on the solubility of silica gel [Kogelbauer *et al.*, 1995].

The pH value where the particle has no charge at all is called the point of zero charge (ZPC). ZPC for silica lies between pH = 1.5 and 3. Looking at the depositing cobalt precursor on silica, the physical and chemical properties of the cobalt species on the silica gel surface are strongly affected by this parameter.

- pH < 5 Cobalt deposits as a cation.
- pH < 2 The silica surface is positively charged. Since cobalt ions in aqueous solution are positively charged, such surfaces do not favour adsorption. Dispersion of cobalt is poor and consequently catalytic activity is low.
- pH =>5 Ion exchange takes place. Silica gel partially dissolves in the solution and can be directly substituted with metallic ions [Ming and Baker, 1995]. Cobalt reacts to form silicates or hydrosilicates which are irreducible. In order to avoid precipitation of cobalt hydroxide, complexing agents such as urea and ethylenediamine are employed to stabilise the cobalt ion.

Silica gel impregnated with cobalt nitrate at pH > 5, results in a catalyst with cobalt silicate species and no reduction peaks under 500°C [Bonneviot *et al.*, 1989, Ming and Baker, 1995]. Puskas *et. al.* (1992) found that silica's can react with cobalt species under the slightly alkaline conditions of the precipitation to form cobalt silicates.

1.4.2.2 Ion Exchange

Most solid mineral supports are oxide surfaces and bear electric charges. Examples of natural ion exchangers are silicates and zeolites (cation exchangers). The framework bears an electric charge and is neutralised by ions of opposite sign. These ions may replace the ions of the support, depending on the pH of the solution and the ZPC of the support [Ertl *et al.*, 1997]. Ion exchange involves the replacement of an ion in the support by another ion species. For example: the support, containing ion A is plunged into an excess solution (total solution volume is larger than total pore volume of the support) containing ion B. Ion B penetrates into the pore structure and then takes the place of ion A. The support partially dissolves in the solution. Ion A passes into the solution until equilibrium is established.

1.4.2.3 Impregnation

The active species can be introduced to a porous support by impregnation with a solution containing a precursor. The impregnation method involves three steps: (1) wetting, (2) drying and (3) activation [Anderson, 1975].

1. Wetting: The impregnation solution is brought into contact with the support for a certain time. The precursor is introduced to the pore space and remains in the dissolved state. It does not become fixed on the surfaces at this stage of the preparation [Ertl *et al.*, 1997].
2. Drying: The catalyst precursor is dried to remove the liquid.
3. Activation: The catalyst is activated by calcination, reduction or other appropriate treatment.

Depending on the pore space, two different methods of impregnation can be followed. If the pores are filled with ambient air before impregnation, it is called dry impregnation or incipient wetness technique. Impregnation with excess volume is used when the pores of the support are filled with the solution liquid before impregnation.

1. Incipient wetness technique. The solution is brought into contact with the previously dried support. The volume of solution added is equal to the total pore volume of the support. The solution moves into the pores by capillary forces. After dry impregnation the sample is dried to remove all liquid.
2. With excess solution. The pores of the support are filled with the solvent before impregnation. The support is then plunged into the solution and kept for the time necessary for total impregnation. The volume of the solution is larger than the total pore volume of the support (excess solution). The diffusion of the precursor into the pores is driven by a concentration gradient. After total impregnation, the catalyst is then drained and dried [Anderson, 1975, Ertl *et al.*, 1997].

For both the techniques the main operating variable is the temperature which influences both the precursor solubility and the solution viscosity, and thus the wetting time. Other variables are pH, temperature and type of solvent. It is important to control the operating conditions during impregnation, in order to make the catalyst reproducible [Anderson, 1975].

The support plays a role during impregnation of transition metal precursors, because transition metal ions can form interaction with the support. Strong metal-support interaction (SMSI) has been observed for the following support minerals: TiO_2, V_2O_5, Vb_2O_5 . A weaker metal-support interaction is observed with SiO_2, Al_2O_3, ZrO_2 and MgO. Key parameters that may

influence the metal-support interaction are: the iso-electric point of the support and pH of solution, temperature, competitive ions and washing [Ertl *et al.*, 1997].

The formation of silicates is of concern, because cobalt silicates are only reducible at temperatures above 550°C, where sintering of the catalyst occurs [Kogelbauer *et al.*, 1995, Puskas *et al.*, 1992]. Cobalt silicate is inactive under FTS conditions and the formation of this metal-support interaction is seen as a permanent deactivation of the catalyst.

Silicate formation seems to be dependent on the preparation method, the type of salt used for catalyst preparation and pH of the impregnating solution [Kogelbauer *et al.*, 1995]. The amount of Co^{3+} formed is less for cobalt acetate than for the nitrate. The pH of the impregnating liquid rises above 5 for acetate, but remains below 5 for cobalt nitrate [Okamoto *et al.*, 1995, Rosynek and Polansky, 1991].

Reuel and Bartholomew (1984) reported a low reduction for cobalt on a silica carrier and explained it by an interaction of metal with support, that is the formation of surface spinals. Certain variables in the preparation have an influence as well, like pH.

A careful selection of metal precursor and competitors, give a large number of metal concentration profiles on the support. The distribution profiles vary between periphery and grain centre, depending on the strength of interaction with the support [Ertl *et al.*, 1997].

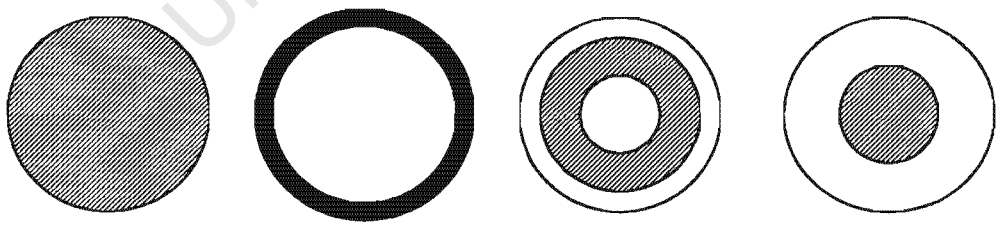

Figure 1-11 : The metal concentration profile in supports

1.4.3 Catalyst Activation

After the catalyst is prepared, most of the time it is not in the final activated state, but still as a precursor compound. The catalyst then has to go through several steps of activation. The active phase of the metal is determined by the reaction. For the Fischer-Tropsch synthesis, the catalyst has to be in the zero valent state. Activation steps consist of drying, calcining and reducing.

The activation procedure can have an influence on the performance of the catalyst. A wide range of investigations has focussed on the behaviour of the supported cobalt Fischer-Tropsch catalyst as a function of support [Reuel and Bartholomew, 1984], of cobalt dispersion [Iglesia *et al.*, 1992], of cobalt precursor [Rosynek and Polansky, 1991] of pretreatment [Bartholomew and Ferrauto, 1976] and of activation [Coulter and Sault, 1995]. In general the catalytic rates and selectivity of the Fischer-Tropsch synthesis are compared with the observed cobalt species to assess the effects that preparation and activation have on the catalyst performance. The alumina supported Co catalyst has displayed two cobalt surface species. The Co_3O_4 is easily reducible and is observed for high loadings (>2 wt%). The relative concentration of this species is dependent on the calcination temperature. The second cobalt phase is composed of Co^{2+} ions that have diffused into the lattice of the support to form a cobalt aluminate. The relative concentration of these embedded ions increases with calcination temperature and decreases with cobalt loading [Coulter and Sault, 1995]. With a silica supported cobalt catalyst, a Co_3O_4 phase forms that is easily reduced to metallic Co at temperatures below 450°C.

1.4.3.1 Drying

Drying is described as the elimination of the solvent (usually water) from the pores of the support [Perego and Villa, 1997]. It takes place at mild temperatures in the range of 80 to 200°C [Sewell, 1996]. Initially drying occurs through evaporation of moisture and is controlled by temperature, relative humidity and flowrate of air over the surface. When the moisture content reduces to 50% the evaporation is controlled by capillary forces. A concentration gradient occurs, which may lead to uneven dispersion [Perego and Villa, 1997]. The solid forms crystallites on the carrier.

Rosynek and Polansky (1991) found no significant changes in dispersion when samples were vacuum dried or air dried after they were both calcined. The vacuum dried samples showed the cobalt more evenly dispersed in the carrier. When the water evaporates from the pores, it causes a concentration gradient. In the rotar vapor system the samples are more uniformly dried than in an oven. This might explain the difference in the uniformity of the dispersion. Vacuum drying prior to calcination gives a high cobalt surface coverage.

Coulter and Sault (1995) found two distinct Co phases on the Co/SiO_2 catalyst when it was dried in air. The one phase was assigned to Co_3O_4 and the other to cobalt silicate. The two components were present in equal amounts. They suggest a sequel transition from the nitrate precursor, to a surface silicate to Co_3O_4 when the catalyst is dried at 100°C. The formation of Co_3O_4 is dependent on drying time. This suggests that the decomposition of $Co(NO_3)_2 \cdot 6H_2O$ in air is kinetically limited and the thermodynamically favoured cobalt phase under these conditions is Co_3O_4 [Coulter and Sault, 1995].

1.4.3.2 Calcination

Calcination is the further heat-treatment at temperatures higher that the drying temperatures. Calcination usually takes place in an oxidising environment, at temperatures higher than those used in the catalytic reaction and catalyst regeneration. Several processes occur during calcination: loss of chemically bonded water or CO_2, decomposition of the precursor, modification of the surface (small crystals grow into bigger ones), modification of structure, and the generation of the active phase. The calcination operating variables are time, temperature, and oxidising stream [Perego and Villa, 1997]. When the silica supported cobalt catalyst is calcined at 400°C, larger particles are formed by the agglomeration of Co_3O_4 particles [Coulter and Sault, 1995].

Calcination thus influences the phase of the cobalt on the support. When bulk zerovalent cobalt is calcined in air, CoO is formed between temperatures of 200°C-400°C., Then CoO is oxidised to Co_3O_4 only above 400°C [Sewell, 1996].

Silica supported Co forms Co_3O_4 at temperatures below 400°C. The decomposition of the nitrate precursor during calcination results in NO_X species, which is a highly oxidative gas. The dispersion of Co might influence how easily it is oxidised to Co_3O_4.

The interaction of cobalt with the silica support increases at calcination temperatures higher that 700°C, and the low temperature (300°C) hydrogen consumption peak disappears [Sewell, 1996]. Coulter and Sault (1995) found that by calcining the catalyst at 400°C, the interaction with the support is decreased. Large Co_3O_4 particles are formed which are reducible at temperatures below 500°C. Non-calcined samples showed a larger interaction with the support. The formation of cobalt silicates can take place during the decomposition of the nitrate precursor, which are at low temperatures. Analyses of species generated during the decomposition of the $Co(NO_3).6H_2O$ precursor indicates that the concentration of gas phase NO_x near the surface determines the nature of the cobalt surface phase.

Calcination conditions do not have an affect on the chain growth probability in the Fischer-Tropsch synthesis [Belambe *et al.*, 1997]. At higher calcination temperatures the number of surface active sites decreases due to a decrease in the reducibility of the catalyst. This causes a decrease in the reaction rate.

1.4.3.3 Reduction

Reduction is the final step of catalyst activation. The metal oxide is transformed into the metallic state by reduction in hydrogen.

$$M_X O_{Y(s)} + H_{2(g)} \rightarrow M_{(s)} + H_2 O_{(g)}$$

The reduction of Co_3O_4 proceeds through two stages. Co_3O_4 rapidly reduces to CoO and then to cobalt metal [van Steen, 1993]. The rate of CoO reduction depends upon the presence of the support.The reducibility of cobalt is enhanced by adding a noble metal. The reduction time has an influence on the metal crystallite size. Small Co^0 particles are formed with short-term reduction, while long-term reduction leads to formation of large bulk-like cobalt crystallites. [Zsoldos *et al.*, 1995].

The support has an influence on the reduction of the catalyst, due to interaction of the metal with the support. Choi (1995) reported the activation energy of reduction increased in the following order: $Co/TiO_2 < Co/Al_2O_3 < Co/SiO_2$,. The surface areas of the supports that he tested also increase in the same order: TiO_2: 50 m^2/g < Al_2O_3: 200 m^2/g: < SiO_2: 600 m^2/g. So the activation energy might be influenced by the surface area due to higher metal support interaction with increase in surface area.

The extent of reduction increases with higher reduction temperatures. Higher metal loading (12 %wt) yields larger metal particles than low loading (5 %wt). Smaller particles have a stronger interaction with the support. Since catalysts with higher metal loading are more readily reduced, metal-support interaction might have an influence on the extent of reduction.

The concentration of cobalt-support species first increases and then decreases with increasing reduction temperature. High temperature reduction may increase the thermal annealing of residual divalent cobalt with the support, forming a highly stable cobalt-support species.

Metal dispersion decreases with increasing reduction temperature due to sintering and forms larger reduced cobalt particles on the support [Sewell *et al.*, 1996].

1.5 Catalyst Characterisation

Characterisation of a catalyst provides information of chemical structure, mechanical structure and texture, and catalytic activity. Chemical structure involves elemental composition and proportion of individual phases that may be present. The texture of the catalyst has to do with size and shape of individual catalyst units. The activity of the catalyst is the measurement of the ability of the catalyst to carry out a particular chemical transformation under specified conditions [Anderson and Pratt, 1985].

1.5.1 Particle Size and Dispersion Measurements

Metal particles are usually not spherical; their shape is not homogenous. With a combination of two or more physical methods, an approximation of the shape and size of the particles can

be obtained. To establish size distribution and or mean size, the particles are assumed to be spherical.

If a collection of n_i spherical particles of diameter d_i is considered, then the area of each of the particles is:

$$A_i = \pi d_i^2$$

and the volume of the particle is:

$$V_i = \frac{\pi d_i^3}{6}$$

There are two types of size distribution:

- Number distribution: plot n_i as a function of d_i,
- Area distribution: plot $n_i d_i^2$ as a function of d_i.

The mean particle size can be expressed as:

- Length-number mean diameter:

$$d_{LN} = \frac{\sum n_i d_i}{\sum n_i}$$

- Volume-area diameter

$$d_{VA} = \frac{\sum n_i d_i^3}{\sum n_i d_i^2}$$

Dispersion is a fraction of the amount of catalyst in metal form that is on the surface of the catalyst.

$$D = \frac{N_S}{N_T}$$

where N_S is the total number of metal atoms present on the surface, and N_T is the total number of metal atoms in the surface and bulk.

Assuming that equal proportions of the 3 low-index planes are found on the polycrystalline surface of fcc material, the number of atoms per unit area can be calculated.

With n_s the mean number of atoms and a_m the surface area occupied by and atom m:

$$a_m = \frac{1}{n_s}$$

The volume (V_{ma}) occupied by an atom can be calculated from :

$$V_{ma} = \frac{M}{\rho N_A}$$

Where M is the atomic mass, ρ is the density of the material and N_A is Avogadro's constant ($6.022*10^{23}$ mol).

The relationship between the particle size and dispersion (D) is given by:

$$D = 6\left(\frac{V_m}{a_m}\right)\Big/ d_{VA}$$

The specific surface area, S_P:

$$S_P = a_m\left(\frac{N}{M}\right)D$$

Particle size can be measured by physical and chemical methods. Chemical methods are for example the measurement of the amount of gas chemisorbed on the catalyst surface. The stoichiometry of adsorption of hydrogen is assumed to be 1:1 for H:Co. Physical methods include electron microscopy and X-ray diffraction.

1.5.1.1 H_2 Chemisorption

The static method of H_2 chemisorption involves pretreatment of the catalyst, followed by evacuation. The catalyst is then brought into contact with a known quantity of adsorbate gas (hydrogen in the case of Co) [Ertl *et al.*, 1997]. The adsorbed gas and the free gas are in dynamic equilibrium. The fractional coverage of the surface depends on the pressure of the overlaying gas. This dependence of the fractional coverage on the pressure at a set temperature is called the adsorption isotherm [Atkins, 1990]. The amount of gas adsorbed is determined by measuring the pressure after the adsorption has reached equilibrium. The volume of the deadspace is calculated by a preliminary calibration. Successive doses of gas allow the determination of the volume of adsorbed gas vs. the equilibrium pressure (adsorption isotherm) [Ertl *et al.*, 1997].

The chemisorption of H_2 on Co is activated [Choi, 1995]. Depending on the % wt loading (5%-10%), the optimum chemisorption temperature for supported cobalt catalyst lies between 100-150°C [Reuel and Bartholomew, 1984].

To evaluate the chemisorbed gas monolayer uptake V_m (saturation of metal surface), a common practise is to back-extrapolate the straight portion of the isotherm to zero pressure. This procedure becomes ambiguous when the isotherm does not have a horizontal region.

When the equilibrium coverage increases significantly with pressure, the saturation of the metal surface is not reached. The volume of the monolayer, V_m is then obtained by fitting the data to an adsorption isotherm of a given type [Ert *et al.*, 1997]. The Langmuir isotherm is based on the assumption that all adsorption sites are equivalent and that the ability of a particle to bind there is independent of whether or not the nearby sites are occupied [Atkins, 1990]. The Langmuir isotherm for dissociative adsorption:

$$V = V_m \frac{b \cdot p^{\frac{1}{2}}}{\left(1 + bp^{\frac{1}{2}}\right)}$$

The isotherm is a plot of 1/V vs. $1/P^{½}$ or $P^{½}/V$ vs. $P^{½}$

The metal dispersion can then be directly obtained from:

$$D = \frac{v_m n}{22414m} \Big/ \frac{wt}{100M}$$

where M is the atomic mass of the metal, m is the mass of the sample (g), n is the chemisorption stoichiometry, v_m is the volume of chemisorbed gas required to form a monolayer and wt is the % metal loading [Ertl *et al.*, 1997].

1.5.1.2 Transition Electron Microscopy

The electron microscope allows the direct observation of the catalyst morphology, with magnification tunable in the range of 10^{-4}-10^{-10} m. It is possible to obtain data on the shape and size of particles as well as the active phases from the images. The transmission electron microscope (TEM) is a most useful tool in particle size measurement [Ertl *et al.*, 1997].

The interaction of the high-energy electron beam with the sold generates a variety of signals, all of which yield information on the nature of the solid. The electrons may undergo two types of scattering: elastic scattering and inelastic scattering. Elastic scattering does not involve transfer of energy to the atom.

The catalyst is set in a resin such as 'Araldite' that is sectioned into thin pieces, using an ultramicrotome with a section thickness of 20-40nm. The specimen should be thin enough to transmit a reasonable fraction of the incident electron beam.

For particles larger than 3nm, diffraction contrast is the dominant method by which the contrast in the image is obtained. The image contrast depends strongly on the particle orientation with respect to the beam. Tilting the specimen by as little as 2° can cause a given particle image to go from maximum to minimum contrast.

If the metal particles are randomly orientated and have a distribution of particle sizes, only a fraction of the particles in any given field will be orientated for maximum diffraction contrast. A good estimate of the average particle size will still be obtained if sufficient fields are examined and sufficient particle images are measured.

Images can be obtained with either bright field or dark field illumination. In bright field illumination, the image is formed by using the direct beam that passes through the microscope's objective aperture. The contrast of the image arises because of the removal of these scattered beams.

In dark field illumination, the image is formed by using a diffracted beam from a crystalline specimen that is allowed to pass through the objective aperture by suitably tilting the specimen with respect to the microscope axis. Dark field illumination, when used in conjunction with bright field illumination, is a powerful technique to assist in phase identification and crystal orientation [Anderson and Pratt, 1985].

It is possible to measure the particle size distribution as well as the mean particle size. Particle sizes can be measured manually. They are first identified on a positive print of the micrograph. To establish a granulometry, a suitable size increment Δd (eg. 1nm) is chosen. The particles are then counted in the intervals 0-Δd, Δd-2 Δd, ..., n Δd-(n+1) Δd. The average diameter d_i for each interval is then $\Delta d/2$, $3\Delta d/2$, ... The number distribution (n_i vs. d_i) and surface distribution ($n_i d_i^2$ *vs. di)* can then be plotted [Ertl *et al.*, 1997].

There are several factors that influence the particle size measurement. Lack of contrast between the particle and support influence the accuracy of the measurement. Particles my be undetected because of electron beam induced changes, such as disaggregation and shift of particles. A few large particles could contribute little to the total active surface, but significantly to the catalyst active mass. This leads to overestimation of the specific surface area and underestimated turnover frequencies. Metals of the first transition row are easily oxidised in air, and oxidised particles are slightly larger than those of the reduced metal [Ertl *et al.*, 1997].

1.6 Temperature Programmed Reduction of Supported Cobalt Catalysts

This thermoanalytical technique measures the response of the solid as the temperature is changed in a reducing atmosphere. Temperature programmed reduction (TPR) applies linear rate of temperature increase while passing a reducing gas over the catalyst bed. The reducible catalyst, or catalyst precursor is exposed to a flow of a reducing gas mixture, typically 5% hydrogen with nitrogen as the make up gas. The rate of reduction is monitored by measuring the H_2 content of the reducing gas at the outlet of the reactor. The experiment allows the determination of the total amount of hydrogen consumed, from which the degree of reducibility of the metal can be calculated [Ertl *et al.*, 1997].

The extent of reduction of supported cobalt catalyst is difficult to determine from TPR, because of unknown quantities of divalent and trivalent cobalt ions. Reduction of the nitrate precursor might also occur. The TPR of the precursor showed the most intense peak to belong to the decomposition of the nitrate. This is accompanied by the evolution of nitrogen oxides, NO, NO_2 and N_2O_4. N_2O_4 can have a higher conductivity than hydrogen and is responsible for a negative peak. The hydrogen consumption peak after the decomposition peak is assigned to the reduction of CoO by Sewell and co-workers (1996). Hydrogen consumption after 500°C is due to some degree of interaction of cobalt with the support, since the bulk cobalt oxide is completely reduced by 500°C. The use of a combined TPR/TPO technique enables the determination of the extent of reduction [Sewell *et al.*, 1996].

1.7 Temperature Programmed Oxidation of Supported Cobalt Catalysts

This technique is an equally valuable technique for the investigation of the redox behaviour of a catalyst, particularly when applied in cyclic TPR/TPO experiments [Ertl *et al.*, 1997].

Bulk cobalt metal undergoes a sequential oxidation. Metallic cobalt is first oxidised to CoO and then to Co_3O_4 (reactions 1 and 2). Co_3O_4 is thermally reduced to CoO at a temperature of 870°C, with a stoichiometric release of oxygen (reaction 3). In the TPO of bulk cobalt metal, the three peaks of the reactions are visible at temperatures of 300°C, 580°C and 780°C.

$$CoO + \tfrac{1}{2}O_2 \rightarrow CoO \qquad (1)$$

$$3CoO + \tfrac{1}{2}O_2 \rightarrow Co_3O_4 \qquad (2)$$

$$Co_3O_4 \rightarrow 3CoO + \tfrac{1}{2}O_2 \qquad (3)$$

The stoichiometric ratio of oxygen uptake by reactions 1 and 2, relative to the oxygen release of reaction 3 should be 4 [Sewell, 1996].

The extent of reduction for a supported metal catalyst is limited due to the interaction with the support and the formation of cobalt silicates. After reduction cobalt is assumed to be present in three forms: Cobalt as reduced metal (zerovalent cobalt), as an oxidisable divalent cobalt species and divalent cobalt-support species which are not oxidisable [Sewell *et al.*, 1996].
The amount of non-oxidisable cobalt-support species can be determined by measuring the oxygen release during the high temperature decomposition of Co_3O_4. This peak represents all cobalt which has been oxidised to trivalent cobalt [Sewell *et al.*, 1996].

The ratio of the oxygen uptake peak to oxygen release peak is dependent on the extent of cobalt reduction. The range of the ratio is between 1 and 4. A ratio of 4 indicates complete reduction of the supported cobalt species. [Sewell, 1996].

CHAPTER 2

Thermodynamic Analysis

2 THERMODYNAMIC ANALYSIS OF Co/SiO_2 CATALYSTS

The objective of this chapter is to evaluate thermodynamically the affect of water on the deactivation of the silica supported cobalt catalyst and to give a background as to whether cobalt dispersion could have any contribution to the affect.

A contradiction is found in the literature where some authors indicate that the cobalt catalyst deactivates when water is co-fed with the syngas [Schanke *et al.*, 1995, Schanke *et al.*, 1996, Kogelbauer *et al.*, 1995, Rothaemel *et al.*, 1997], and others show a positive affect on the product spectra and selectivity [Nijs and Jacobs, 1980, Schulz *et al.*, 1995a, Iglesia, 1997]. The questions that arise then are whether the deactivation of cobalt due to water is thermodynamically possible and does the particle size of cobalt has any influence on the deactivation.

Cobalt has a high FTS activity and low water-gas shift activity. The cobalt catalyst can therefore be best applied in slurry reactor technology because of the good heat transfer of the system. Due to the nature of the slurry reactor, high partial pressures of water are generated when operated at high conversions. The water present in the reactor could lead to a deactivation of the catalyst by a possible re-oxidation of the active metal.

2.1 Thermodynamic Analysis

Figure 2-1 shows the Gibbs free energy for the oxidation of bulk cobalt with water over a temperature range. The Gibbs free energy for the reaction of cobalt with water to form cobalt oxide is positive over the whole range of temperatures at which the catalyst is prepared and treated (see Figure 2-1). This cause of deactivation does not seem thermodynamically possible.

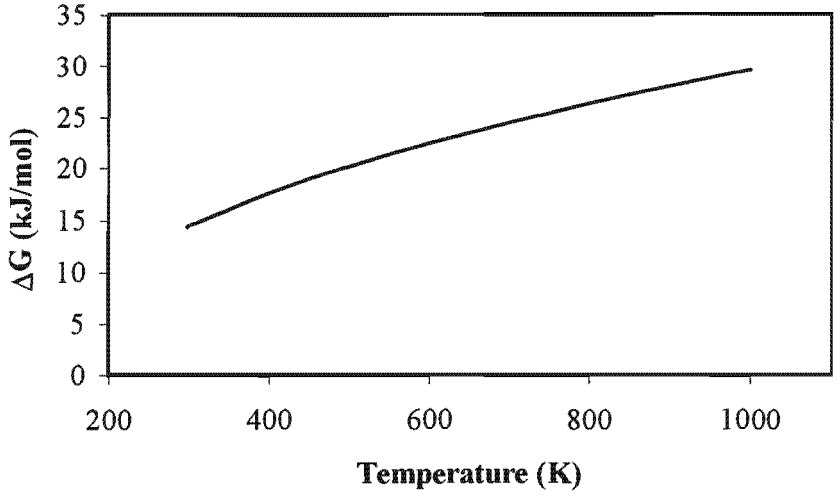

Figure 2-1: The Gibbs free energy for Co + H_2O ⟶ CoO + H_2 [thermodynamic data: Knacke *et al.*, 1991]

In the consideration of the oxidation of bulk cobalt that has been described above, the affect of change in surface energy has not been taken into account. Although the re-oxidation of bulk cobalt with water is thermodynamically not favoured, the re-oxidation of the metal surface might be feasible. The surface atoms of a solid are exposed to a different environment than the atoms in the bulk of the solid. They have fewer neighbours than the bulk atoms do. The neighbours of each surface atom may be distributed anisotropically. Therefore the thermodynamic properties associated with the surface region is defined separately from the bulk thermodynamic properties. Studies of small particles have shown that when the particles become very small and dispersion tend to unity, the characteristics of theses systems are very different from those of the bulk phase [Somorjai, 1994]. Significant surface oxidation is found when the Co/Al_2O_3 is treated with low H_2O/H_2 ratio [Schanke *et. al.*, 1996].

Consider a large crystalline solid that is bounded by surface planes. Let N be the number of atoms in the solid and E^o the energy of the solid per atom. The specific surface energy, E^s (energy per unit area) is then defined by the relation:

$$E = NE^o + \wp E^s$$

where E is the total energy of the solid and $\wp$ is the surface area. The surface work content, A^s (energy per unit area) is defined by the equation

$$A^s = E^s - TS^s$$

where S^s is the entropy per unit area of surface created (specific surface entropy) and T is the temperature in degrees Kelvin. The surface free energy G^s (energy per unit area) is defined by the equation

$$G^s = H^s - TS^s$$

where H^s is the heat absorbed by the system per unit surface area (specific surface enthalpy). The total free energy of the system G can also be expressed as

$$G = NG^\circ + \wp G^s$$

where G^o is the free energy per atom and G^s is the free energy per unit area of surface. Thus the Gibbs free energy for small particles can be written in the form of two contributions:

$$\Delta G = \Delta G^i + \Delta G^s$$

The surface contribution is the sum of the isothermal work (γdA) plus the energy contributed by transferring dN atoms to and from the surface:

$$\Delta G = \Delta G^i + \gamma dA + \Sigma_i \mu_i \Gamma_i dA$$

with $$\Gamma_i = \frac{dN_i}{dA}$$

since $$\frac{dN_i}{dA} = 0$$

and $$F_i dA = 0$$

The Gibbs energy per mole of material then is:

$$\Delta g = \Delta g^{i} + \frac{(\gamma)}{n} dA$$

Taking the molar density in account of the material:

$$l_m = \frac{n}{V}$$

and assuming spherical geometry, i.e.:

$$A = \Pi d_p^2$$

$$V = \frac{\Pi d_p^3}{6}$$

the Gibbs free energy per mole can be given by:

$$\Delta g = \Delta g_i + (\gamma)\, 6\, d(\frac{1}{d_o})$$

For Co $\longrightarrow$ CoO (large particles), i.e. as $d_p \rightarrow \infty$, the following limit can be developed:

$$\lim_{d_p \to \infty} \Delta g = \Delta g_i$$

The molar Gibbs free energy for large particles equals thus the interactive Gibbs free energy. The Gibbs free energy which were measured using both materials (ΔG^b) is approximately equal to the interactive Gibbs free energy:

$$\Delta g^{i} \approx \Delta g^{b}$$

In the thermodynamical consideration regarding small cobalt crystallites, the contribution of the surface energy has now to be taken into account. As a limit the complete oxidation of small cobalt crystallites to small cobalt oxide crystallites can be achieved. The change in the Gibbs free energy for the reaction can now be formulated as a contribution of the Gibbs free energy for the reaction of bulk cobalt plus the contribution of the change in surface energy.

$$\Delta g^R = \Delta g^{bR} - \int_{d_p,Co}^{0} (\gamma)\, d(\frac{1}{d_p}) + \int_{0}^{d_pCoO} (\gamma)\, d(\frac{1}{d_p})$$

If after the oxidation the particle size remain constant then:

$$\Delta g^R = \Delta g^{b,R} + \frac{((\gamma)_{CoO} - (\gamma)_{Co})}{d_p}$$

The surface energy for the oxides is lower than that of the metals [Somorjai, 1994]. The second term of the equation is thus negative. This becomes more negative when the particle size decreases. This simplified calculation shows that re-oxidation of very small cobalt crystallites may become thermodynamically feasible.

Once the surface of the cobalt is oxidised and in contact with the support, the Gibbs free energy for the formation of cobalt silicates is negative [thermodynamic data: Knacke *et al.*, 1991], indicating a possible formation of a metal support interaction (see Figure 2-2).

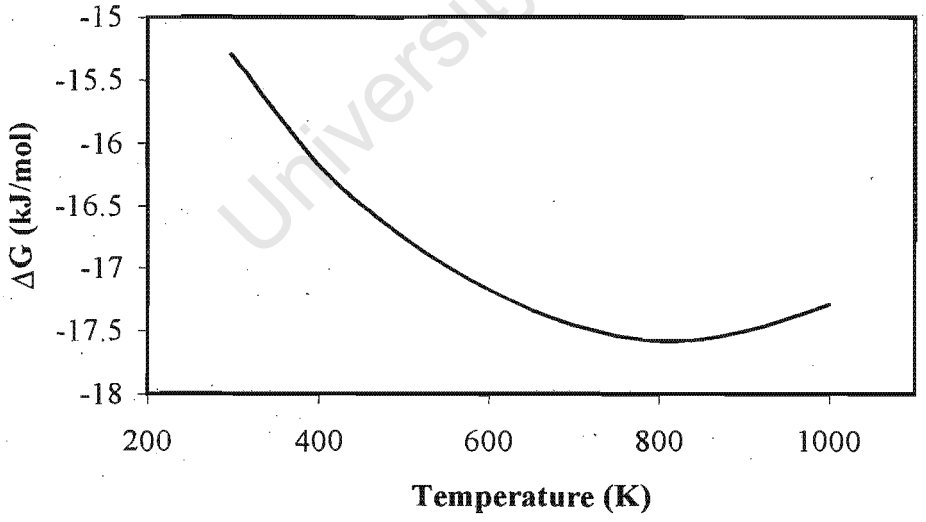

Figure 2-2: The Gibbs free energy for 2CoO + SiO2 ⟶ 2CoO.SiO2 [thermodynamic data: Knacke *et al.*, 1991]

The thermodynamical data is taken at 200°C and 5 bar, which are typical Fischer-Tropsch conditions for the cobalt catalyst. The assumption here is that all the cobalt present in metal form is in direct contact with the support. Thus is a case similar to a very high dispersion of cobalt on the support. The result is that all the cobalt in direct contact with the support forms an interaction with the support under these hydrothermal conditions (see Figure 2-3). These results confirm with the findings of Kogelbauer *et al.* (1995) where they showed a decrease in cobalt reducibility due to cobalt silicate formation after hydrothermal treatment.

As seen in Figure 2-3, most of the metallic cobalt forms a metal support interaction, but not all. A small amount of the metal is oxidised to CoO.. The Δ Gibbs free energy for these reactions can be seen in Appendix VI, as calculated with HSC Chemistry for Windows.

2.2 Expected Influence of Dispersion on Deactivation

Cobalt catalysts with a high dispersion are expected to have a higher activity, since more of the metal should be available for CO and H_2 chemisorption and dissociation. For high dispersion of cobalt, a high surface carrier is needed, but it is found that on high surface silicas that more cobalt silicate surface species are formed than on low surface silicate [Rosynek and Polansky, 1991]. Since high cobalt dispersions result in high cobalt silicate concentrations, the increase of available metallic surface cobalt expected for higher dispersions is thus cancelled out [Coulter and Sault, 1995]. Johnson *et al.* (1991) observed a decreasing activity with increasing dispersion. This might be due to metal support interaction. Metal support interaction is necessary to obtain high dispersions. Therefore, the optimum situation is one of give and take, to get maximum dispersion of cobalt with the minimum of strong-metal-support-interaction.

2.3 Formation of Cobalt Silicates During Catalyst Synthesis

When the cobalt nitrate precursor for the Co/SiO_2 catalyst is decomposed during drying, it initiates the formation of a surface cobalt silicate. The CoO intermediate reacts with SiO_2 to form a cobalt silicate surface compound. When the drying in air is prolonged the surface silicate converts into Co_3O_4. Drying in vacuum disperses the nitrate precursor on the support and forms cobalt silicate islands. When the air-dried samples are annealed in ultra high vacuum (UHV), the surface silicate is stabilised against reduction or oxidation, through the

migration of Co^{2+} ions into the support. A well-ordered bulk cobalt silicate is then formed. The relative concentration of these embedded ions increases with calcination temperature and decreases with cobalt loading [Coulter and Sault, 1995].

Coulter and Sault (1995) showed by analyses of species generated during the decomposition of the $Co(NO_3)_26H_2O$ precursor, that the concentration of the gas phase NO_x near the surface determines the nature of the cobalt surface phase.

When assumed that all the metal atoms in direct contact with the support, form a bond with the support and are thus inactive, then a metal dispersion of 100% would give a totally deactivated surface due to the metal support interaction. In Figure 2-4, the expected deactivation due to cobalt-silicate formation during catalyst preparation is shown.

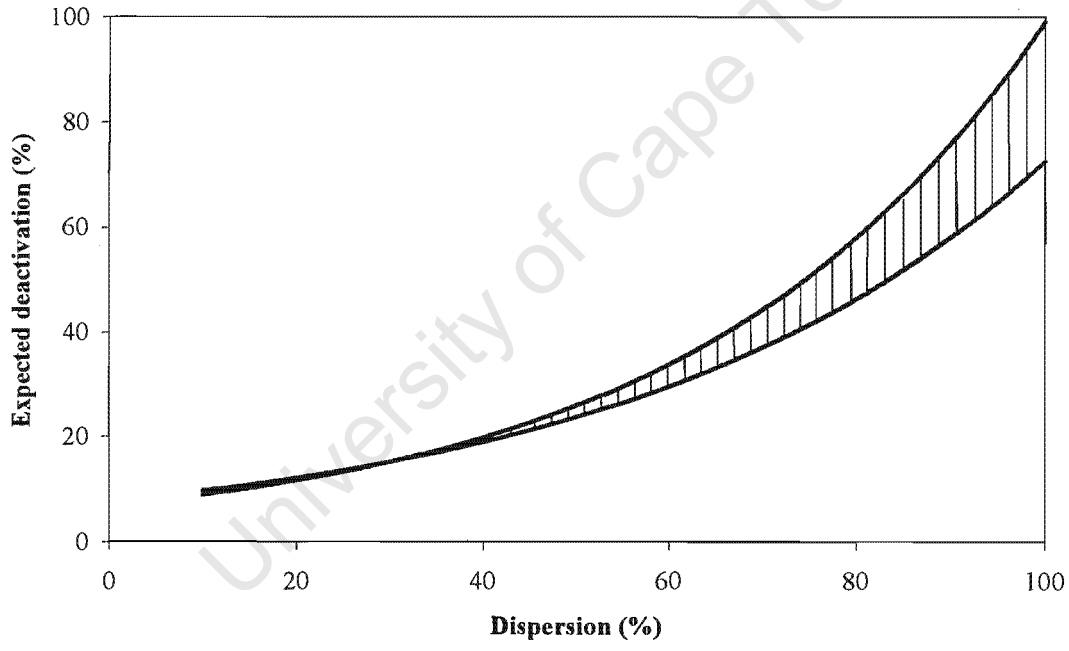

Figure 2-4: The expected deactivation at impregnation

CHAPTER 3

Experimental

3. EXPERIMENTAL

3.1 Catalyst Synthesis

Supported cobalt catalysts are highly active in Fisher-Tropsch synthesis. Both the identity of the metal precursor and the support have a decisive effect on the characteristics of the catalyst [Niemelä and Krause, 1996]. Cobalt nitrate is conventionally used as a precursor because it is simple to prepare and easy to decompose to cobalt metal.

The precursor can be brought into contact with the support by precipitation [Perego and Villa, 1997], impregnation [Niemelä *et al.*, 1997] and contact with cobalt nitrate melt [Iglesia *et al.*, 1995].

The overall activity is related to the activation treatments that the cobalt catalysts undergo [Belame *et al.*, 1997, Coulter and Sault, 1995, Niemelä *et al.*, 1997, Iglesia, 1997]. Drying, calcination and reduction temperature and time influence the surface properties and extent of reduction of the cobalt catalyst.

3.1.1 The Support

Silica was chosen because a great amount is known about the silica as a support and less carbonaceous deposit and migration from metal to support occurs on Co/SiO_2 than on the Co/Al_2O_3 catalyst [Boskovic and Smith, 1997].

Silica gel, Davisil™, grade 646, 35-60 mesh, 99+ %, was supplied by Aldrich Chemical Company, Inc. The mean pore diameter is 150Å, and the surface area: 300m^2/g [van Steen *et al.*, 1996]. The pH of 5 wt.% slurry in water is 7 according to Aldrich Chemical Company, Inc. The pore volume was taken as 2.3 cm^3/g [van Steen *et al.*, 1996] in the catalyst preparation.

Table 3-1: The calcination heating programme

Temperature Range (°C)	*Heating Rate (°C/min)*	*Holding Time (hrs.)*
0-100	10	1
100-200	10	1
200-300	0.5	0
300-400	10	1

Because of the exothermic nature of the decomposition of the nitrate precursor, cobalt particles can agglomerate to form bigger crystallites [Iglesia, 1997]. A slow heating rate over the decomposition temperature range (200-300°C) might result in smaller cobalt crystallites.

The catalysts were named according to their treatments, $Co/SiO_2(N)$-c6, $Co/SiO_2(N)$-c4 and $Co/SiO_2(N)$-s-c4, where –c indicates the calcination step and the number 4 or 6 the temperature of calcination i.e. 400 or 600°C respectively and –s represents the slow heating rate.

3.2.2 Reduction

All the catalysts were reduced for 16 hours at 400°C. The calcined catalysts were heated up at 10°C/min in pure hydrogen (60 ml (STP)/min). Two catalysts were directly reduced, without the calcination step. $Co/SiO_2(N)$ was reduced in the classic way by heating up at 10°C/min in pure hydrogen. The other catalyst, $Co/SiO_2(N)$-s, underwent a more complex reduction heating programme (see Table 3-2).

According to Bartholomew and Farruto (1976) the heating rate during reduction has an effect on metal surface area, of alumina supported nickel. The dispersion should increase when a slow heating rate of less than 5 °C/min was applied. They showed that it is possible to control catalyst dispersion by controlling either the amount of water removed by drying prior to reduction, or by controlling the heating rate and the partial pressure of water during reduction.

Table 3-2: The reduction heating programme

Temperature Range (°C)	*Heating Rate (°C/min)*	*Holding Time (hrs.)*
0-100	10	1
100-200	10	4
200-300	0.5	0
300-400	10	16

Since the decomposition of the nitrate precursor takes place as an exothermic step function, and the concentration of NO_X species can influence the amount of metal-support interaction [Coulter and Sault, 1995], the heating rate should be slow over this temperature region. It is possible to minimise the exothermic heat release by controlling the temperature and to dilute hydrogen with an inert gas.

The two pauses in the reduction heating rate programme were at the boiling point of water (100°C) and at the start of the decomposition of the nitrate precursor (200°C). During the heating up phase a 5% H_2/He stream at 60 ml/min was used as the reducing gas.

Denomination of the directly reduced catalysts was as follows: $Co/SiO_2(N)$ for the catalyst prepared in the classic way, and $Co/SiO_2(N)$-s, where –s indicates a slow heating rate during reduction.

3.2.3 Treatment with H_2/H_2O Gas Mixture

There are various ways of testing the influence of water on the cobalt Fisher Tropsch catalyst. Water can be fed with the reaction feed under FTS conditions,[Iglesia, 1997, Schanke *et al.*, 1996, Schulz *et al.*, 1995a]. Alternatively the catalyst can be exposed to water vapour before testing the catalyst under FTS conditions [Kogelbauer *et al.*, 1995, Schanke *et al.*, 1996].
A fraction of each catalyst was exposed to water vapour prior to FTS and was then compared with the original catalyst on characterisation and reaction level.

The catalyst was loaded in a fixed bed stainless steel reactor (see Figure 3-1), fitted with an internal thermocouple. The flow rate of the reducing gas was measured and adjusted with a needle valve to obtain 60 ml (STP)/min. Typically 3g of catalyst was placed in the isothermal zone. The catalyst was then reduced in 60 ml (STP)/min H_2 by heating up to 400°C and keeping at this temperature for 16 hours. Before starting the water treatment, the catalyst was cooled down to 200°C in H_2 flow and the saturator was stabilised for 30 min on the bypass. Water was introduced to the feed stream by bubbling hydrogen through a jacketed saturator filled with deionised water. The saturator, fitted with a thermocouple was kept at 60°C by circulating water from the heated water bath through the jacket. A H_2/H_2O ratio of 4 was obtained with total flowrate of 60 ml (STP)/min. The gas lines carrying the water vapour were heated to 130°C to ensure no condensation of water in the lines. The cold trap captured the water at room temperature and kept the exit line from blocking up. The catalyst was exposed to this water treatment for 24 hours at atmospheric pressure.

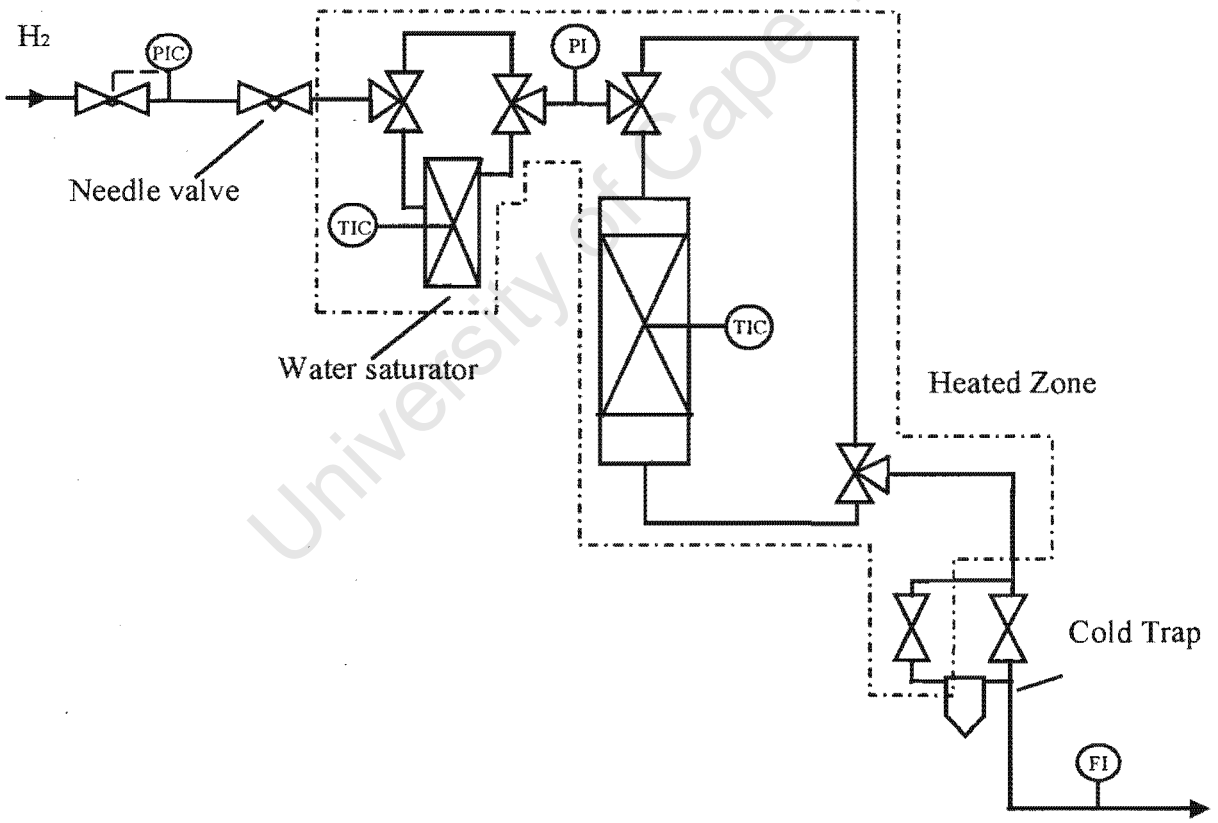

Figure 3-1: Layout of the water treatment equipment

Water-treated catalysts were indicated with a –w added to the original catalyst name.

The original catalysts were temperature treated at 200°C in hydrogen for the same time (24 hrs) as the time of exposure to water vapour. This was to ensure that the catalysts were comparable. After the catalyst was reduced and cooled down, the reactor was opened and the catalyst was exposed to the atmosphere. The catalysts were stored in a desiccator at room temperature. The contact with air caused the metal surface to oxidise and had to be re-reduced *in situ* at 200°C for 4 hours before Fischer-Tropsch synthesis, TPO and H_2 chemisorption measurements.

3.3 Nomenclature of the Catalysts

Table 3-3 gives an overview of the catalysts used in this study. The following abbreviations were used to indicate the type of precursor used in the preparation method and activation procedure: N for cobalt nitrate. –cX represent a calcination before reduction at X00 °C. –s indicates a slow heating rate and –w is added to the catalyst name when the catalyst was exposed to water treatment before reaction (see Table 3-3).

Table 3-3: Composition and nomenclature of catalyst

Catalyst name	*Calcination*	*Reduction*	*Steam treatment*
$Co/SiO_2(N)$	—	400°C, 16 hrs.	H_2 treatment 200°C 24 hrs. $H_2/H_2O = 0$
$Co/SiO_2(N)$-w	—	400°C, 16 hrs.	H_2O treatment 200°C 24 hrs. $H_2/H_2O = 4$
$Co/SiO_2(N)$-s	—	400°C, 16 hrs. slow heating rate[1)]	H_2 treatment 200°C 24 hrs. $H_2/H_2O = 0$
$Co/SiO_2(N)$-s-w	—	400°C, 16 hrs. slow heating rate[1)]	H_2O treatment 200°C 24 hrs. $H_2/H_2O = 4$
$Co/SiO_2(N)$-c6	Calcined 600°C, 24 hrs	400°C, 16 hrs.	H_2 treatment 200°C 24 hrs. $H_2/H_2O = 0$
$Co/SiO_2(N)$-c6-w	Calcined 600°C, 24 hrs	400°C, 16 hrs.	H_2O treatment 200°C 24 hrs. $H_2/H_2O = 4$
$Co/SiO_2(N)$-c	Calcined 400°C, 3 hrs.	400°C, 16 hrs.	H_2 treatment 200°C 24 hrs. $H_2/H_2O = 0$
$Co/SiO_2(N)$-c-w	Calcined 400°C, 3 hrs.	400°C, 16 hrs.	H_2O treatment 200°C 24 hrs. $H_2/H_2O = 4$
$Co/SiO_2(N)$-s-c	Calcination programme[2)]	400°C, 16 hrs.	H_2 treatment 200°C 24 hrs. $H_2/H_2O = 0$
$Co/SiO_2(N)$-s-c-w	Calcination programme[2)]	400°C, 16 hrs.	H_2O treatment 200°C 24 hrs. $H_2/H_2O = 4$

[1)] Reduced using a temperature programme shown in Table 3-2.
[2)] Calcined in air by using a temperature programme shown in Table 3-1.

3.4 Catalyst Characterisation

Catalyst characterisation is an integral step in the design of a catalyst. It aids linking structural and electronic properties of the active compound with catalytic performance. The catalysts were characterised using thermochemical, adsorptive and spectroscopic techniques. Thermochemical characterisation included temperature programmed reduction (TPR), temperature programmed oxidation (TPO). Hydrogen chemisorption was the only adsorptive

characterisation technique applied and spectroscopic techniques used were atomic absorption spectroscopy (AAS) and transmission electron microscopy (TEM).

3.4.1 Thermochemical Characterisation Techniques

The extent of reduction of supported cobalt catalysts can be determined by using a combined TPR/TPO technique. Because of the unknown stoichiometry of the reduction it is difficult to determine the degree of Co/SiO_2 reduction from only TPR measurement. [Sewell *et al.*, 1996].

TPR spectrum describes the hydrogen consumption as a function of temperature, which is increased linearly to 1000°C. The TPO spectrum describes the oxygen consumption as a function of temperature, which is raised linearly from 40 to 1000°C.

3.4.1.1 Temperature Programmed Reduction

The reduction behaviour of the catalysts was studied via temperature programmed reduction. 0.15g finely grounded catalyst was loaded on a porous fritt in a quartz mini reactor. The quartz reactor has a thermowell in which a thermocouple was inserted to control the temperature (see Figure 3-2). A reducing gas consisting of 5.84% H_2/N_2 was passed over the catalyst bed at 60 ml (STP)/min. The hydrogen/nitrogen mixture was calibrated by temperature programmed reduction of pure metal oxides (CuO, NiO and Co_3O_4, see Appendix I). The thermal conductivity of the reactor exit stream was measured with a thermal conductivity detector (TCD). The hydrogen consumption could be calculated from the change in thermal conductivity.

After catalyst reduction the temperature was lowered to 40°C where at the TCD was stabilised for at least 4 hours. Upon stabilisation of the detector, the oxidising gas (2% O_2/He) was diverted through the reactor at 60 (STP) ml/min and the temperature was raised linearly from 40°C to 1000°C at 10°C/min. The reactor temperature was kept at 1000°C for 30 minutes to ensure complete oxidation of the reduced metal catalyst. The oxygen uptake during TPO was calculated by measuring the oxygen concentration in the outlet stream as a function of temperature using a linear temperature programme and constant inlet flowrate. The oxygen release and uptake during TPO do not have a significant influence on the flowrate. The data were collected and stored by microcomputer for further processing.

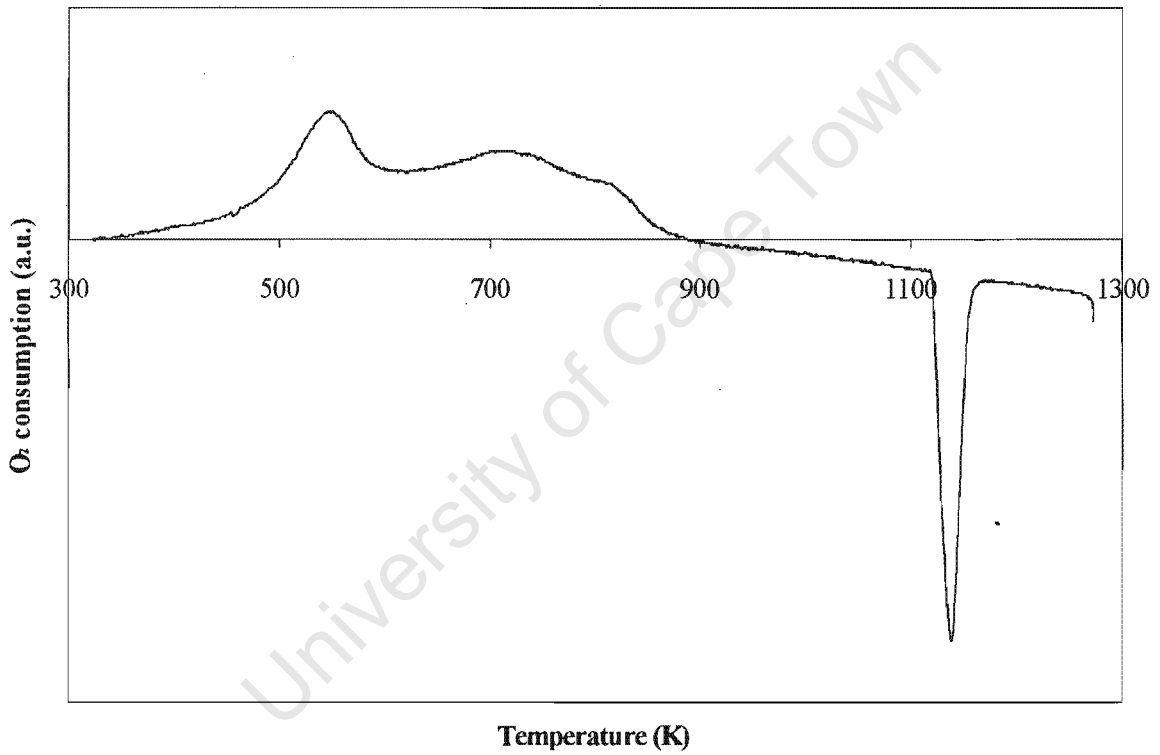

Figure 3-3: TPO spectrum of cobalt metal. (Reducing gas = 60 ml (STP)/min 5% H_2/N_2, reduction temperature = 500°C. Oxidising gas = 60 ml (STP)/min 2% O_2/He, temperature programming rate = 10°C/min, $m_{cat} \approx 0.50g$)

The TPO of unsupported cobalt metal is characterised by two oxygen consumption maxima occurring at 300 and 580°C, corresponding to the sequential oxidation of metallic cobalt to CoO and to Co_3O_4 (reactions 1 and 2). At 870°C a thermal reduction of Co_3O_4 to CoO

occurs with a stoichiometric release of oxygen (reaction 3). The stoichiometry of the cobalt oxidation reaction and thermal reduction during TPO is illustrated below.

$$Co + \tfrac{1}{2} O_2 \longrightarrow CoO \qquad (1)$$

$$3\ CoO + \tfrac{1}{2} O_2 \longrightarrow Co_3O_4 \qquad (2)$$

$$Co_3O_4 \longrightarrow 3\ CoO + \tfrac{1}{2} O_2 \qquad (3)$$

From the reaction stoichiometry, the ratio of oxygen uptake caused by reactions 1 and 2 relative to the oxygen release caused by reaction 3, should be 4. The ratio of peak areas corresponding to oxygen uptake and oxygen release during TPO was 4.07, which confirms the reaction stoichiometry during the experiment. The TPO calibration procedure and calculation of % reduction can be seen in Appendix II.

In the case of supported cobalt catalysts, the degree of reduction may be limited due to interaction with the support. After hydrogen reduction, cobalt may be present as zerovalent cobalt, as unreduced divalent cobalt species that can be oxidised and as divalent cobalt-support species, which cannot be oxidised. The presence of residual trivalent cobalt species after reduction at 500°C is highly unlikely [van't Blik and Prins, 1986] and should therefore not influence the TPO calculations.

The ratio of oxygen uptake to the oxygen release peak will be between 1 and 4, depending on the extent of reduction. A ratio of 1 indicates that the cobalt species present after hydrogen reduction are divalent in nature and therefore the oxygen uptake is the same as the oxygen release (reactions 2 and 3). A ratio of 4 indicates complete reduction of the supported cobalt.

The high temperature oxygen release peak corresponds to the oxygen release from all the trivalent species present on the catalyst, excluding the cobalt species that could not be oxidised to trivalent cobalt. These non-oxidisable species are probably in the form of a stable cobalt support species. Knowing the total content of cobalt on the catalyst sample and by measuring the amount of high temperature oxygen release, the extent of cobalt support formation can be quantified.

Three different types of cobalt species were observed from the TPO measurement:

Zerovalent cobalt:	the amount of metallic cobalt after reduction
Oxidisable divalent cobalt:	the amount of residual unreduced cobalt that has not been reduced by 500°C but can be oxidised during TPO
Non-oxidisable divalent cobalt:	the amount of cobalt that cannot be reduced by 500°C and cannot be oxidised up to 1000°C

3.4.2 Adsorptive Characterisation Techniques

Most catalysts of practical importance are porous and possess large specific areas. Although the catalytic activity may not be directly related to the total surface, the determination of surface area is considered to be an important requirement in catalyst characterisation.

Catalyst particles present a size distribution that can be very narrow or very broad. Hydrogen chemisorption together with transmission electron microscopy can give an approximation of both particle size and shape.

3.4.2.1 Hydrogen Chemisorption

Hydrogen chemisorption is the recommended as the most reliable technique to measure cobalt crystallite size in Co/SiO_2 catalysts [Reuel and Bartholomew, 1984]. The chemisorption of hydrogen is highly activated, i.e. a larger amount of hydrogen adsorbs with increasing temperature. The degree of activation increases with decreasing metal loading and increasing amount of metal support interaction. Thus under the appropriately selected conditions, hydrogen yields a monolayer surface coverage for supported cobalt catalysts.

The cobalt dispersion on the 5% Co/SiO_2 catalysts was measured by hydrogen chemisorption at 100°C assuming a 1:1 H:Co surface stoichiometry. These measurements were carried by using a Pyrex glass volumetric adsorption apparatus: Micromeritics ASAP 2000, capable of 0.13 Pa dynamic vacuum. The catalyst was reduced in a 60 ml (STP)/min H_2 stream. The time and temperature were the same as the pre-treatment for Fischer-Tropsch reaction, i.e.

10°C/min to 200°C and then kept for 4 hours. The reduction took place *in situ*, to prevent any oxidation of cobalt due to atmospheric exposure.

After reduction, the reactor was evacuated for 4 hours, 2 hours at 200°C and another 2 hours, while cooling down to 100°C. Evacuation is to remove any residual adsorbed hydrogen or water present on the catalyst surface, due to the activation procedure. Chemisorption isotherms were measured at four hydrogen pressures between 15 and 46 kPa. These isotherms can be extrapolated to zero pressure to calculate the total chemisorption uptakes when the catalyst surface reached total saturation. The Langmuir isotherm should be fitted to the data to obtain the saturation volume if complete saturation was not reached. A sample calculation is given in Appendix III.

3.4.3 Spectroscopic Characterisation Techniques

3.4.3.1 Transmission Electron Microscopy

Electron microscopy offers the advantage of allowing the direct observation of catalyst morphology with magnification tuneable in the range of $10^{-4} - 10^{-10}$ m.

The catalyst samples were crushed and wetted with a few drops of distilled water. Copper grids with a thin film of carbon acting as a support for the specimen were floated on the droplets of the sample. Excess sample was blotted with filter paper and the sample was allowed to dry.

The samples were viewed in bright field mode in a JEOL 200CX transmission electron microscope using an acceleration voltage of 200kV.

The cobalt particles were visible as darker units on the silica grains. The magnification used was from 20 000 times to 100 000 depending on the cobalt particle size on the catalyst sample.

3.4.3.2 Atomic Absorption Spectroscopy

Atomic absorption spectroscopy is a useful tool in determining the catalyst composition. Each atom emits a characteristic spectrum. The spectrum consists of a series of densely spaced spectral lines. This provides the basis for spectrographic analyses of the composition of the vaporised mixture of atoms.

Atomic absorption spectroscopy (AAS) was used to determine the cobalt content of the catalyst. 0.2g-0.3g of the reduced cobalt catalyst was wetted with a few drops of deionozed water. 4 ml of cold 40% HF was added and left overnight for complete digestion. The mixture was then diluted with dionised water to obtain a Co ppm value that lies in the optimum range of the using a Varian Spectra AA-30 spectrometer (1-200 μg/ml). Only a few interferences have been observed for cobalt in an air-acetylene flame. Ni, Cr, W in concentrations of 1000 μg/ml, Si; 200 μg/ml and Cu, Mo 500 μg/ml have been shown to interfere with cobalt readings in an air-acetylene flame [Welz, 1976]. Ni, Cr, W, Cu and Mo were not present on the catalyst sample.

Calibration was done with cobalt nitrate in solution with and without HF added. Standards were made up to 50 mg/l, 80 mg/l, 100 mg/l and 150 mg/l. A sample calculation of the AAS results can be found in Appendix IV.

3.5 Fischer-Tropsch Synthesis

The Fischer-Tropsch synthesis converts CO and H_2 into hydrocarbon chains over a metal catalyst. The process can be performed in a fixed bed or slurry reactor on lab scale.

3.5.1 Experimental Set-up

1g of catalyst (35-60 mesh) was tested under Fischer-Tropsch conditions in a fixed bed reactor at a reaction temperature of 190°C and total pressure of 5 bar, WHSV of 200 hr^{-1} (See Appendix VII) and H_2:CO molar ratio of 2:1. The reactor was operated at low CO conversions (<15%), to achieve a pseudo-gradientless behaviour [Rothaemel *et al.*, 1997].

A flowsheet of the experimental set-up is shown in Figure 3-4. The flowrate of CO and H_2 was controlled by a Brooks and a Unit mass flow controller to be 3.5 ml (STP)/min and 7 ml (STP)/min. Calibration of the mass flow controllers can be seen in Appendix V. The mixer in the reactant feed line consisted of a ¼ inch tube filled with small glass beads to ensure proper mixing of the feed. The function of the 4-way valve was to switch from the inert Ar gas flowing over the catalyst bed to syngas at the start of reaction. Argon flowrate automatically controlled by the pressure regulator and a needle valve. When the syngas was flowing over the catalyst bed, argon was bypassed and served as a make-up gas to maintain a total pressure of 5 bar in the reactor.

The catalyst bed was packed in the isothermal region directly above the glass fritt (see Figure 3-5). Silonised glass wool was placed above the catalyst bed to keep the bed in place. The synthesis gas entered at the top of the reactor and was then passed over the catalyst bed. The by-pass line entered at the side of the glass reactor and was mixed with the syngas and products at the reactor exit. The temperature inside the catalyst bed was measured with a thermocouple. The glass reactor was kept in place with a fitting, sealed by an o-ring. The top of the reactor was tightened and sealed by a copper seal.

The catalyst was heated up at 10°C/min in hydrogen (60 ml (STP)/min) to 200°C for 4 hours prior to FTS to re-reduce the surface oxide that formed when the catalyst was exposed to the atmosphere. The catalyst was then cooled down to 190°C in argon, while the syngas on bypass and internal standard flowrates were stabilised.

A stainless steel U-tube filled with glass beads acted as a wax trap. Setting the wax trap at 180°C ensured that the heavy waxes would be trapped and would not to settle in the exit line and eventually cause a blockage. The reactor exit line was set at 200°C to maintain a product mixture in the gas phase.

Cyclohexane served as the internal standard in the analyses of the FTS product spectra. N_2, the carrier gas for cyclohexane, was diverted through a cylohexane saturator at 1.5 ml (STP)/min. A 0.1 ml (STP)/min cyclohexane flow was obtained by setting the temperature of the saturator at 10°C.

FTS product samples were taken with the ampoule sampling technique. Samples were taken at 10 min., 30 min., 1 hr., 2 hrs. and 24 hrs. after the start of the reaction.

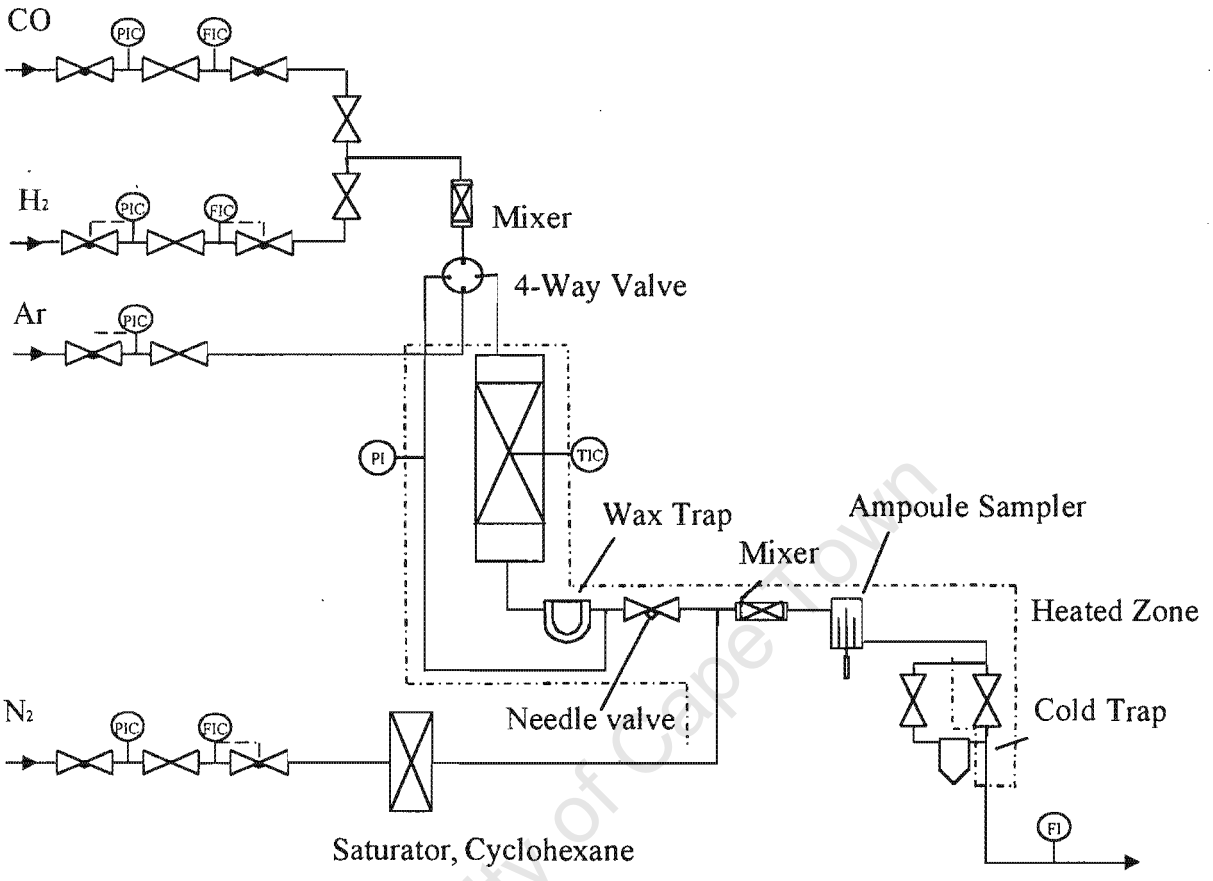

Figure 3-4: The flowsheet of the fixed bed reactor

The exit gas was passed through a cold trap set at room temperature to entrap hydrocarbons in the liquid phase at room temperature. The total flowrate was measured with a bubble meter.

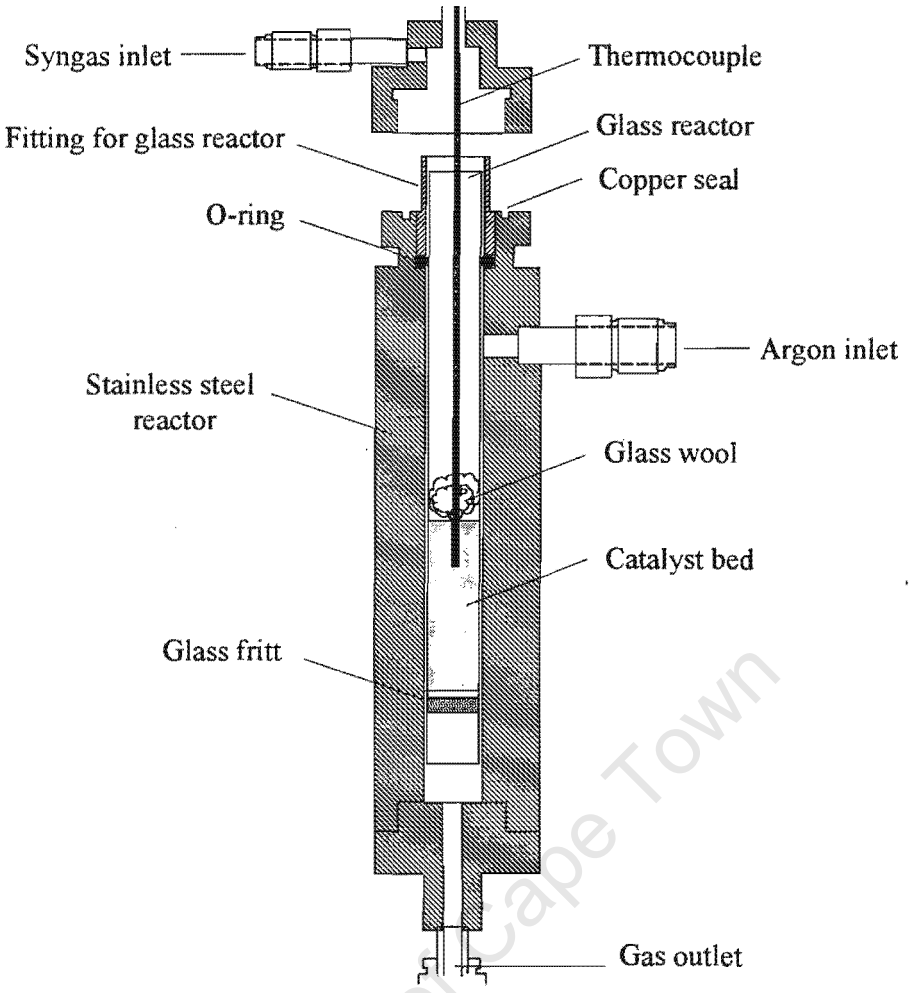

Figure 3-5: The glass reactor

3.5.2 Analyses

The products were separated with gas chromatography, using a 100m RH-1 (PONA equivalent) column 0.32 ID x 1.00 µm, and analysed with a flame ionisation detector. The temperature programme started at 40°C and was kept for 8 minutes, heated up at 5°C/min and was kept at 270°C for 40 minutes. The total time for the temperature programme to run was 94 minutes. This allowed enough time for the heavy hydrocarbons to flush through the column. It was not possible to lower the temperature to sufficient sub-ambient temperatures that is required for the separation of C1-C3 hydrocarbons.

CHAPTER 4

Results

4. RESULTS

4.1 Introduction

The effect of several treatments on the silica supported cobalt catalyst for Fischer-Tropsch synthesis was investigated. With the aim to create silica supported cobalt catalysts with different crystallite sizes, the catalysts were calcined at different temperatures or directly reduced with different heating rates. A portion of these catalysts was then water-treated, prior to Fischer-Tropsch synthesis, and then compared with the original catalyst, both with regard to their physical and chemical properties and their characteristics in Fischer-Tropsch synthesis.

4.2 Catalyst composition

The catalysts were prepared by incipient wetness technique. Cobalt was loaded unto the silica in the form of cobalt nitrate. The amount of cobalt nitrate used was calculated in order to obtain 5wt % cobalt on silica. To test if 5wt% Co was indeed loaded, spectroscopic techniques such as AAS and ICP were employed to analyse the cobalt content.

4.2.1 Elementary Analyses

A cobalt lamp and an air-acetylene flame were utilised to determine the amount of cobalt present in the sample. 0.2-0.3g of catalyst was digested with 4ml of 40% cold HF and diluted with deionised water. The solution was transferred to a polypropylene volumetric flask and made up to 100 ml with deionised water. Further dilution with deionsed water took place according to the optimum Co ppm range of the Varian atomic adsorption spectrometer.

Calibration was done with and without adding HF to the standard solution. HF showed no interference with the Co in the air-acetylene flame as is expected. Ni, Cr, W in concentrations of 1000 μg/ml, Si in concentrations of 200 μg/ml and Cu, Mo in concentrations of 500 μg/ml have been shown to interfere with cobalt readings in an

air-acetylene flame [Welz, 1976]. The silica-support blank sample showed no interference with the cobalt reading in this case.

Table 4-1: wt % Co in the $Co/SiO_2(N)$ catalyst determined by AA and ICP[1)]

Catalyst[2)]	*AAS* *wt % Co*	*ICP* *Wt % Co*
$Co/SiO_2(N)$	3.98	4.50
$Co/SiO_2(N)$-w	3.95	4.70
$Co/SiO_2(N)$-s	4.16	4.84
$Co/SiO_2(N)$-s-w	4.60	5.35
$Co/SiO_2(N)$-c4	4.38	4.76
$Co/SiO_2(N)$-c4-w	4.29	5.07
$Co/SiO_2(N)$-s-c4	3.90	4.63
$Co/SiO_2(N)$-s-c4-w	4.16	4.94
$Co/SiO_2(N)$-c6	4.14	-
$Co/SiO_2(N)$-c6-w	4.15	-
Silica	0.00	-

1) wt.% was taken on reduced wet catalyst sample. Assume all Co present as metallic cobalt.
2)-s: slow heating rate
-c4: calcined at 400°C
-w: water-treated

The cobalt content of the catalysts lies between 3.95 and 4.6 wt % (AAS) and 4.5 and 5.35 wt % (ICP). Each catalyst was prepared separately. For a reference, two samples of a $Co/SiO_2(N)$ were analysed by AA and ICP, and the values show these instruments to be accurate. AAS: 3.98 and 3.95 wt %, while ICP gave 4.72 and 4.8 wt % Co/SiO_2. The variation in the cobalt loading (see Table 4-1) is due to the experimental preparation procedure and is not a function of the instrument.

The reason most of the values are beneath $5\%Co/SiO_2$ is because of the hydrophilic behaviour of cobalt nitrate. The amount of cobalt nitrate weighed was based on the assumption of 6 moles of crystal water per mole of cobalt nitrate. Due to the hygroscopic nature of cobalt nitrate the amount of water associated with it can be higher and thus the final cobalt loading obtained can be lower than 5 wt.%.

The ICP values are constantly higher than the results from the AAS. Because the AAS was done in the Department of Chemical Engineering and the calibration procedure was checked several times, it was decided to use these values in the further calculations.

4.3 The Effect of Calcination Temperature

Three different catalysts were prepared by calcining at different temperatures, each at a different calcination heating rate. $Co/SiO_2(N)$-c4 was heated up to 400°C in air at 10°C/min, where $Co/SiO_2(N)$-s-c4 was also calcined at 400°C, but with a slower calcination heating rate of 0.5°C/min. $Co/SiO_2(N)$-c6 was calcined at 600°C and heated up at 20°C/min. All three catalysts were then reduced in pure hydrogen at 400°C for 16 hours after being heated up from room temperature with a heating rate of 10°C/min.

Calcining in air at 400°C causes the formation of larger cobalt crystallites [Coulter and Sault, 1995]. Metal support interaction is initiated during the decomposition of the nitrate precursor in the drying phase already.

Calcination might result in diffusion of Co^{2+} species into the support where they occupy tetrahedral or octahedral lattice sites [Chin and Hercules, 1982]. With more Co^{2+} species migrating into the support, less become available for reduction to the metal. Less active sites are then expected to be formed.

4.3.1 Particle Size Measurement

Hydrogen chemisorption and transmission electron microscopy were used to determine the crystallite size of the cobalt particles on the silica support.

The two techniques are focussing on different variables of the particle size distribution. Hydrogen chemisorption measurements are based on a H_2 volume chemisorbed on a 0.5g of 5%$Co/SiO_2(N)$ catalyst sample. Assuming the area of one Co atom in fcc structure is 6.59 $Å^2$, the average particle diameter can be calculated.

Transmission electron microscopy looks at high magnification at a very small sample weight of the catalyst.

4.3.1.1 Hydrogen Chemisorption

Hydrogen chemisorption measurements were performed at 100°C, due to the activated nature of hydrogen chemisorption on cobalt [Reuel and Bartholomew, 1984]. Prior to hydrogen chemisorption, the catalyst was re-reduced *in situ* with hydrogen (±100 ml (STP)/min) at 200°C for 4 hours and then evacuated for 2 hrs at 200°C and 2 hours at 100°C, to remove any residual hydrogen.

The chemisorption data and the calculated average particle size for the catalyst with different calcination procedures are given in Table 4-2.

Table 4-2: Volume H_2 absorbed, surface area, dispersion and average particle diameter of silica supported cobalt catalysts, calcined at different temperatures

Catalyst	*Linear back-extrapolation*			
	V_{H2}/g_{cat}	A_s	D[4]	d_{avg}
	(cm^3/g_{cat})	(m^2/g_{cat})	(%)	(nm)
$Co/SiO_2(N)$-c6[1]	0.253	0.94	2.8	28.0
$Co/SiO_2(N)$-c4[2]	0.358	1.32	5.4	22.5
$Co/SiO_2(N)$-s-c4[3]	0.305	1.12	4.1	21.0

[1] -c6: calcined at 600°C heating rate 20°C/min
[3] -c4: calcined at 400°C, heating rate 10°C/min
[3] -s-:slow heating rate (0.5°C/min)
[4] D = dispersion of metal atoms, see Appendix III for sample calculation

The average particle size increases with increase in calcination temperature. This is in agreement with the findings of Belambe *et al.* (1997). Calcining at 600°C resulted in d_{avg} of 28 nm and calcining at 400°C gave an average particle size of ± 22 nm. These obtained dispersions and particle sizes are similar to those obtained by Niemelä *et al.* (1997).

Increasing the calcination temperature form 200°C to 500°C resulted in small changes in the temperature programmed reduction spectra, see Figure 4-1. The low temperature peak shifted to higher temperatures with the increase of calcination temperature. This shift in the peak could be due to a weak metal support interaction that increases with a higher calcination temperature. If the reduction process is auto-catalytic, i.e. the reduced metal catalyses the further reduction, an increase in reduction temperature is expected for larger crystallites. The area of hydrogen consumed > 700 K becomes larger with increase in calcination temperature indicating a higher strong-metal-support-interaction with increase of calcination temperature (see Table 4-3).

Table 4-3: Hydrogen consumption during TPR and reduction peak temperatures for calcined catalysts

Catalyst	*Fraction of H_2 consumption below 700K*	*Fraction of H_2 consumption above 700K*	*Total H_2: Co ratio (mole: mole)*	T_{low} *(K)*	T_{high} *(K)*
Calcined at 500°C	0.51	0.48	0.947	630	1128
Calcined at 400°C	0.57	0.43	0.920	625	1120
Calcined at 300°C	0.59	0.41	0.894	618	1098
Calcined at 200°C	0.49	0.51	0.940	613	943

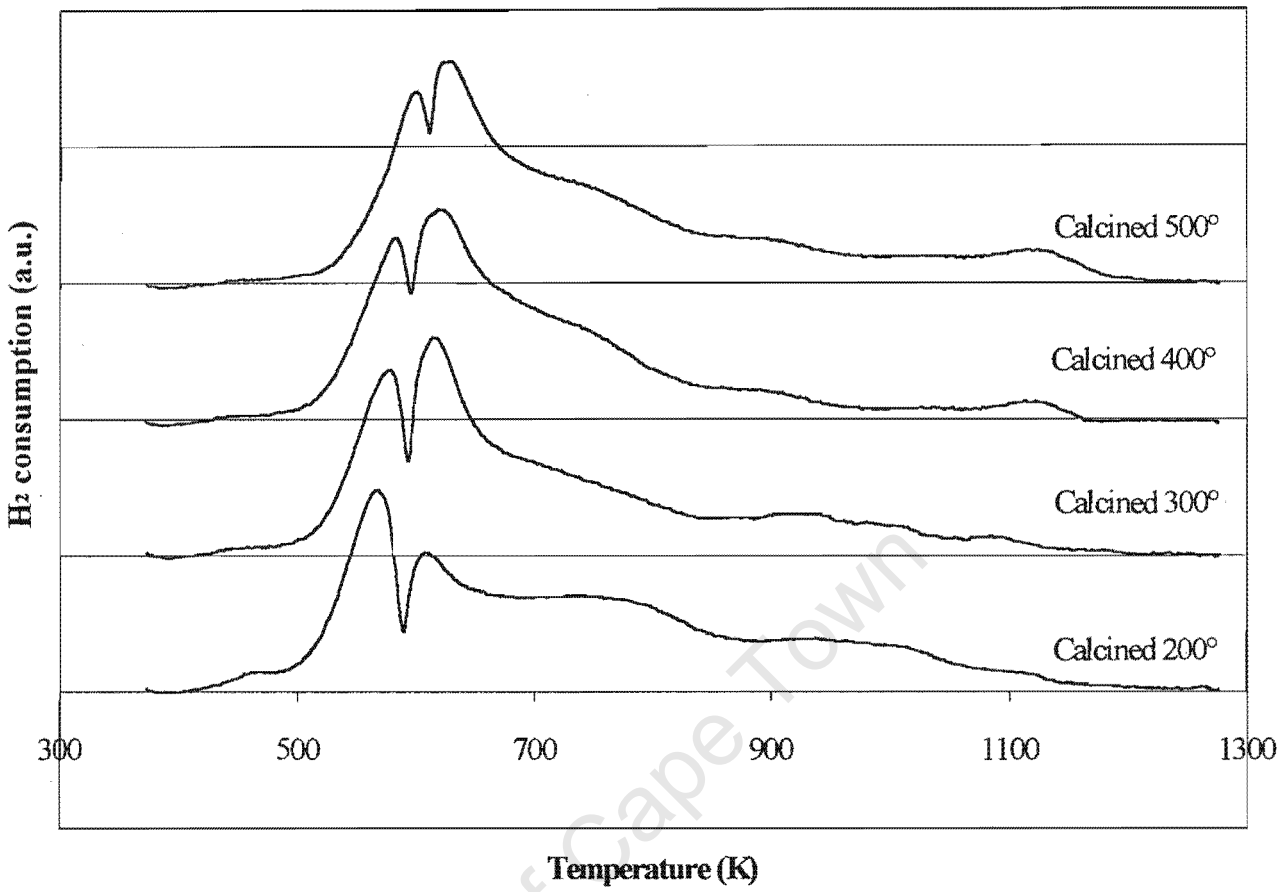

Figure 4-1. Effect of calcination temperature on the TPR spectra of Co/SiO_2 catalysts. (Calcination in air in muffle furnace, heating rate 10°C/min. Reducing gas = 60 ml (STP)/min 5% H_2/N_2, temperature programming rate = 10°C/min, $m_{cat} \approx 0.15g$)

These results are in agreement with the findings of Sewell (1996).

Co is known to undergo a two step reduction. Co_3O_4 first reduces to CoO and then to cobalt metal. These two distinct peaks can be seen in the TPR spectra of the catalyst calcined at 400°C with a normal heating rate (10°C/min). Hydrogen consumption above 700K can be attributed to strong-metal-support-interaction.

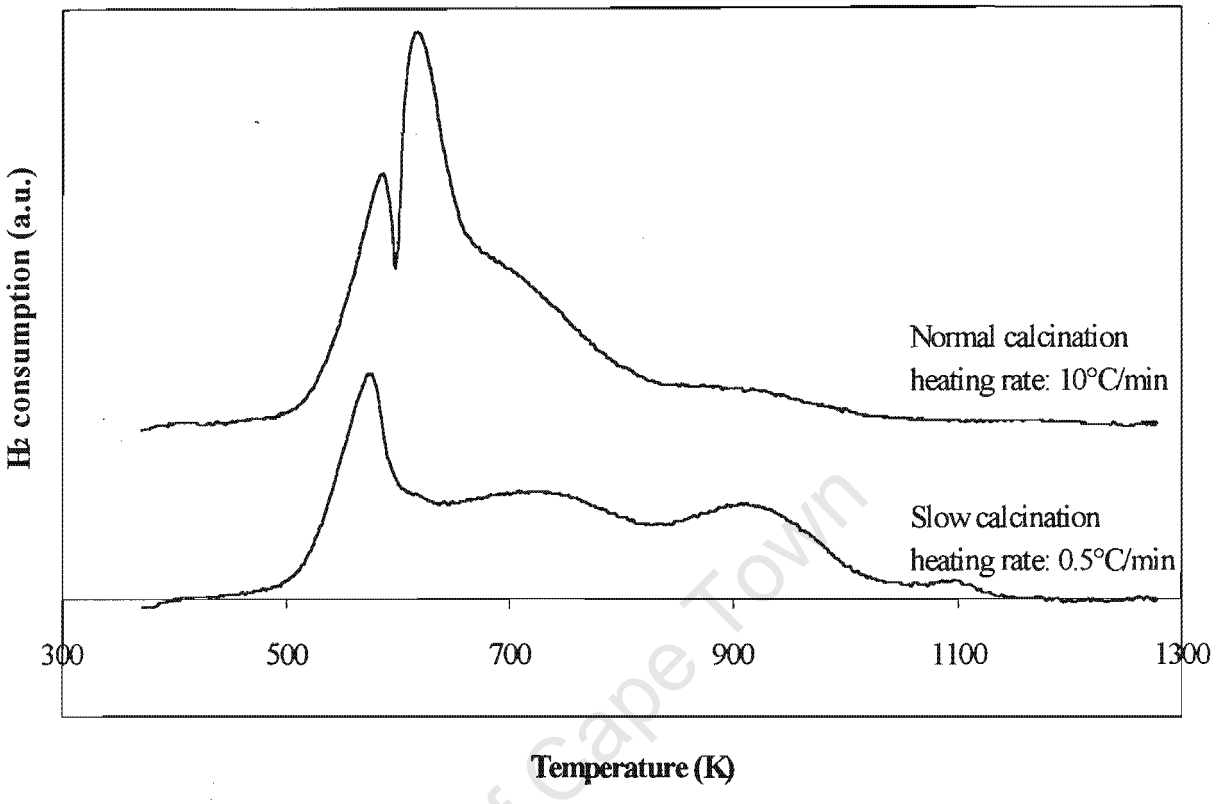

Figure 4-2: TPR spectra of the effect of calcination heating rate on the Co/SiO_2 catalysts. (Calcination in air. Reducing gas = 60 ml (STP)/min 5% H_2/N_2, temperature programming rate = 10°C/min, $m_{cat} \approx 0.15g$)

Only the first reduction peak is visible in the TPR spectra of the catalyst calcined with a slow heating rate (0.5°C/min) (see Figure 4-2). The second reduction peak is broader and not as intense when compared to normal calcination heating rate. The hydrogen consumption above 700K increased indicating a higher amount of strong metal support interaction with a slower calcination heating rate (see Table 4-4).

Table 4-4: Hydrogen consumption during TPR and reduction peak temperatures for catalysts calcined at different heating rates

Catalyst	*Fraction of H_2 consumption below 700K*	*Fraction of H_2 consumption above 700K*	*Total H_2: Co ratio (mole: mole)*	*T_{low} (K)*	*T_{high} (K)*
Calcined at 400°C 10°C/min	0.66	0.32	0.116	620	892
Calcined at 400°C 0.5°C/min	0.46	0.54	0.832	582	923

4.3.3 Temperature Programmed Reduction of Reduced Catalysts

After the calcination step, the catalysts calcined at 400°C (heating rate 10°C/min), calcined at 400°C (heating rate 0.5°C/min) and calcined at 600°C (heating rate 20°C/min) were all reduced the same way. The reduction was in pure hydrogen and the temperature was raised from room temperature to 400°C at 10°C/min. The temperature was kept at 400°C for 16 hours. The TPR spectra after reduction look fairly similar for the three catalysts (see Figure 4-3). The low temperature peak still present after the catalyst reduction is due to a surface oxidation that occurs when the reduced catalyst is exposed to air at room temperature.

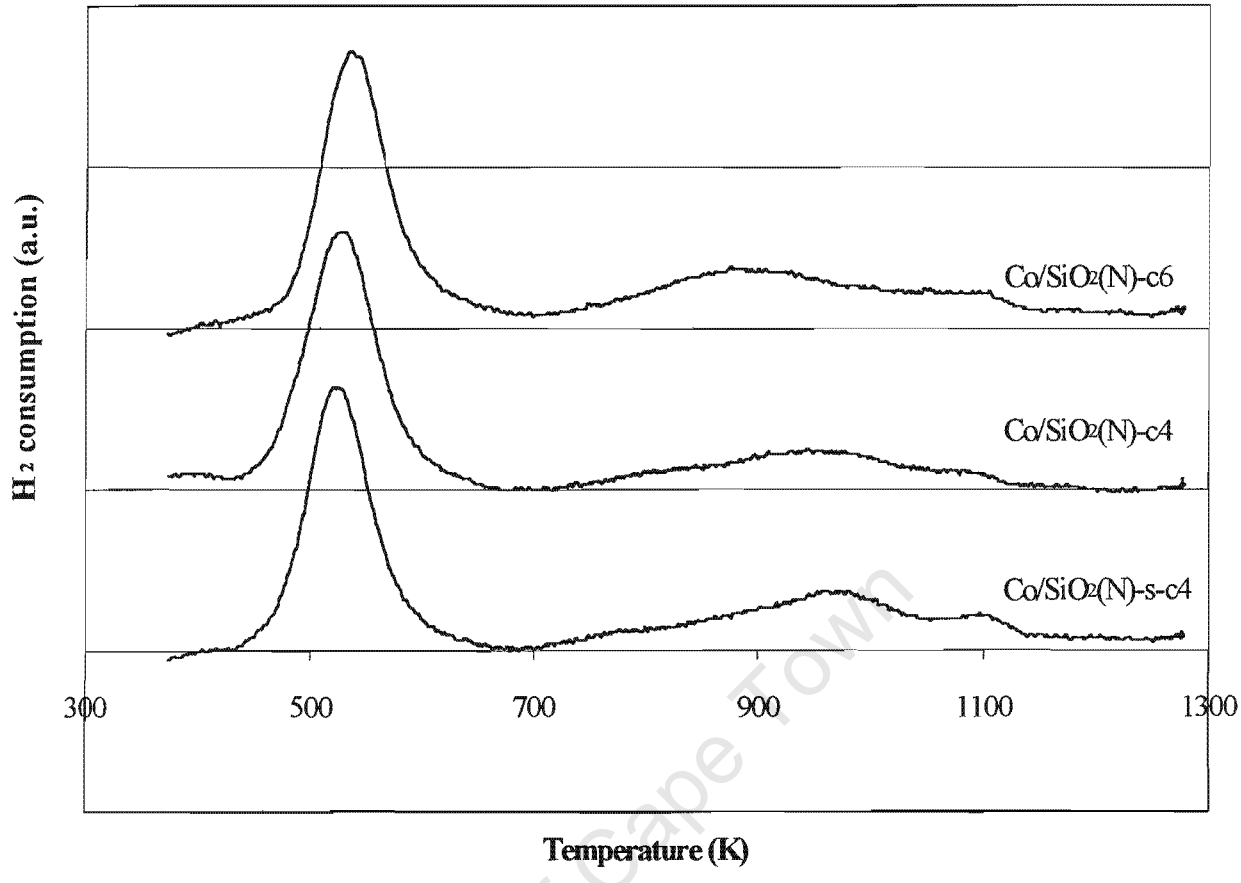

Figure 4-3: Effect of calcination heating rate on the reduction behaviour of reduced Co/SiO_2 catalysts. (Calcination in static air in muffle furnace. Catalysts reduced in hydrogen prior to TPR. TPR reducing gas = 60 ml (STP)/min 5% H_2/N_2, temperature programming rate = 10°C/min, $m_{cat} \approx 0.15g$)

Table 4-5 gives the H_2 consumption and the peak temperatures at which the rate of reduction is a maximum, seen also in Figure 4-3. The low temperature peak shifts to a higher temperature as the calcination temperature and heating rate increases. The opposite happens with the high temperature peak. As the calcination temperature increases the high temperature peak shifts to a lower temperature.

Table 4-5: Hydrogen consumption during TPR and reduction peak temperatures for calcined and subsequently reduced catalysts. Calcination in muffle furnace (static air). Reduction at 400°C for 16 hours with heating rate of 10°C/min.

Catalyst	*Fraction of H_2 consumption below 700K*	*Fraction of H_2 consumption above 700K*	*Total H_2: Co ratio (mole: mole)*	T_{low} *(K)*	T_{high} *(K)*
$Co/SiO_2(N)$-c6[1)]	0.53	0.47	0.728	542	895
$Co/SiO_2(N)$-c4[2)]	0.70	0.30	0.562	533	959
$Co/SiO_2(N)$-s-c4[3)]	0.57	0.43	0.700	526	970

[1)] -c6: calcined at 600°C heating rate 20°C/min
[3)] -c4: calcined at 400°C, heating rate 10°C/min
[3)] -s-: slow heating rate (0.5°C/min)

The low temperature peak (H_2 consumption below 700K) is due to a surface oxidation that occurs when the reduced catalyst is exposed to the atmosphere at ambient conditions. When the calcination temperature increases and the cobalt particles agglomerate, less cobalt surface becomes available for this oxidation, and therefore causes a decrease in low temperature hydrogen consumption as seen in Table 4-5.

The high temperature hydrogen consumption increases with higher calcination temperature. Cobalt species, which are reduced at temperatures above 700K in the TPR of the reduced catalyst, can be attributed to unreduced Co-species. The amount of H_2 consumed above 700K is thus an indication of the degree of reduction. A high H_2 consumption above 700K corresponds to a lower degree of reduction.

4.3.4 Temperature Programmed Oxidation of Reduced Catalysts

The extent of reduction of a supported cobalt catalyst is difficult to determine by only using TPR, due to the unknown stoichiometry of the catalyst reduction. By using a combined TPR/TPO technique, it is possible to determine the extent of cobalt reduction and to estimate the extent of cobalt-support species formation [Sewell *et al.*, 1996]. A full description of the technique is given in Chapter 3.4.

A typical TPO spectrum of Co/SiO_2 is given in Figure 4-4. The spectrum indicates oxygen uptake and release of the reduced Co/SiO_2 catalyst in a 60 ml (STP)/min 2%

O_2/He stream as the temperature was raised from 40 to 1000°C. The reduction of the catalyst took place in a 60 ml (STP)/min 5%H_2/N_2 stream heated up from room temperature to 200°C at 10°C/min and kept for 4½ hours prior to the TPO.

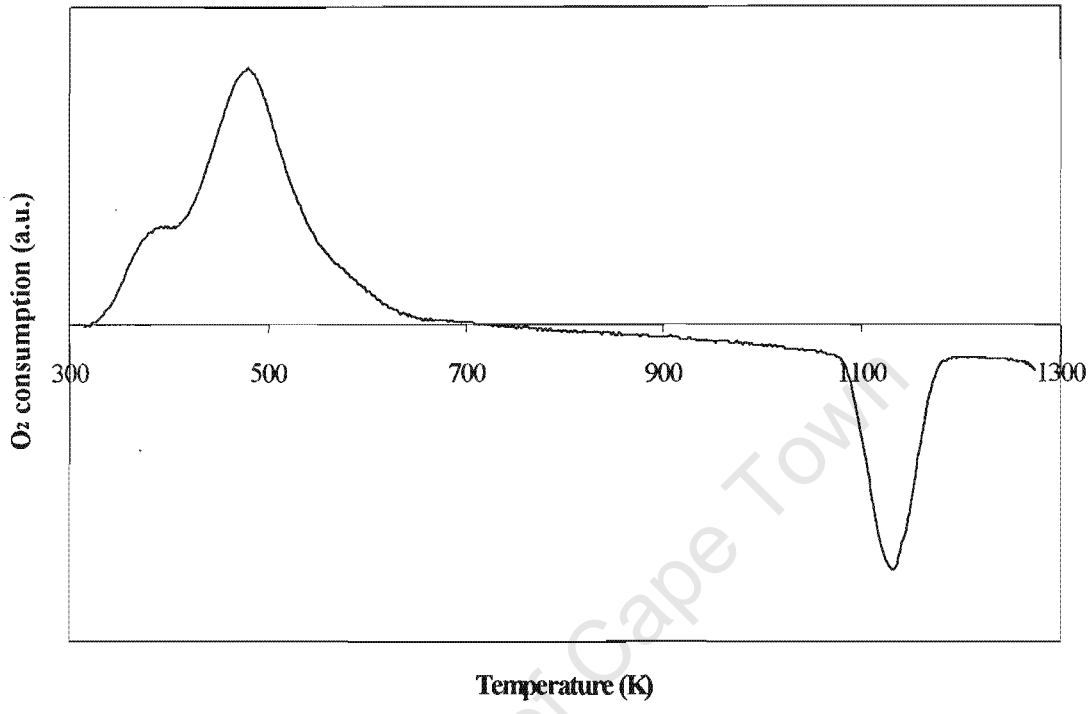

Figure 4-4: A typical TPO spectrum of the Co/SiO_2 catalysts reduced at 200°C (10°C/min) for 4½ hours prior to TPO. Oxidising gas = 60 ml (STP)/min 2% O_2/He, temperature programming rate = 10°C/min, $m_{cat} \approx 0.5$g)

The first peak, including the shoulder peak, is oxygen consumed due to the oxidation of Co^0 to Co^{2+} and subsequently the oxidation of Co^{2+} to Co^{3+}. At high temperatures Co_3O_4 undergoes a thermal reduction to CoO. This can be seen as the high temperature oxygen release peak at 1115 K, (see Figure 4-4.)

Table 4-6: Composition and metal oxidation temperatures during TPO for $Co/SiO_2(N)$, calcined at different temperatures.

Catalyst	*Zerovalent Co (mole %)*	*Oxidisable Co^{2+} (mole %)*	*Non-oxidisable Co^{2+} (mole %)*	*$T_{oxidation}$ (K)*
$Co/SiO_2(N)$-c6[1)]	93	4	3	490
$Co/SiO_2(N)$-c4[2)]	-	-	-	-
$Co/SiO_2(N)$-s-c4[3)]	88	5	6	471

[1)] -c6: calcined at 600°C heating rate 20°C/min
[3)] -c4: calcined at 400°C, heating rate 10°C/min
[3)] -s-:slow heating rate (0.5°C/min)

The slow calcination heating rate resulted in a smaller crystallite size (see Table 4-2). The catalysts exhibit a very similar degree of reduction (see Table 4-6).

4.3.5 Fischer-Tropsch Synthesis

The catalysts were tested under Fischer-Tropsch conditions (190°C and 5 bar) in a fixed bed reactor. H_2: CO was fed in a ratio of 2:1 at 10.5 ml (STP)/min over 1g of 5 wt.% Co/SiO_2 catalyst. Samples were taken at 10 min., 30 min., 1 hr., 2 hrs. and 24 hrs. after start of the reaction. Steady state was assumed to be reached after 24 hours.

CO hydrogenation activity is expected to decrease when the cobalt catalyst undergoes high temperature treatment. High temperature treatment (>400°C) can result in cobalt crystallite agglomeration (see Table 4-2) that would lead to a decrease in the number of active sites [Niemalä *et al.*, 1997].

4.3.5.1 Hydrocarbon Yield

The hydrocarbon yield was measured as a function of time on stream. The yield of hydrocarbons increased during the first hour (see Figure 4-5). Subsequently a decrease in the activity of all catalysts is observed.

A decrease in hydrocarbon yield with increase in calcination heating rate and calcination temperature is observed. $Co/SiO_2(N)$-s-c4 and $Co\text{-}SiO_2(N)$-c4 exhibited a

similar hydrocarbon yield and a similar trend with time on stream. The catalyst calcined at 600°C with a calcination heating rate of 20°C/min (Co/SiO_2-c6) had the lowest hydrocarbon yield with TOS, of the three catalysts.

After 24 hours the hydrocarbon yield for Co/SiO_2(N)-s-c4 was 2.86 C%, for Co/SiO_2(N)-c4 was 2.25 C% and for Co/SiO_2(N)-c6 was 1.7 C%.

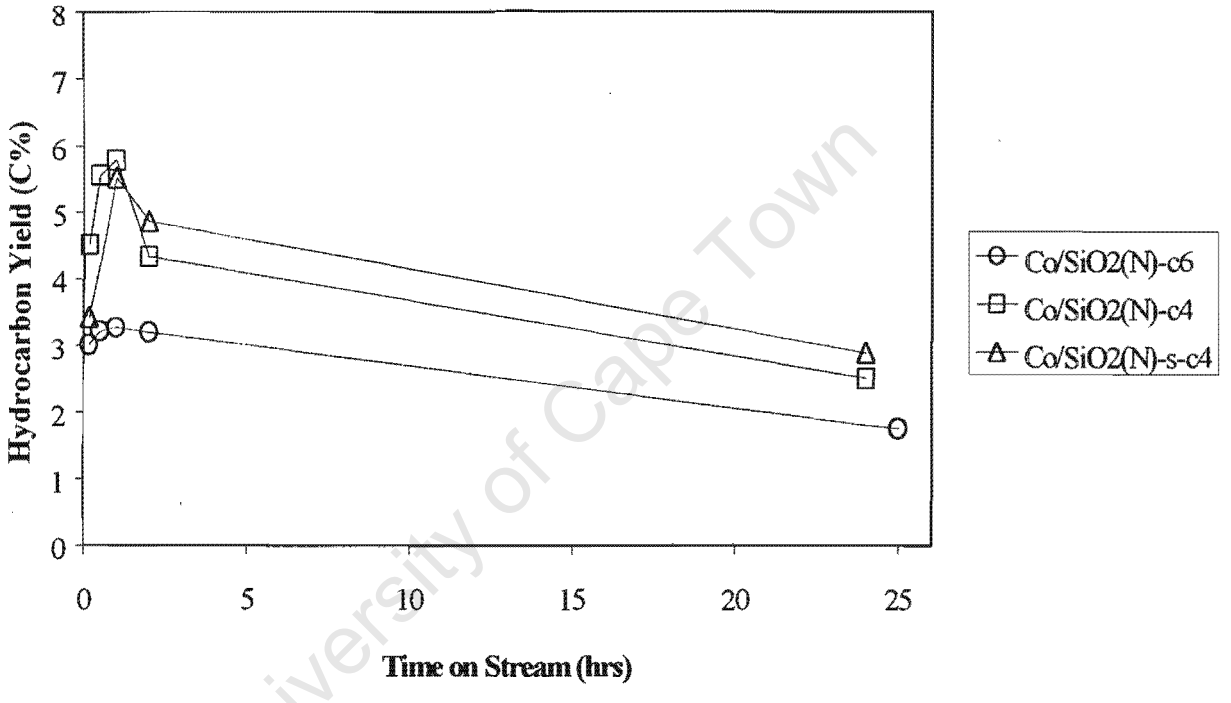

Figure 4-5: The hydrocarbon yield with time on stream for the Co/SiO_2(N) catalyst calcined at different temperatures.

4.3.5.2 Chain Growth Probability

The chain growth probability for the calcined catalysts range from α = 0.78 to 0.84 (Table 4-7). The samples were taken at 24 hours for Co/SiO_2(N)-c4 and Co/SiO_2(N)-s-c4 and at 25 hours for Co/SiO_2(N)-c6.

Table 4-7: The chain growth probability of the calcined catalysts

Catalyst	*Chain growth probability*
$Co/SiO_2(N)$-c6[1)]	0.78
$Co/SiO_2(N)$-c4[2)]	0.84
$Co/SiO_2(N)$-s-c4[3)]	0.78

[1)] -c6: calcined at 600°C heating rate 20°C/min
[3)] -c4: calcined at 400°C, heating rate 10°C/min
[3)] -s-: slow heating rate (0.5°C/min)

Fan *et al.* (1997) noticed that a higher calcination temperature (150-450°C) favored carbon-chain growth, resulting in a larger growth probability and low conversions. Belambe *et al.* (1997) concluded from their experiments that calcination did not affect the chain growth probability with the Ru promoted Co/Al_2O_3 catalyst and had only a minor effect on methane selectivity. Calcination only has an effect on the overall activity, but not on the intrinsic activity of the cobalt catalyst [Belambe *et al.*, 1997]. The calcination was in flowing air in the range of 200-400°C held for 10 hours, heated up at 1°C/min. Niemelä *et al.* (1997) observed higher reduction temperature treatment (300-450°C) not to influence the chain growth probability of Co/SiO_2.

4.4 The Effect of Reduction Heating Rate

Two catalysts were prepared by directly reducing the catalyst precursor in hydrogen. One catalyst was heated at 0.5°C/min ($Co/SiO_2(N)$-s) in 5%H_2/He and the other was heated at 10°C/min ($Co/SiO_2(N)$) in pure hydrogen. Both catalysts were reduced in pure hydrogen at 400°C for 16 hours. The reason for using a slow reduction heating rate is to control the exothermic step of the nitrate precursor decomposition (200-300°C). By controlling the heating rate and the composition of the reducing atmosphere (5%H_2/He), smaller Co crystallites have been reported to form [Iglesia, 1997]. The exothermic decomposition of the nitrate precursor, the oxidation of CoO to Co_3O_4 during oxidative treatments and high H_2O concentrations that develop during rapid reduction of oxides and nitrates by H_2 may lead to the agglomeration of cobalt particles and low metal dispersion.

4.4.1 Particle Size Measurements

To see the influence of the heating rate on the particle size, TEM and H_2 chemisorption were utilised to determine individual particle size and the average particle diameter.

4.4.1.1 Hydrogen Chemisorption

The effect of slow reduction heating rate on the cobalt particle crystallite size can be seen by calculating the mean particle diameter from the hydrogen chemisorption measurements. Prior to the hydrogen chemisorption measurement, the catalysts were re-reduced *in situ* at 200°C for 4 hours in hydrogen (100 ml (STP)/min) to reduce the surface oxide that formed when the catalyst was exposed to air at room temperature. The heating rate was 10°C/min.

Table 4-8: Volume H_2 adsorbed, surface area, dispersion and average particle diameter of silica supported cobalt catalysts, directly reduced at different heating rates

Catalyst	*Linear back-extrapolation*			
	V_{H2}/g_{cat}	A_s	$D^{3)}$	d_{avg}
	(cm^3/g_{cat})	(m^2/g_{cat})	(%)	(nm)
$Co/SiO_2(N)^{1)}$	0.418	1.5	4.4	18
$Co/SiO_2(N)$-s$^{2)}$	0.416	1.53	6.95	16

[1)] Directly reduced 10°C/min
[2)]-s: slow reduction heating rate (0.5°C/min)
[3)] D = dispersion of metal atoms

By slowly heating (0.5°C/min) the nitrate precursor in a 5%H_2/He stream, a smaller average cobalt particle size (16 nm) is obtained than when the catalyst is reduced in the classic way (10°C/min) in pure hydrogen (18 nm). The dispersion increased from 4.4% to 6.95% when the reduction heating rate was slowed down.

4.4.1.2 Transmission Electron Microscopy

The catalysts were reduced in hydrogen (60 ml (STP)/min) heating up from room temperature to 400°C at 10°C/min and held for 16 hours. The samples were then

crushed, wetted and mounted on a carbon film supported by a copper grid. The crushed grains were viewed in bright-field mode in a JEOL 200CX transmission electron microscope using an acceleration voltage of 200kv.

The particles formed during a normal reduction heating rate (10°C/min) are about 50 nm, on the catalyst sample. When the reduction heating rate was slowed down to 0.5°C/min, smaller particles were formed (30 nm) (See Figure A8-2 in Appendix VIII).

4.4.2 Temperature Programmed Reduction

The two directly reduced catalysts show similar reduction behaviour (see Figure 4-6). The low temperature peak is a surface oxidation that occurs when the reduced catalyst is exposed to air. After 6 months the TPR of the $Co/SiO_2(N)$ catalyst was repeated. A larger shoulder peak to the low temperature hydrogen consumption peak is visible. This might be due to further oxidation of the catalyst due to prolonged exposure to air at room temperature.

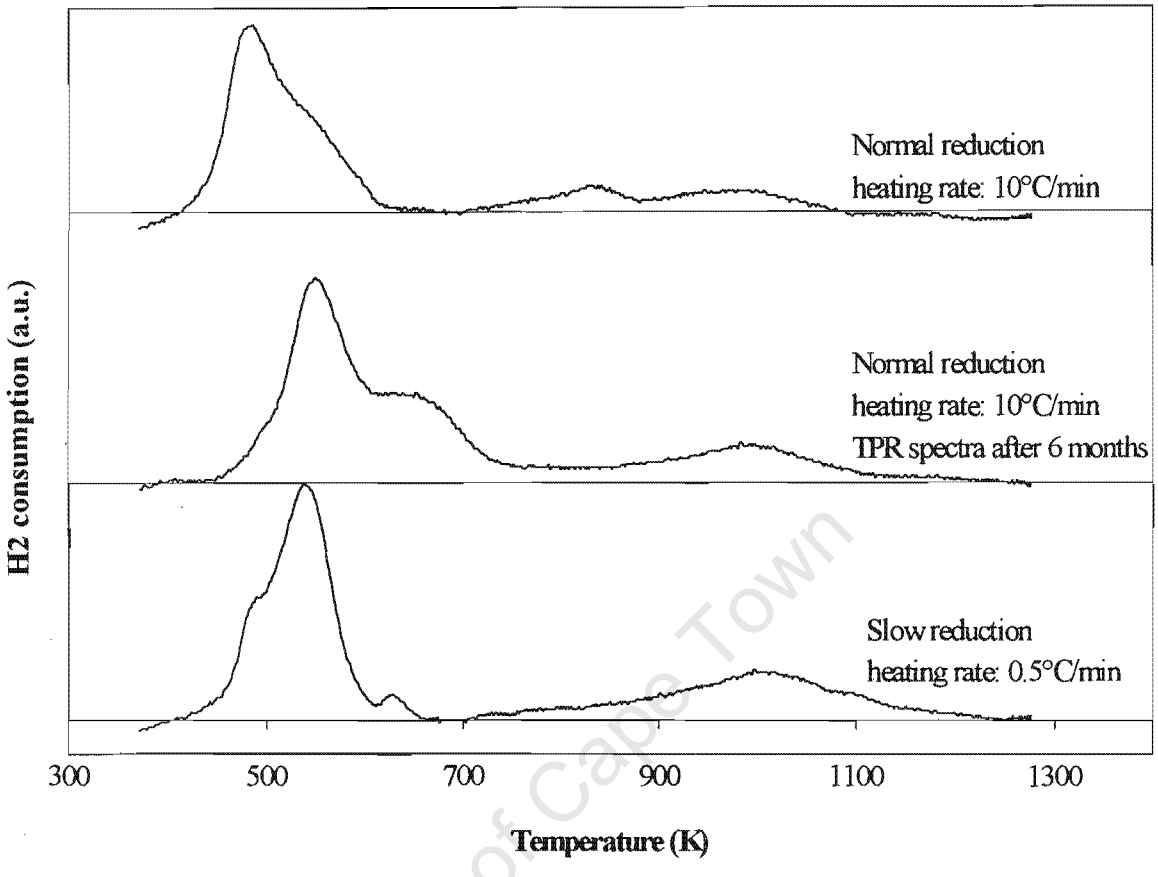

Figure 4-6: TPR spectra of the effect of reduction heating rate on the Co/SiO_2 catalysts. (Reducing gas = 60 ml (STP)/min 5% H_2/N_2, temperature programming rate = 10°C/min, $m_{cat} \approx 0.15g$)

Integration of the peaks corresponds to the amount of hydrogen consumed. According to the hydrogen consumption values (see Table 4-9), the catalyst prepared with a slow reduction heating rate exhibits a larger high temperature peak. The low temperature peak is slightly smaller for $Co/SiO_2(N)$-s than for $Co/SiO_2(N)$.

Table 4-9: Hydrogen consumption and peak maximum during for silica supported catalysts reduced at different heating rates

Catalyst	*Fraction of H_2 consumption below 700K*	*Fraction of H_2 consumption above 700K*	*Total H_2: Co ratio (mole: mole)*	*T_{low} (K)*	*T_{high} (K)*
$Co/SiO_2(N)$[1)]	0.77	0.23	0.522	485	992
$Co/SiO_2(N2)$[2)]	0.73	0.27	0.648	546	1003
$Co/SiO_2(N)$-s[3)]	0.64	0.36	0.692	544	1008

[1)] Directly reduced 10°C/min
[2)] Directly reduced 10°C/min, TPR spectra after 6 months
[3)]-s: slow reduction heating rate (0.5°C/min)

4.4.3 Temperature Programmed Oxidation

The combined technique of TPR with TPO proves that cobalt forms a higher interaction with the support when the catalyst is slowly heated (0.5°C/min) in a 5%H_2/He atmosphere.

Table 4-10: Composition and metal oxidation temperatures during TPO for $Co/SiO_2(N)$, directly reduced with different reduction heating rates

Catalyst	*Zerovalent Co (mole %)*	*Oxidisable Co^{2+} (mole %)*	*Non-oxidisable Co^{2+} (mole %)*	*$T_{oxidation}$ (°C)*
$Co/SiO_2(N)$[1)]	90	1	9	478
$Co/SiO_2(N)$-s[2)]	88	9	3	482

[1)] Directly reduced 10°C/min
[2)]-s: slow reduction heating rate (0.5°C/min)

The degree of reduction decreases slightly when a slow (0.5°C/min) heating rate is used. The reduction behavior of these two catalysts is very similar (Table 4-10).

4.4.4 Fischer-Tropsch Synthesis

The original catalysts were tested under Fisher-Tropsch conditions in a fixed bed reactor to see if particle size would cause any change in the catalyst FTS behavior. The reaction temperature was 190°C and the pressure 5 bar.

FTS turnover rates are not dependent on Co dispersion and support identity over the dispersion range of 0.01 and 0.12, at typical FTS conditions [Iglesia, 1997].

Niemelä and Krause (1996) found that conversion on the Co/SiO_2 catalyst deactivates according to dispersion after 5 hours of operation, i.e. the higher the dispersion the higher the rate of decrease. The type of precursor used influenced the results. A higher dispersion was obtained with a catalyst prepared from cobalt carbonyl. A carbonyl type precursor catalyst undergoes a higher amount of carbon deposition than the nitrate type precursor catalyst. The deactivation of the catalyst with higher dispersion was partly due to carbon deposition and agglomeration of cobalt crystallites.

4.4.4.1 Hydrocarbon Yield

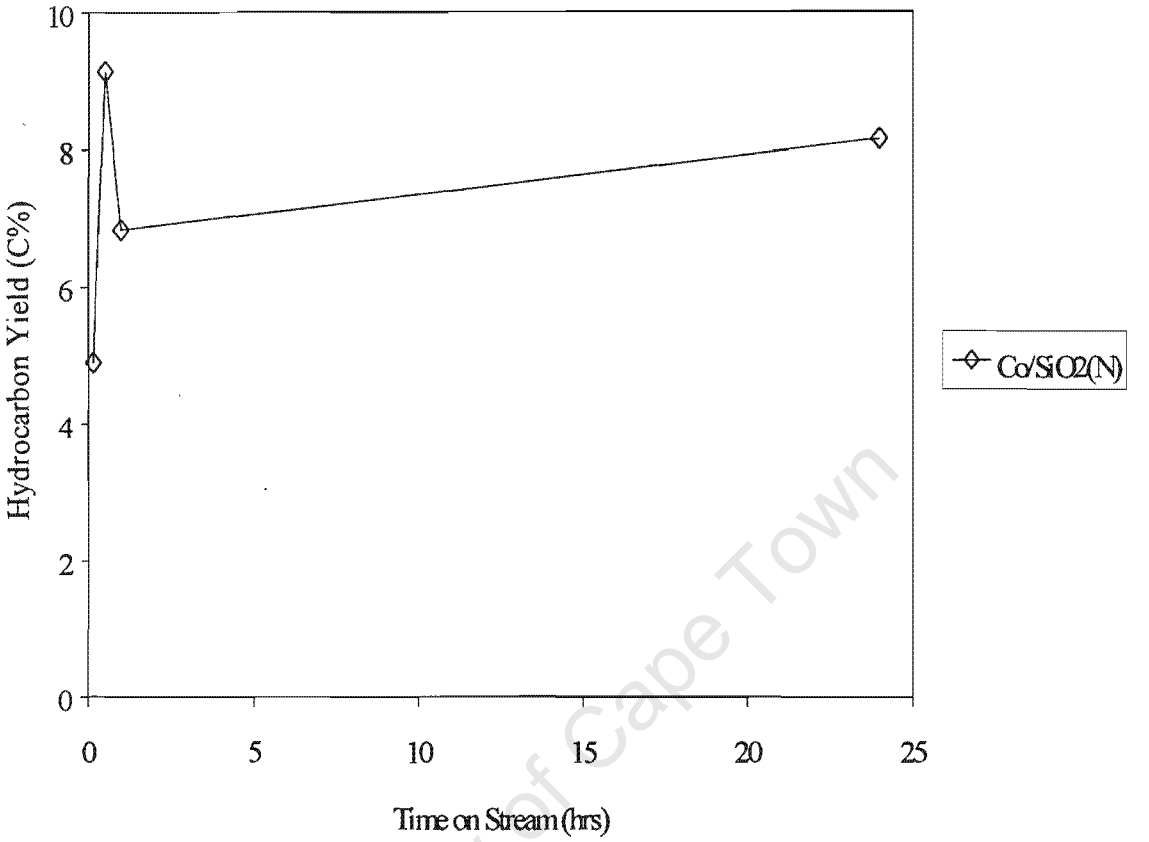

Figure 4-7: The hydrocarbon yield with time on stream for the $Co/SiO_2(N)$ catalyst

An initial increase in hydrocarbon yield is observed in the first hours of synthesis. The hydrocarbon yield stabilizes at 8.1% after 24 hours for the $Co/SiO_2(N)$ catalyst. The hydrocarbon yield of the slowly reduced catalyst is not available due to problems with ampoule sampling.

4.4.4.2 Chain growth probability

Table 4-11: The chain growth probability of the silica supported cobalt catalysts, directly reduced with different heating rates

Catalyst	*Chain growth probability*
$Co/SiO_2(N)^{1)}$	0.84
$Co/SiO_2(N)$-$s^{2)}$	0.89

[1)] Directly reduced 10°C/min
[2)]-s: slow reduction heating rate (0.5°C/min)

A higher chain growth probability is observed with the cobalt catalyst with a higher dispersion (see Table 4-11).

4.5 The Effect of Water Treatment

A portion of each catalyst was treated with a water-hydrogen mixture after reduction at 400°C. The water treatment was at 200°C for 24 hours to simulate the re-oxidation behaviour of the catalyst during Fischer-Tropsch synthesis. A H_2/H_2O mixture (4:1) was passed over the catalyst bed at 60 ml (STP)/min. The original catalyst underwent a temperature treatment (200°C) in hydrogen for the same amount of time as a baseline cast.

4.5.1 Particle Size Measurements

The hydrogen chemisorption measurement was representative of the deactivation induced by water-treatment. To see if water treatment had any effect on the particle size of the cobalt TEM were used to determine the particle size before and after water treatment.

4.5.1.1 H_2 Chemisorption

Table 4-12: The change in volume of hydrogen chemisorbed on the Co/SiO_2 catalyst due to water treatment.

Catalyst	*Before water treatment*	*After water treatment*
	V_{H2}/g_{cat} (cm^3/g_{cat})	V_{H2}/g_{cat} (cm^3/g_{cat})
$Co/SiO_2(N)$[1)]	0.418	0.207
$Co/SiO_2(N)$-s[2)]	0.416	0.154
$Co/SiO_2(N)$-c6[3)]	0.253	0.232

[1)] Directly reduced 10°C/min
[2)]-s: slow reduction heating rate (0.5°C/min)
[3)] -c6: calcined at 600°C heating rate 20°C/min

Hydrogen chemisorption is a measurement related to the active sites available for dissociative hydrogen chemisorption, by measuring the volume of hydrogen uptake.

Changes in hydrogen uptake are accompanied by changes in catalytic activity and therefore a good indication of catalyst deactivation.

Water treatment resulted in a decrease of hydrogen uptake for each catalyst (see Table 4-12). This decrease can be an indication of a decrease in active sites possibly caused by enhanced metal-support-interaction induced by water treatment.

4.5.1.2 Transition Electron Microscopy

The particle size of the sample from $Co/SiO_2(N)$, according to TEM, is 50 nm before and after water treatment. Water treatment does not seem to change the particle size of the catalyst. (see Appendix VIII, Figure A8-3)

4.5.2 Temperature Programmed Reduction

The effect of water treatment on the reduction behaviour of the Co/SiO_2 catalyst was studied with TPR.

4.5.2.1 Calcined catalysts

The low temperature peak (see Figure 4-8) due to an oxidation occurring at room temperature, is still present after water treatment, but not necessarily at the same temperature and intensity.

In Figure 4-8 the TPR spectra of the water-treated catalyst are compared with the original calcined and reduced catalyst. A trend of a decreased intensity of the low temperature peak after water treatment is visible. Water treatment reduced the surface oxidation due to atmospheric exposure. Treatment with water seems to increase the high temperature H_2 consumption.

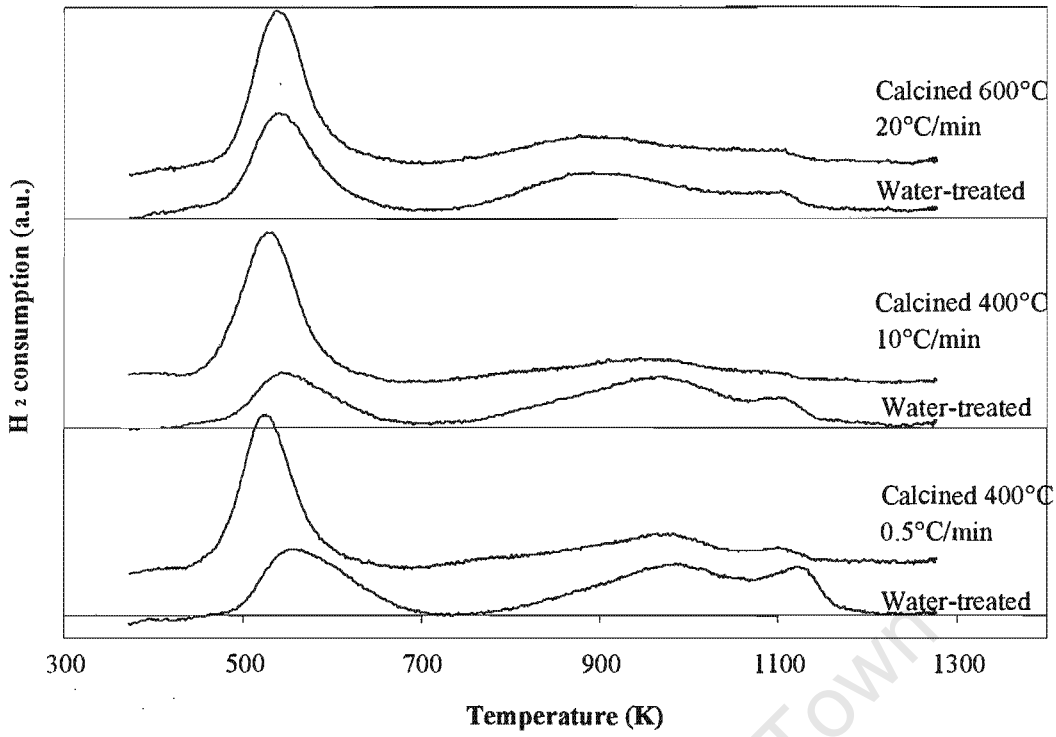

Figure 4-8: TPR spectra of the effect of water treatment on the calcined and reduced Co/SiO_2 catalysts. (Calcination in air in furnace. Reducing gas = 60 ml (STP) /min 5% H_2/N_2, temperature programming rate = 10°C/min, $m_{cat} \approx 0.15g$)

When the catalyst is steam-treated, the low temperature peak of Co/SiO_2(N)-c4 and Co/SiO_2(N)-s-c4 shifts to a slightly higher temperature in the TPR spectra (260°C to 276°C and 253°C to 284°C, Table 4-13).

Table 4-13: Hydrogen consumption during TPR and peak maximum temperatures for calcined and water-treated Co/SiO_2 catalysts.

Catalyst	*H_2: Co ratio Peak below 700K (mole: mole)*	*H_2: Co ratio Peak above 700K (mole: mole)*	*T_{low} (K)*	*T_{high} (K)*
Co/SiO_2(N)-c6	0.385	0.343	542	895
Co/SiO_2(N)-c6-w	0.317	0.407	543	895
Co/SiO_2(N)-c4	0.395	0.167	533	959
Co/SiO_2(N)-c4-w	0.198	0.397	549	966
Co/SiO_2(N)-s-c4	0.402	0.298	526	970
Co/SiO_2(N)-s-c4-w	0.242	0.419	557	987

A shift in the high temperature peak, due to water treatment, is also observed for both catalysts calcined at 400°C. Not only does water treatment shift the hydrogen consumption peaks to higher temperatures for both these catalysts, but it also changes the amount of hydrogen consumed. The hydrogen consumption for the high temperature peak of Co/SiO_2(N)-c4 increases from 0.167 (H_2: Co mole: mole ratio) to 0.397 mole: mole. The same increase is observed for the catalyst calcined with a slow calcination heating rate, Co/SiO_2(N)-s-c4: high temperature peak increases from 0.298 mole: mole to 0.419 mole: mole. This increase in the high temperature peak is accompanied by a decrease in the low temperature peak.

Co/SiO_2(N)-c6 and Co/SiO_2(N)-c6-w showed no change in peak temperature. The high temperature peak had a slight increase in hydrogen consumption and the low temperature peak a slight decrease. The changes in these values are not as explicit as those for the catalysts calcined at 400°C.

4.5.2.2 Directly Reduced Catalysts

Two catalysts were directly reduced in hydrogen with different heating rates. A portion of each catalyst was then exposed to water treatment. The TPR spectra of these catalysts show a shift in the low temperature peak to a higher temperature for both catalysts after water treatment. The peak intensity decreases after water

treatment. No marked changes are observed for the high temperature peak (see Figure 4-9).

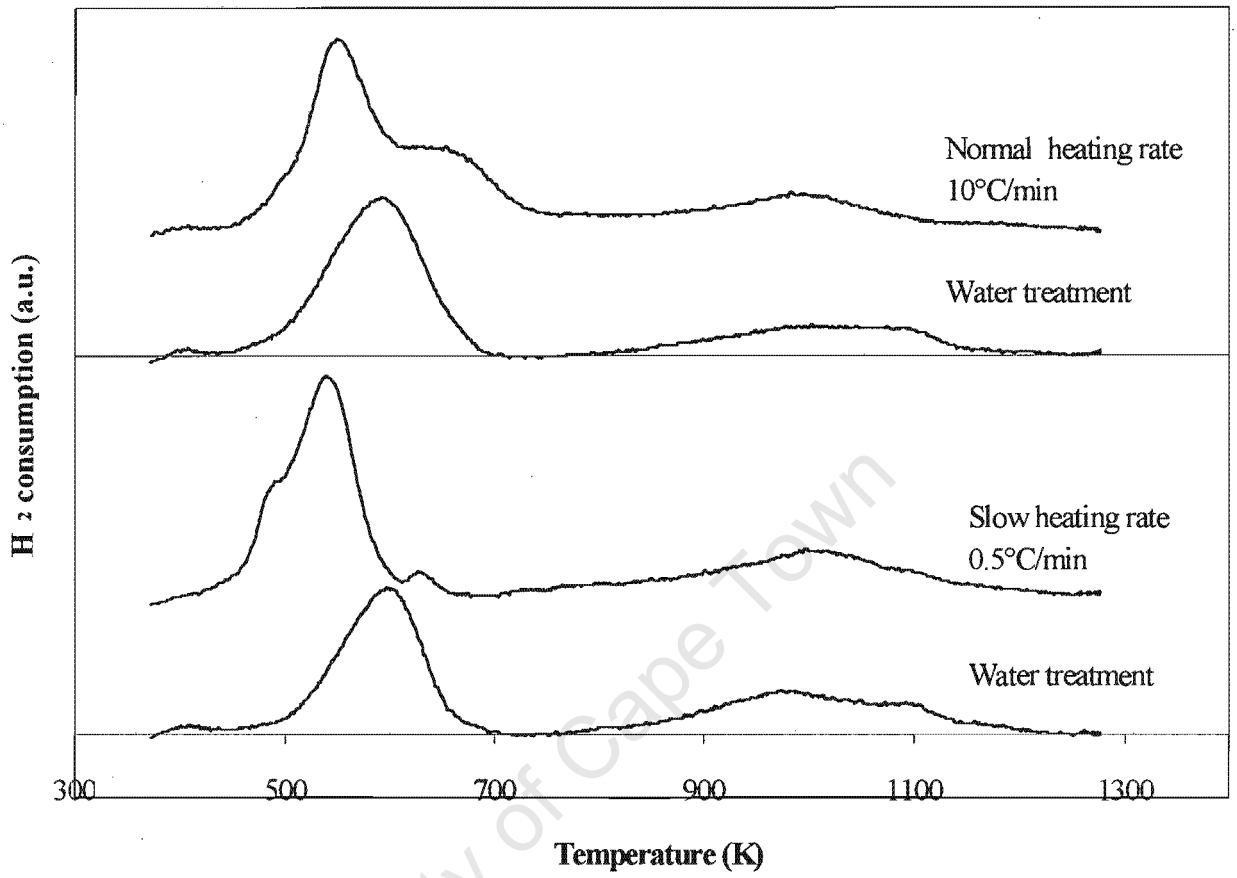

Figure 4-9: TPR spectra of the effect of water treatment on directly reduced Co/SiO_2 catalysts. Reducing gas = 60 ml (STP)/min 5% H_2/N_2, temperature programming rate = 10°C/min, $m_{cat} \approx 0.15g$)

The slow reduction heating rate catalyst exhibits a decrease in hydrogen consumption (0.442 to 0.325 mole: mole, Table 4-14) in the low temperature peak after water treatment. The high temperature peak shows a small decrease in area.

Co/SiO_2(N) was reduced using the standard way in hydrogen with a heating rate of 10°C/min. After water-treating the catalyst, the low temperature peak displayed a lower amount of hydrogen consumed (0.486 to 0.433 mole H_2: mole Co, Table 4-14). The high temperature peak had only slight increase in hydrogen consumption (0.162 to 0.187 mole H_2: mole Co, Table 4-14).

Table 4-14: Hydrogen consumption during TPR and reduction peak temperatures of directly reduced Co/SiO_2 catalysts and the water-treated counterpart.

Catalyst	*H_2: Co ratio Peak below 700K (mole: mole)*	*H_2: Co ratio Peak above 700K (mole: mole)*	*T_{low} (K)*	*T_{high} (K)*
$Co/SiO_2(N)$[1)]	0.471	0.177	551	1003
$Co/SiO_2(N)$-w[2)]	0.433	0.187	591	1028
$Co/SiO_2(N)$-s[3)]	0.442	0.251	540	1006
$Co/SiO_2(N)$-s-w*	0.325	0.244	600	955

[1)]Directly reduced 10°C/min
[2)]-w: water treatment
[3)]-s: slow reduction heating rate (0.5°C/min)

$Co/SiO_2(N)$-s-w does not show an increase in the high temperature H_2 consumption peak. When the low temperature peak is reduced at 200° prior to reaction, the T_{max} of this peak influences the degree of reduction. A shift to a higher temperature in T_{max} decreases the degree of reduction of the catalyst if the catalyst is re-reduced at 200°C. The shift occurs after water treatment and might be ascribed to the formation of weak-metal-support-interaction. Alternatively the possible autocatalytic effect of H_2 reduction of cobalt might cause the shift in the peak maximum temperature. Because of the deactivation of the catalyst due to re-oxidation and formation of strong-metal-support-interaction, less active sites are available. Less cobalt metal area are therefore available to enhance the reduction rate and this causes an increase in the low temperature T_{max}.

4.5.3 Temperature Programmed Oxidation

The valence state of cobalt on the Co/SiO_2 catalyst before and after water treatment was studied with TPO. Together with TPR, the water treatment was found to decrease the reducibility of the catalysts by oxidising the cobalt and enhancing metal support interaction.

4.5.3.1 Calcined Catalyst

The catalyst was re-reduced at 200°C for 4½ hours, to reduce the surface oxide that formed due to exposure to air after catalyst reduction at 400°C. The catalyst was heated up in 5%H_2/N_2 (60 ml (STP)/min) at 10°C/min. After reduction at 200°C, the gas was switched to He for the stabilisation of the TCD, whereupon the catalyst was cooled down. After reaching a stable signal a 2%O_2/He mixture was passed over the catalyst bed at 60 ml (STP)/min and the temperature was raised linearly form 40 to 1000°C at 10°C/min.

Table 4-15 shows that water treatment of the calcined catalysts decreases the reducibility of the catalyst, i.e. less zerovalent cobalt is present on the catalyst. The degree of reduction of the catalysts calcined at 600°C decreased form 93% to 85% after water treatment. The catalyst calcined at 400°C decreased from 88% to 75% in % reducibility after water treatment. The amount of oxidisable divalent cobalt, but especially the amount of non-oxidisable Co, increases with water treatment. The formation of non-oxidisable Co^{2+} during H_2-treatment is seen as a permanent deactivation because these divalent cobalt species can only be reduced at temperatures where sintering of the catalyst would occur.

Table 4-15: Composition and metal oxidation temperatures during TPO for calcined Co/SiO_2(N) and the water-treated equivalent

Catalyst	*Zerovalent Co (mole %)*	*Oxidisable Co^{2+} (mole %)*	*Non-oxidisable Co^{2+} (mole %)*	*$T_{oxidation}$ (K)*
Co/SiO_2(N)-c6	93	4	3	490
Co/SiO_2(N)-c6-w	85	10	5	491
Co/SiO_2(N)-c4	-	-	-	-
Co/SiO_2(N)-c4-w	76	21	3	490
Co/SiO_2(N)-s-c4	88	5	6	471
Co/SiO_2(N)-s-c4-w*	76	8	16	478

4.5.3.2 Directly Reduced Catalyst

The degree of reduction of both catalysts decreases after water treatment. The TPO-technique shows water treatment to increase the amount of non-oxidisable Co as well as the amount of oxidisable Co^{2+} (see Table 4-16). Silicate formation increased from 9 mole % to 11 mole % for $Co/SiO_2(N)$ and from 3 mole % to 13mole % for $Co/SiO_2(N)$-s after water treatment.

Table 4-16: Composition and metal oxidation temperatures during TPO for directly reduced $Co/SiO_2(N)$ and the water-treated counterpart

Catalyst	*Zerovalent Co (mole %)*	*Oxidisable Co^{2+} (mole %)*	*Non-oxidisable Co^{2+} (mole %)*	*$T_{oxidation}$ (K)*
$Co/SiO_2(N)$	90	1	9	478
$Co/SiO_2(N)$-w	83	6	11	482
$Co/SiO_2(N)$-s	88	9	3	482
$Co/SiO_2(N)$-s-w	83	4	13	489

In Appendix II, the TPO spectra of the catalysts and their water-treated counterparts are shown. The stream treatment has a slight influence on the TPO spectra. The oxidation peak is shifted with a few °C in some cases.

4.5.4 Fischer-Tropsch Synthesis

The water-treated catalysts were tested at the same conditions as the original catalysts: 190°C and 5 bar in a fixed bed reactor. The flow rate of syngas was 10.5 ml (STP)/min and the composition was 66.67% H_2 and 33.33% CO.

Iglesia (1997) observed an increase in FTS reaction rates when water was co-fed with reactants at low conversion. These water effects are dependent on the support identity and can lead to support effects on the turnover rates at low conversions.

4.5.4.1 Hydrocarbon Yield

A decrease of hydrocarbon yield after water treatment, would be an indication of deactivation of the Co/SiO_2 catalysts caused by water. The catalyst calcined at 400°C before reduction showed a hydrocarbon yield between 4.3 and 5.8% in the first two hours and then decreased to 2.5% after 24 hours. When the catalyst was treated with water the hydrocarbon yield decreased significantly to 2.6 % in the first two hours and even further to 1.7% after 24 hours (see Figure 4-10). It can therefore be concluded that the catalyst has been deactivated by the water treatment.

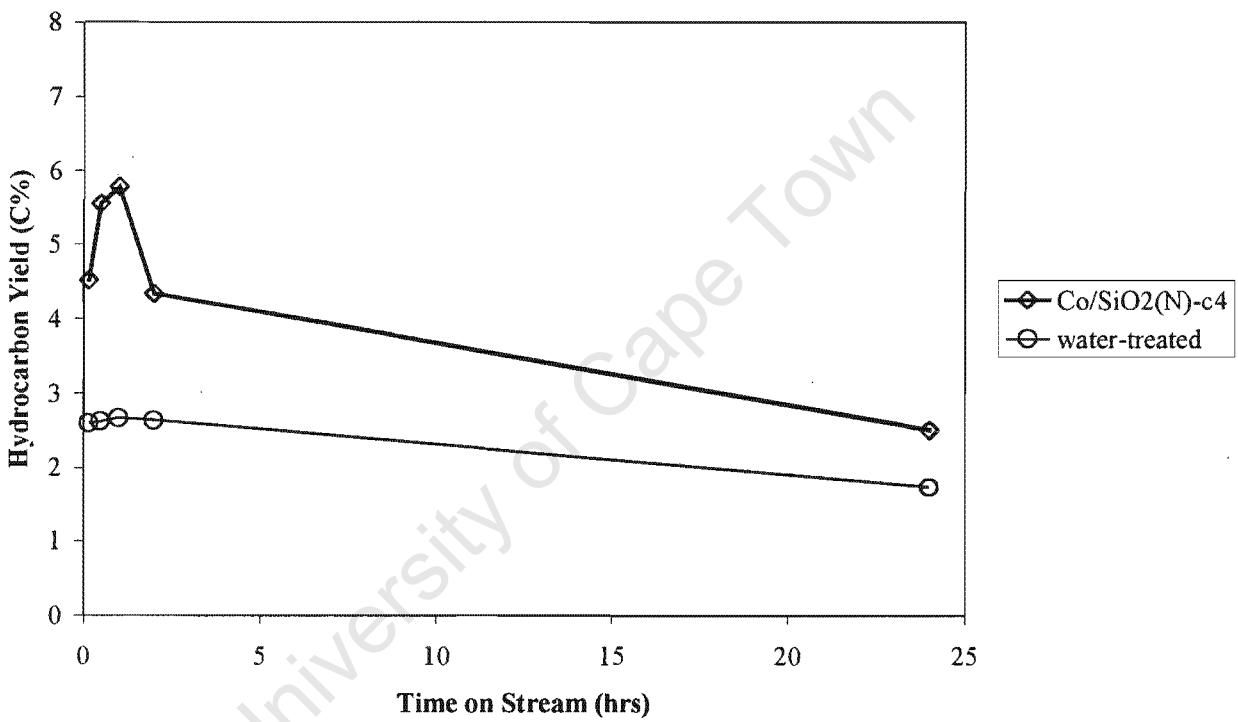

Figure 4-10: The comparison of hydrocarbon yield with time on stream for the Co/SiO_2(N) catalyst calcined at 400°C with the water-treated counterpart

Calcining the catalyst at 600°C before reduction resulted in a hydrocarbon yield between 3 and 3.2% in the first two hours and 1.7% after 24 hours. After water treatment the catalyst gave a hydrocarbon yield between 2.4 and 3.3% in the first two hours and 2.1% after 24 hours.

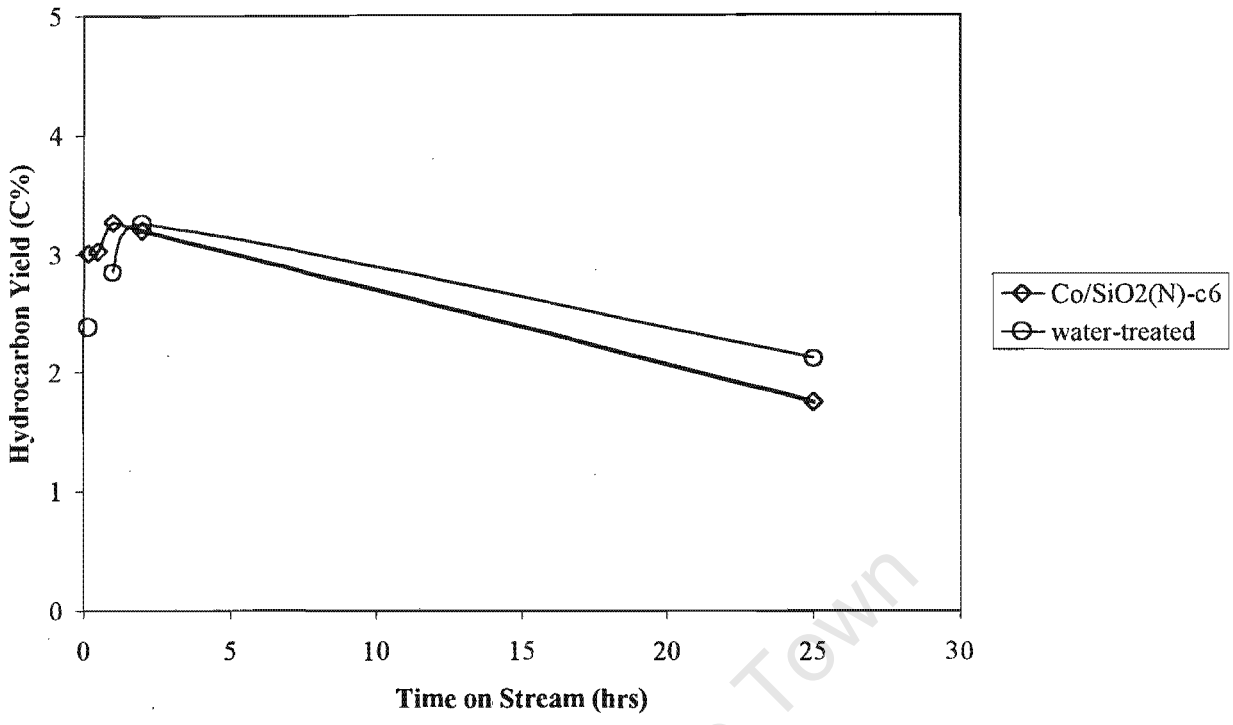

Figure 4-11: The comparison of hydrocarbon yield with time on stream for the $Co/SiO_2(N)$ catalyst calcined at 600°C , with the water-treated counterpart

The influence of water treatment on the catalyst calcined at 600°C is not as pronounced as for the catalyst calcined at 400°C (see Figure 4-11). This is because the catalyst is already in a semi-deactivated state because of the particle agglomeration that took place when the catalyst was calcined at 600°C.

Water-treated $Co/SiO_2(N)$ exhibited a hydrocarbon yield constantly lower than the non-water-treated $Co/SiO_2(N)$ (see Figure 4-12). $Co/SiO_2(N)$ was prepared with no calcination step before reduction. The hydrocarbon yield during Fisher-Tropsch synthesis was 4.9% (10 minutes) and increased to 9.1% (30min) and was 7.5% after 2 hours. After 24 hours the hydrocarbon yield was 8.1%.

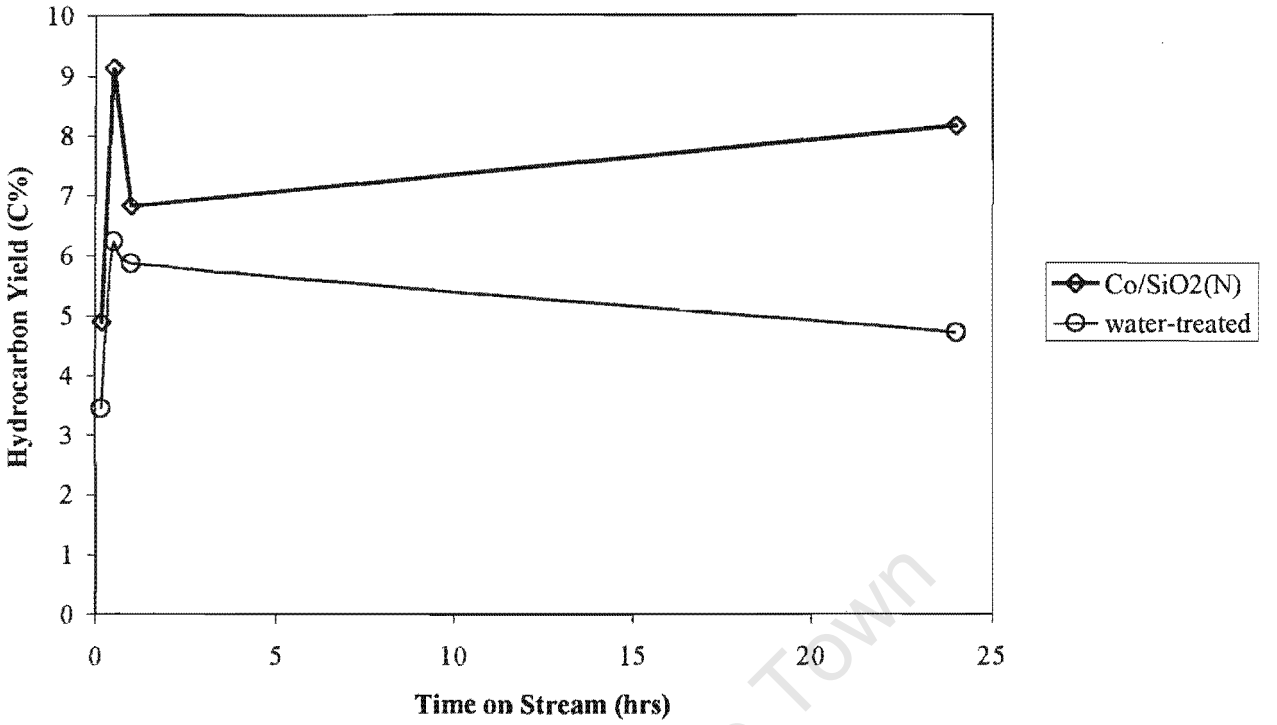

Figure 4-12: Hydrocarbon yield with time on stream for the directly reduced $Co/SiO_2(N)$ catalyst, compared with the water-treated equivalent

A severe deactivation in hydrocarbon yield was observed when $Co/SiO_2(N)$ was treated with water. After 10 minutes of reaction the hydrocarbon yield was 3.4% and it increased to 6.19 % after 2 hours. The hydrocarbon yield was 4.7% after 24 hours.

4.5.4.2 Chain Growth Probability

The chain growth probability decreased after treating the calcined catalysts with water. For $Co/SiO_2(N)$-c6 the chain growth probability decreased from 0.78 before water treatment to 0.74 after water treatment. The chain growth probability of $Co/SiO_2(N)$-c4 decreased from 0.83 before water treatment to 0.75 after water treatment.

Table 4-17: The chain growth probability of the calcined Co/SiO_2 catalysts compared with the calcined and water-treated Co/SiO_2 catalysts

Catalyst	*Chain growth probability*	*Chain growth probability of water-treated catalyst*
Co/SiO_2(N)-c6	0.78	0.74
Co/SiO_2(N)-c4	0.83	0.75

There was an increase in the chain growth probability after water treatment for the Co/SiO_2(N) catalyst, from 0.835 to 0.887. The chain growth probability for the slowly reduced catalyst, Co/SiO_2(N)-s decreased from 0.888 to 0.846 after treatment with water (see Table 4-18).

Table 4-18: The chain growth probability of the directly reduced Co/SiO_2 catalysts compared with the water-treated Co/SiO_2 catalysts

Catalyst	*Chain growth probability*	*Chain growth probability of water-treated catalyst*
Co/SiO_2(N)	0.84	0.89
Co/SiO_2(N)-s*	0.89	0.85

*-s: slow reduction heating rates

Water, a product of FTS may influence the chain growth probability, selectivity and rate of primary CO hydrogenation on some catalysts [Iglesia, 1997].

Schulz *et al.* (1995)a observed a slight increase in chain growth probability for Ru promoted Co catalyst when water was co-fed in the syngas stream to the slurry reactor. These reactions were carried out after one week of steady state operation. The increase in chain growth probability when water is added in the reactant feed is supported by the results of Iglesia, (1997)

4.5.4.3 Olefin Selectivity

Figure 4-13 shows the olefin content in the fraction of linear C8 hydrocarbons as a function of time on stream for the catalyst calcined at 600°C and the water-treated equivalent. The olefin selectivity in the C8 fraction obtained with the catalyst

$Co/SiO_2(N)$-c6 increases with time on stream and decreases with time on stream for the water-treated equivalent. The olefin selectivity in the C8 fraction at steady state decreases from ca. 0.6 to 0.2 after water treatment.

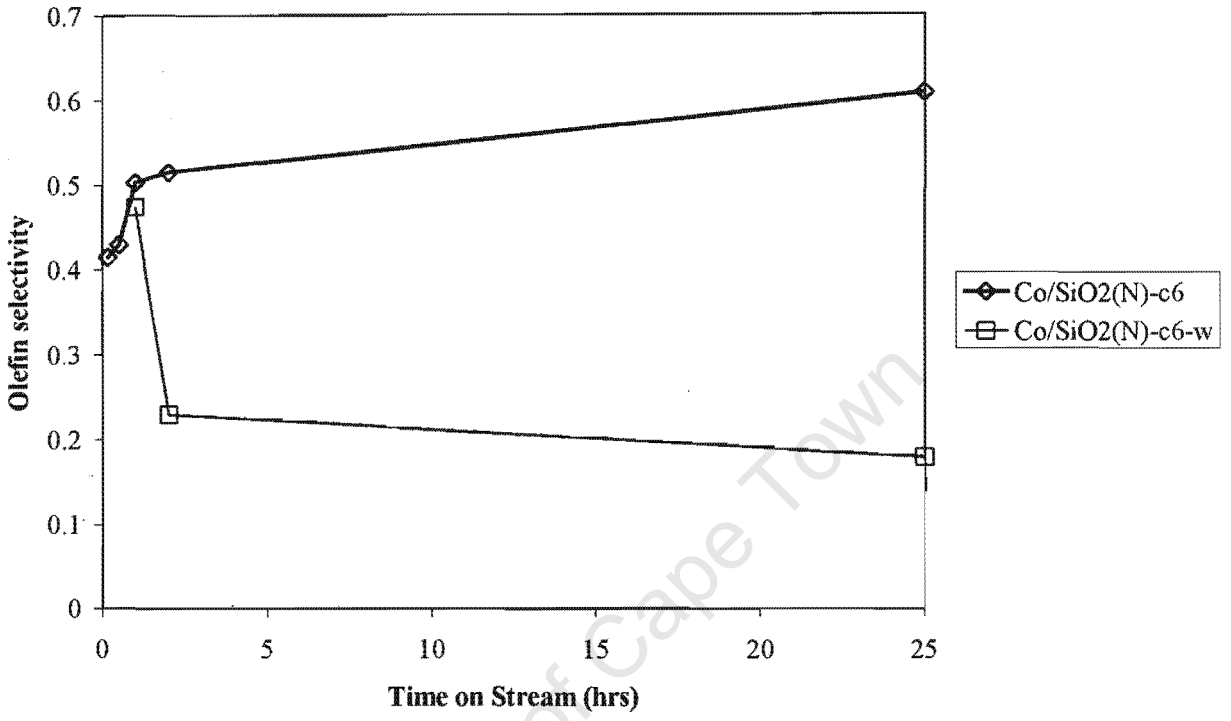

Figure 4-13: Olefin content in the fraction of linear C8 hydrocarbons as a function of time on stream for the cobalt catalyst calcined at 600°C and its water-treated equivalent.

Figure 4-14 shows the olefin selectivity in the fraction of C8 hydrocarbons a to increase with time on stream for the catalyst calcined at 400°C. An increase in the olefin selectivity with time on stream is also observed for the water-treated catalyst. The olefin selectivity in the C8 fraction decreases from 0.75 to 0.55 (24 hours on stream) after the catalyst has been water-treated.

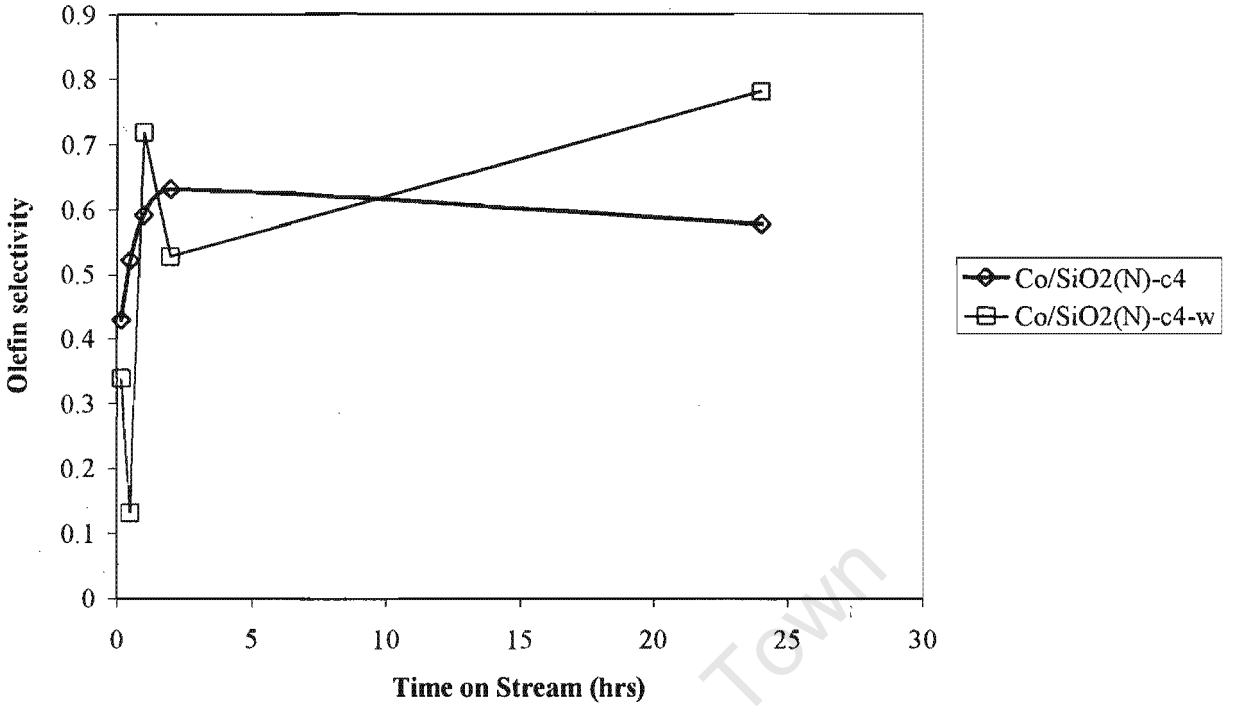

Figure 4-14: Olefin content in the fraction of linear C8 hydrocarbons as a function of time on stream for the cobalt catalyst calcined at 400°C and its water-treated equivalent.

For the directly reduced catalyst an increase olefin selectivity in the C8 fraction with reaction time is observed for both the original and the water-treated catalyst (see Figure 4-15). The olefin selectivity at 24 hours time on stream decreases after water treatment from 0.55 to 0.4.

In the first two hours, the olefin selectivity increases significantly for all the catalysts. When the reaction reach a steady state and the pores are filled with liquid products and a liquid-gas equilibrium is achieved, the olefin selectivity seems to remain fairly constant.

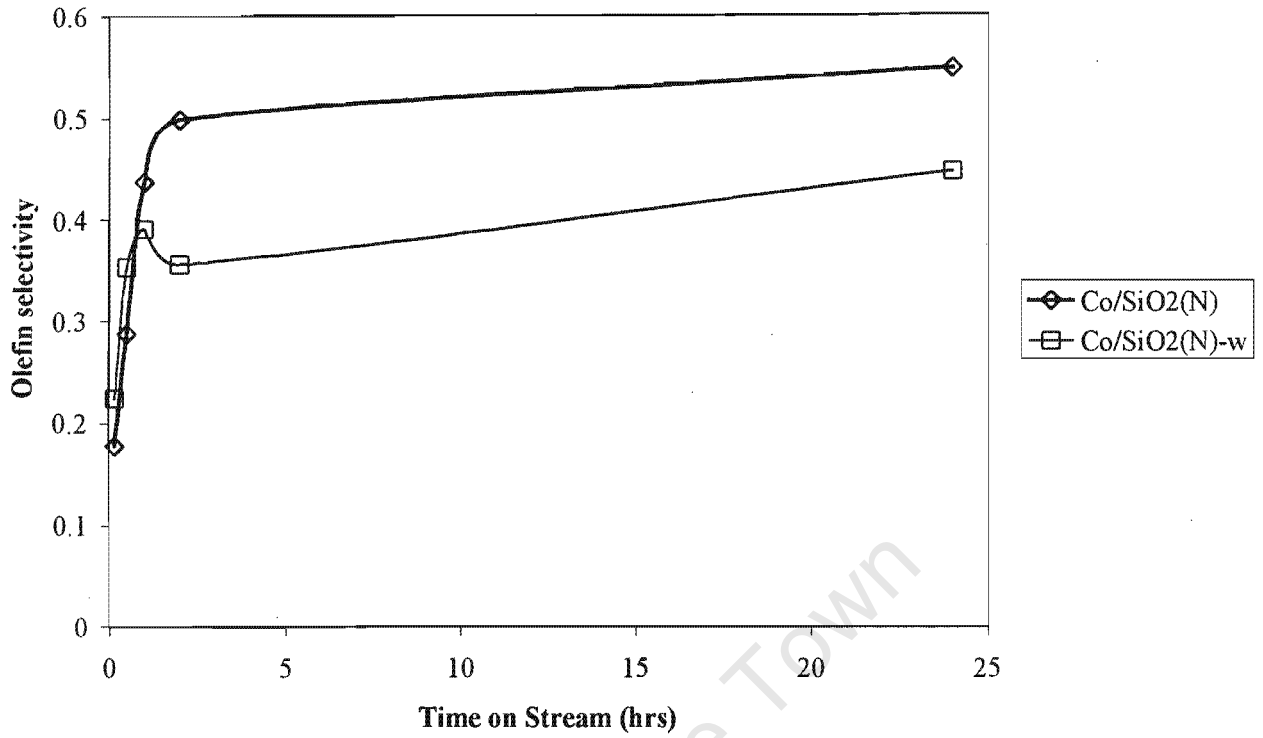

Figure 4-15: Olefin content in the fraction of linear C8 hydrocarbons as a function of time on stream for the directly reduced cobalt catalyst (heating rate = 10°C/min) and its water-treated equivalent.

Figure 4-16 shows the olefin selectivity in the C8 fraction as a function of time on stream for the catalyst directly reduced with a slow heating rate (0.5°C/min). A similar trend of increase in olefin selectivity is observed for the catalyst that was reduced using a slow heating rate in comparison to the usual applied heating rate (0.5 vs. 10 °C/min). The water-treated catalyst has a similar olefin selectivity to the original catalyst.

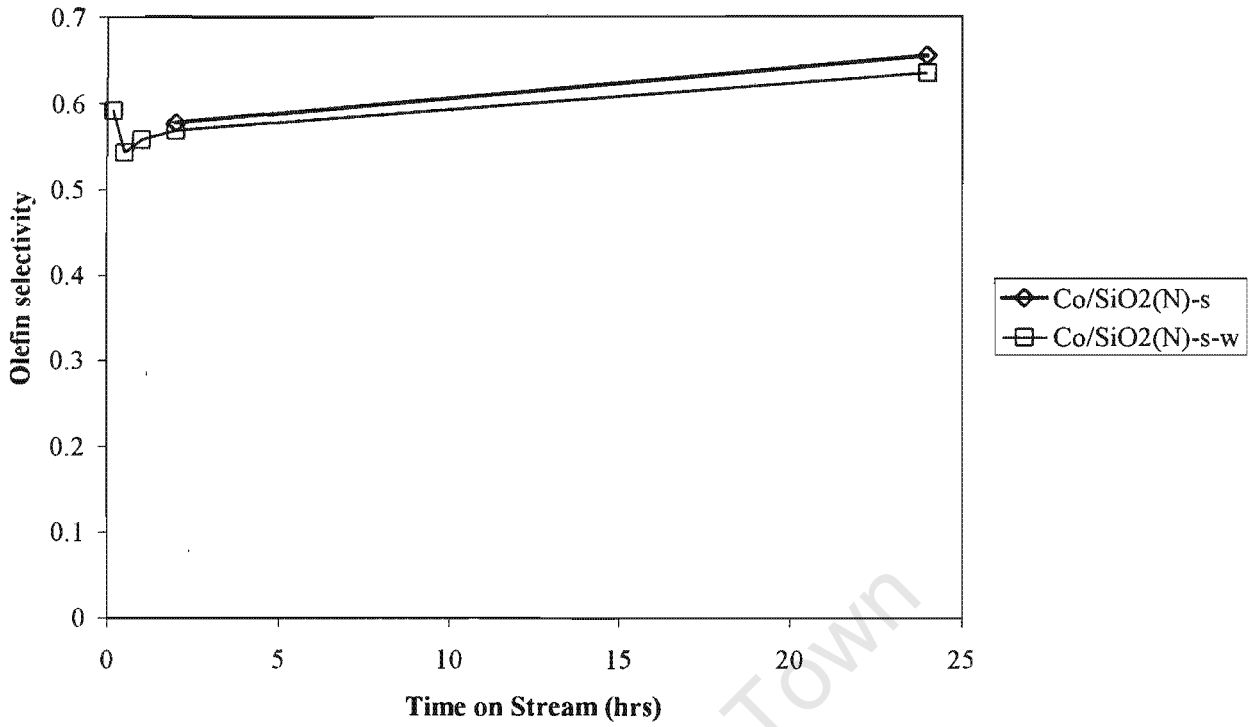

Figure 4-16: Olefin content in the fraction of linear C8 hydrocarbons as a function of time on stream for the directly reduced cobalt catalyst (heating rate = 0.5°C/min) and its water-treated equivalent.

4.5.4.4 α-Olefin selectivity

The Fischer-Tropsch synthesis generates α-olefins as a primary product [Schulz *et al.*, 1988]. Primary product formation of β-olefins can be neglected. Readsorption of olefins can lead to double bond shift or olefin hydrogenation that decreases the α-olefin selectivity.

Figure 4-17 shows the α-olefin selectivity in the fraction of C8 olefins as a function of time on stream for the catalyst calcined at 600°C. The α-olefin selectivity increases and then decreases in the first 2 hours and stabilises towards 0.8 (25 hours) for the water-treated catalyst and 0.45 for the original catalyst.

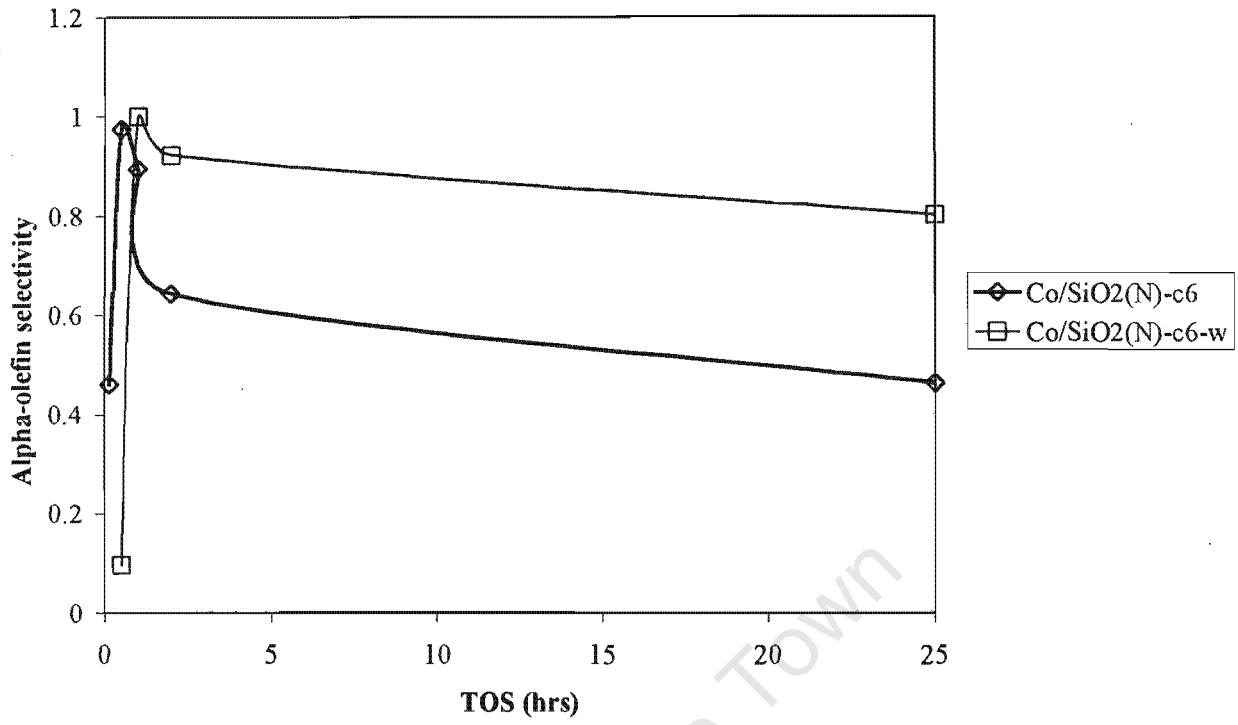

Figure 4-17: α-Olefin selectivity based on the C8 carbon fraction of the catalyst calcined at 600°C and the water-treated equivalent

Figures 4-18 and 4-19 show the α-olefin selectivity for the catalyst that has been reduced directly without an intermittent calcination step. The α-olefin selectivity shows a increase during the first two hours after which it reaches a stable value. The water-treated catalysts show a higher α-olefin selectivity. The catalyst reduced at a heating rate of 10°C/min showed a steady-state α-olefin selectivity of 0.5 (original catalyst) and 0.9 (water-treated catalyst) after 24 hours. The catalyst reduced at a heating rate of 0.5°C/min showed a much lower α-olefin selectivity 0.35 (original catalyst) and 0.55 (water-treated catalyst) at steady-state (after 24 hours TOS).

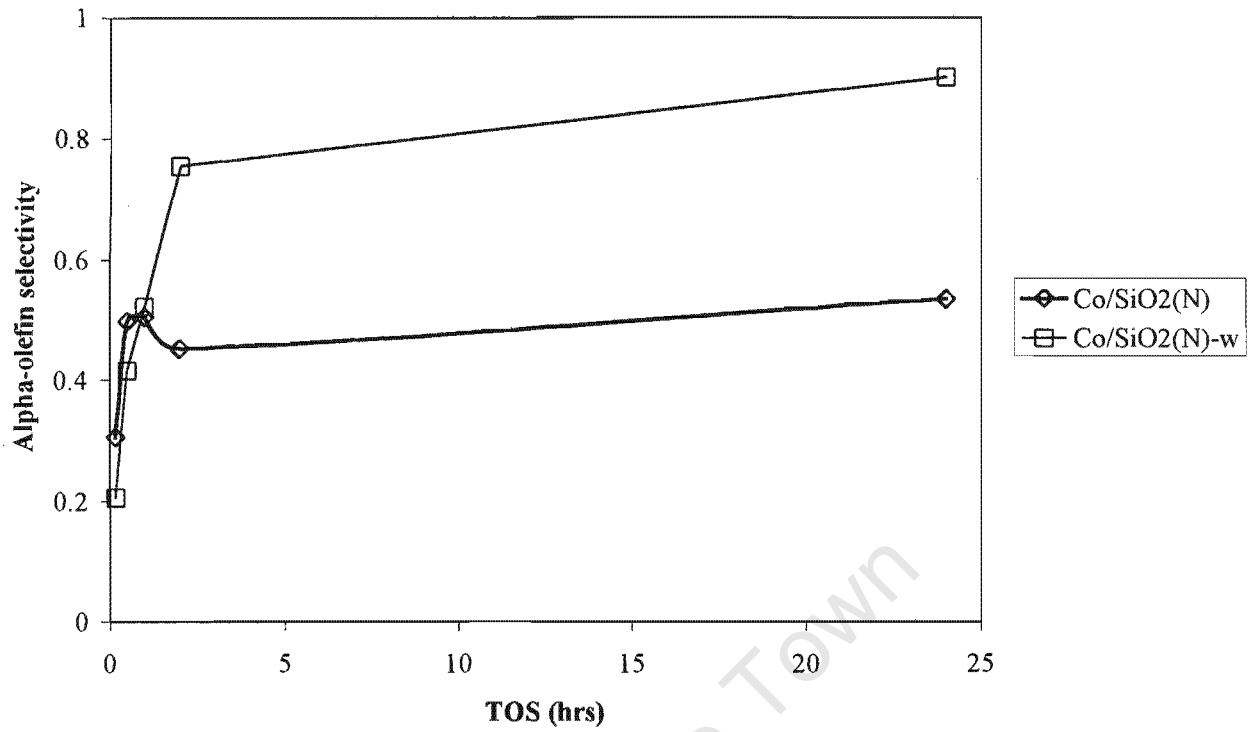

Figure 4-18: α-Olefin selectivity based on the C8 carbon fraction of the directly reduced catalyst (heating rate = 10°C/min) and the water-treated equivalent

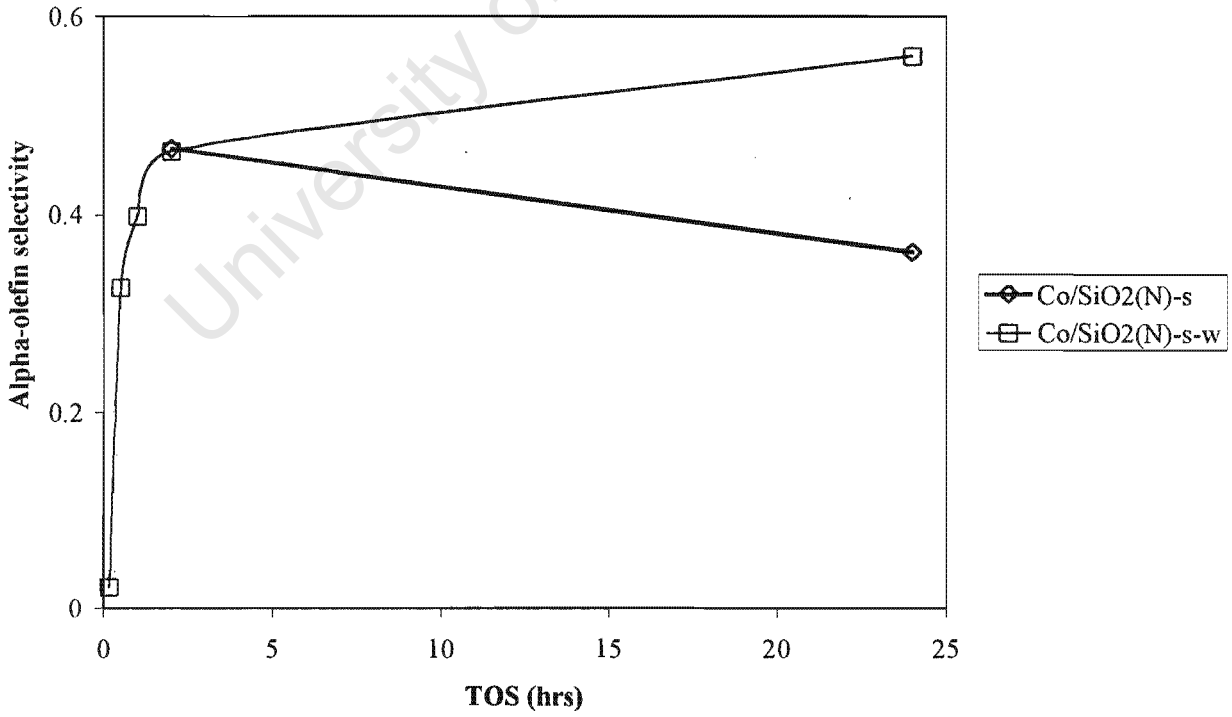

Figure 4-19: α-Olefin selectivity based on the C8 carbon fraction of the directly reduced catalyst (heating rate = 0.5°C/min) and the water-treated equivalent

The higher α-olefin selectivity obtained with the water-treated catalyst is due to a lesser amount of α-olefin readsorption. Since α-olefin readsorption increase with increase in site density [Iglesia *et al.*, 1992], a higher α-olefin selectivity indicates a decrease in site density after water treatment.

CHAPTER 5

Discussion

5. DISCUSSION

The aim of the project was to test the influence that the crystallite size of cobalt has on the possible re-oxidation of cobalt with water. Thermodynamic considerations lead to the conclusion that oxidation with water becomes more likely if the particles become smaller. Once the particle is oxidised it becomes inactive in the Fischer-Tropsch synthesis. Furthermore, the oxidised particle is very likely to form an interaction with the support (i.e. cobalt silicate) that cannot be regenerated. These species with a strong-metal-support-interaction are only reducible at temperatures where sintering of catalyst and support occurs which can be viewed as a permanent deactivation.

5.1 The Effect of Co Crystallite Size

The Fischer-Tropsch reaction is known to be structure insensitive [Johnson *et al.*, 1991, Iglesia, 1997]. The structure sensitivity that has been reported previously [Reuel and Bartholomew, 1984], is due to marked effects in the extent of reduction that changes when modifying the dispersion. Although the Fischer-Tropsch synthesis is not structure sensitive, the deactivation of the catalyst might be related to the particle size of the cobalt crystallites [Niemelä and Krause, 1996] and the influence of the particle size is thus of importance. Niemelä and Krause (1996) concluded that the conversion on the Co/SiO_2 catalyst decreases with time according to the dispersion, i.e. higher dispersion gives a higher rate of deactivation. The same observation was made by Krishna and Bell (1992) when testing the Ru/TiO_2 catalyst.

5.1.1 The Influence of Preparation Method on the Catalyst's Reducibility

To test the influence of cobalt crystallite size, catalysts with different cobalt particle sizes were prepared by varying the activation method. The average particle size determined from H_2 chemisorption varied from 16 nm, by directly reducing the catalyst with a slow heating rate, to 28 nm, by calcining the catalyst at 600°C before reduction. Crystal agglomeration that leads to the formation of larger cobalt crystallites takes place when the supported cobalt catalyst is treated at higher temperatures [Coulter and Sault, 1995]. When the cobalt nitrate precursor is directly

reduced, the concentration of NO_x species formed on the surface of the cobalt determines the cobalt phase. NO_x is a strong oxidation gas and a high concentration will lead to agglomeration of Co_3O_4 particles on the support. By controlling the decomposition of cobalt nitrate via slow reduction heating rate, the concentration of NO_x species is lower and allows the mobile Co^{2+} to distribute over the surface and constitute a well-dispersed cobalt phase [Arnoldy and Moulijn, 1985, Iglesia, 1997].

Because of the high dispersions and high surface areas, supported catalysts are typically in a state of high surface free energy. During heating and/or catalytic reactions, these materials therefore have a high tendency to sinter and thus to decrease the exposed surface area and surface free energy of the system. The extent of sintering depends on several parameters including time of treatment, temperature, gas phase composition and the properties of the support and of the active phase. The formation of highly dispersed particles on a support is governed by nucleation and growth mechanisms. For sintering to occur, particles or atoms, molecules or clusters of the active phase must become mobile. The Tamman temperature (K):

$$T_{Tam} \approx 0.5 T_{melt}^{bulk}$$

is considered to be sufficient to make atoms or ions of the bulk of a solid sufficiently mobile for bulk-to surface migrations [Ertl *et al.*, 1997]. The Hüttig temperature:

$$T_{Hut} \approx \frac{1}{3} T_{melt}^{bulk}$$

is enough to make species already located on the surface sufficiently mobile to undergo agglomeration or sintering. With the melting temperature of Co: T_{melt} = 1768.15K, the Tamman temperature is T_{Tam}= 884K (611°C) and the Hüttig temperature is T_{Hut} = 589 K (316°C).

The maximum dispersion will then be obtained by keeping the temperature below the Hüttig temperature of cobalt, before the Co^{2+} ions become mobile and start to agglomerate. Niemelä *et al.* (1997) investigated the influence of reduction temperature and found maximum dispersion for catalysts reduced at 350°C.

Because the surface characteristics of the catalyst is affected by the calcination temperature [Chin and Hercules, 1982] care should be taken when ascribing observed changes to a particles size effect.

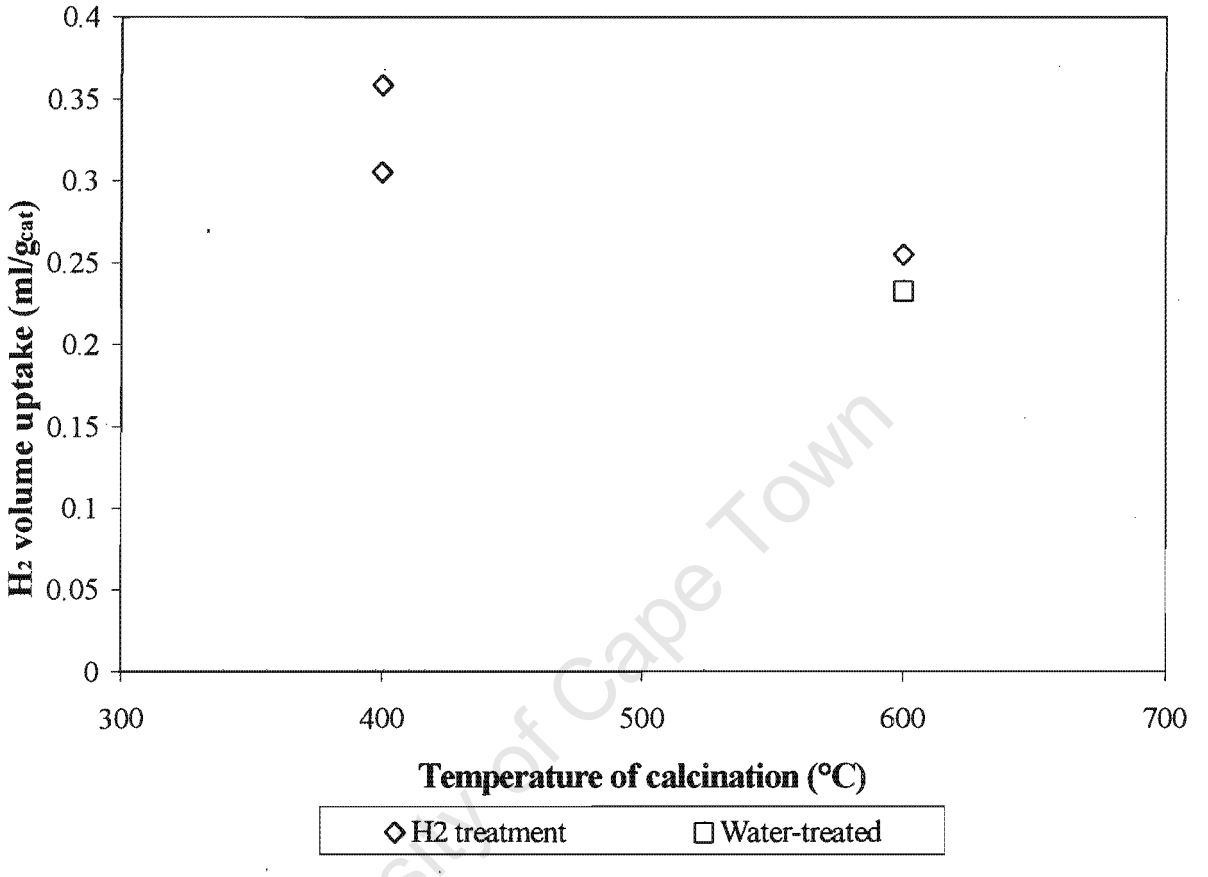

Figure 5-1: The influence of calcination temperature on the hydrogen chemisorption volume uptake

The decrease of hydrogen uptake (see Figure 5-1) with increase in calcination temperature is probably due to particle agglomeration [Niemelä *et al.*, 1997] and migration of Co^{2+} ions into the support [Chin and Hercules, 1982]. The diffusion is limited to the first few layers of the support under typical calcination conditions [Chin and Hercules, 1982].

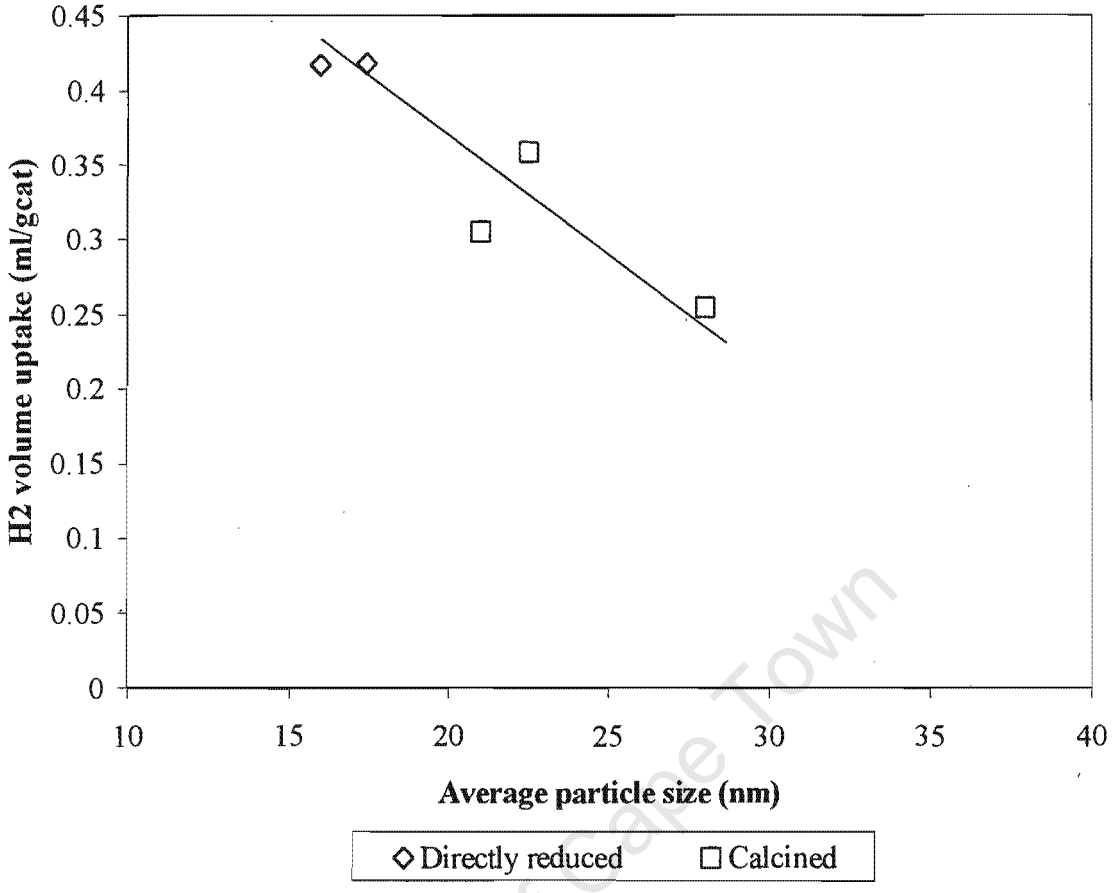

Figure 5-2: The influence of pre-treatment to obtain different particle sizes on the volume of hydrogen uptake

The volume of hydrogen uptake during hydrogen chemisorption decreases linearly with increase in particle size (see Figure 5-2). This is expected as the particle size was calculated from hydrogen chemisorption data with the degree of reduction (TPO) taken into account.

Particles agglomerate to form bigger cobalt crystallites [Coulter and Sault, 1995] and this results in loss of active sites and therefore causes a decrease in H_2 volume uptake. The pre-treatments show an influence on the degree of reduction. The degree of reduction increased with increase in particle size (see Figure 5-3). This is in contradiction with what Chin and Hercules (1982) found on the Co/Al_2O_3 catalyst i.e: the higher calcination temperature decreased the degree of reduction. Because the Co/SiO_2 catalyst reduces more easily and less sintering occurs than the Co/Al_2O_3 catalyst [Niemela *et al.*, 1997], it is possible for the silica supported catalyst to have a

higher degree of reduction at a higher temperature than for the Co/Al_2O_3 catalyst. Rosynek and Polansky (1991) found that isothermal reduction at 400°C is much less complete for an uncalcined catalyst than for the calcined materials. Calcining at higher temperatures results in a higher degree of reduction, similar to that seen in Figure 5-3.

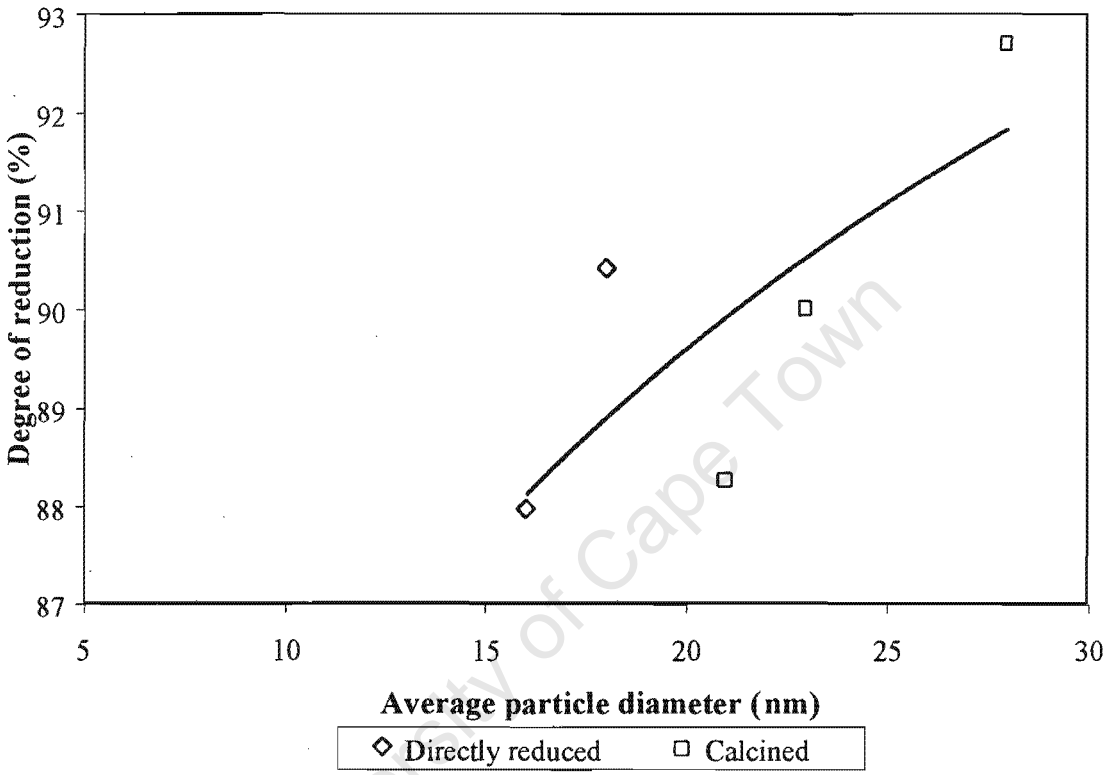

Figure 5-3: The influence of pre-treatment in order to obtain different particle sizes on the degree of cobalt reduction

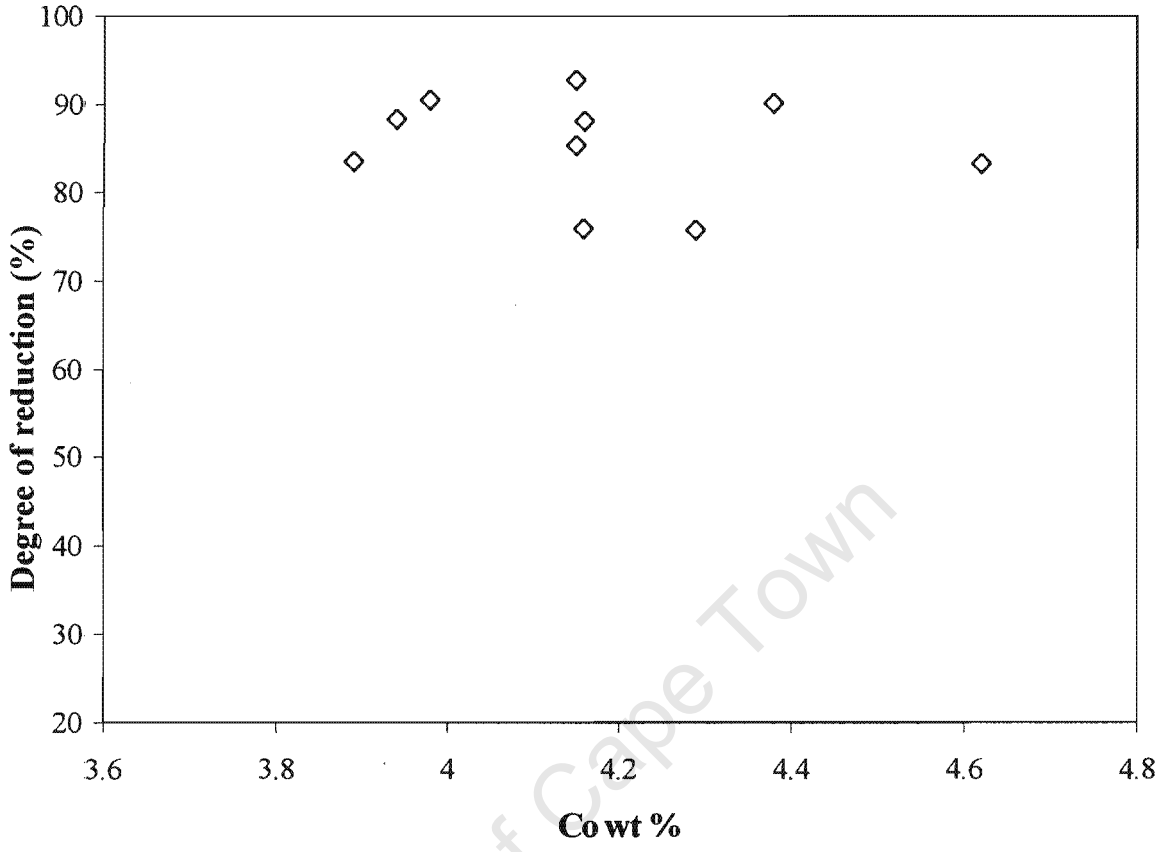

Figure 5-4: The influence of cobalt loading on the degree of reduction

5.1.2 Characterisation Methods

5.1.2.1 Atomic Adsorption Spectroscopy

The Co wt. % on the support varied with each catalyst, because the catalysts were prepared separately. This variation did not have a direct influence on the degree of reduction (see Figure 5-4).

The Co loading on the support also did not have an effect on the average particle diameter (see Figure 5-5).

The exact particle distribution could not be determined by TEM, for at least 100 photographs are needed to construct reliable statistical data. The mean particle size could be determined by H_2 chemisorption.

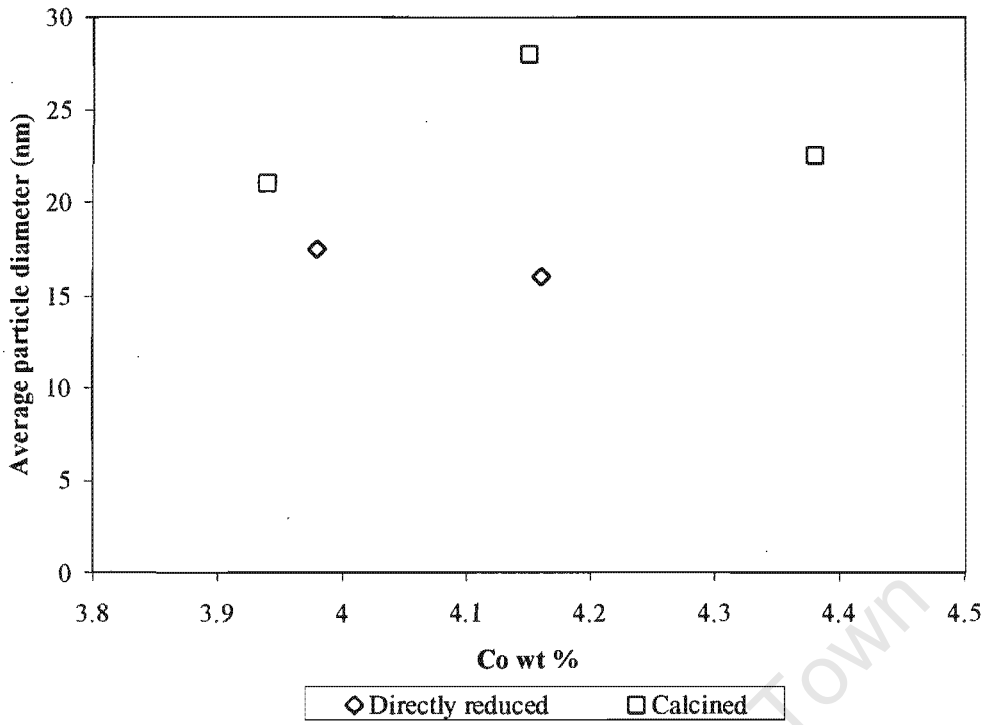

Figure 5-5: The influence of the cobalt wt % on the average particle diameter

5.1.2.2 Temperature Programmed Reduction

Hydrogen consumption above 700 K can be ascribed to the reduction of cobalt silicate. These peaks are visible at 1025 K. Figure 5-6 shows the temperature at which the maximum hydrogen consumption was observed for the low temperature region (T < 700K) and the high temperature region (T > 700K).

T_{max} decreased with increase in particle size. This effect could be the results of the higher calcination temperature used to obtain larger cobalt crystallites. The tendency of T_{max} for the high temperature consumption peak to decrease with increasing calcination temperature was observed by Arnoldy and Moulijn (1985).

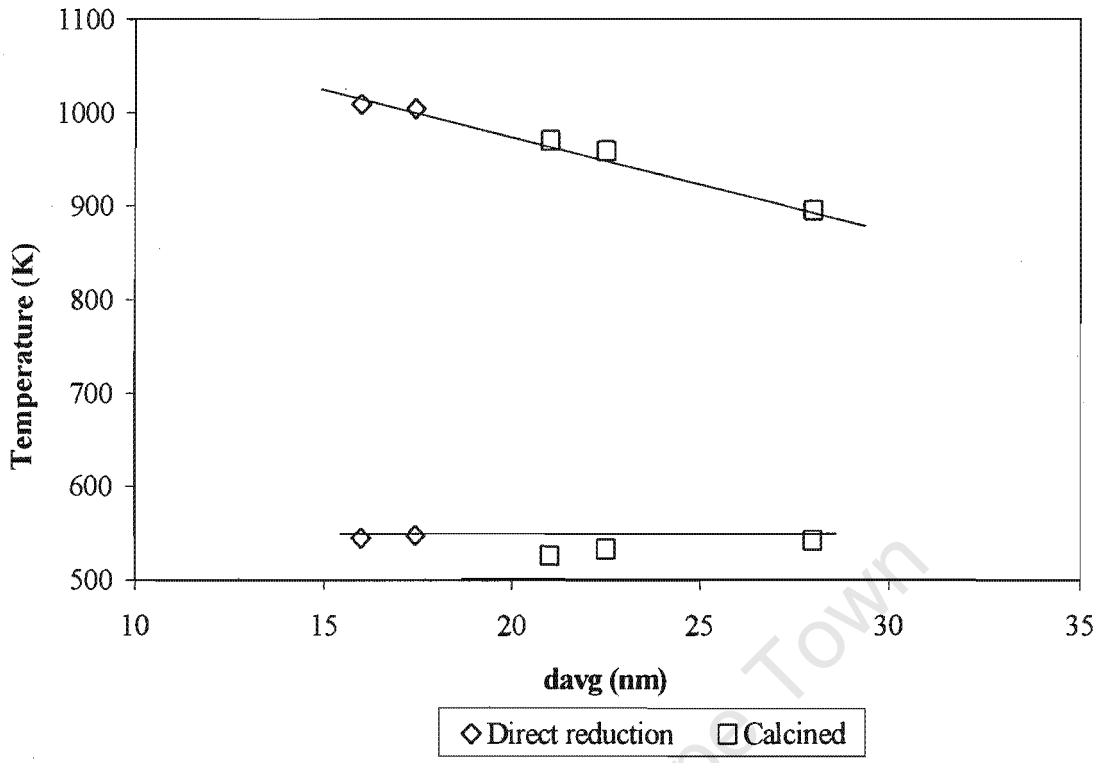

Figure 5-6: The high (T > 700K) and low (T < 700K) temperature peak maximum in the TPR spectra of the original catalysts, as a function of particle size

The low temperature hydrogen consumption peak is due to reduction of surface oxides that formed when the catalyst was exposed to the atmosphere after reduction. This low temperature peak is in the reduction region where supported Co_3O_4 and CoO reduce to cobalt metal, and indicates a re-oxidation of cobalt metal to CoO at room temperature. Arnoldy and Moulijn (1985) found a similar re-oxidation at room temperature of bulk CoO to Co_3O_4 after CoO had been prepared through the thermal reduction of Co_3O_4.

Arnoldy and Moulijn (1985) identified 4 different reduction regions of the Co/Al_2O_3 catalyst, depending on the calcination procedure and temperature. Originally it was thought that cobalt oxide existed on the support in one of two phases: β-phase that is a crystalline phase and a δ-phase where Co^{2+} ions are dispersed in the surface layers of the support. Cobalt oxide exits above 1025 K only as Co^{2+} in a metal support compound, and below 1025K as Co^{2+} and Co^{3+} [Arnoldy and Moulijn, 1985]. The

two regions observed in TPR spectra of the reduced Co/SiO_2 catalysts behave similar with increase in calcination temperature than the Co/Al_2O_3 catalyst.

T_{max} for the low temperature peak stayed constant within error of measurement, just above 500 K and is again consistent with the findings of Arnoldy and Moulijn (1985).

5.1.3 Fischer-Tropsch Synthesis

The degree of reduction varied with the particle size, due to differences in the preparation method in order to get the different particle sizes.

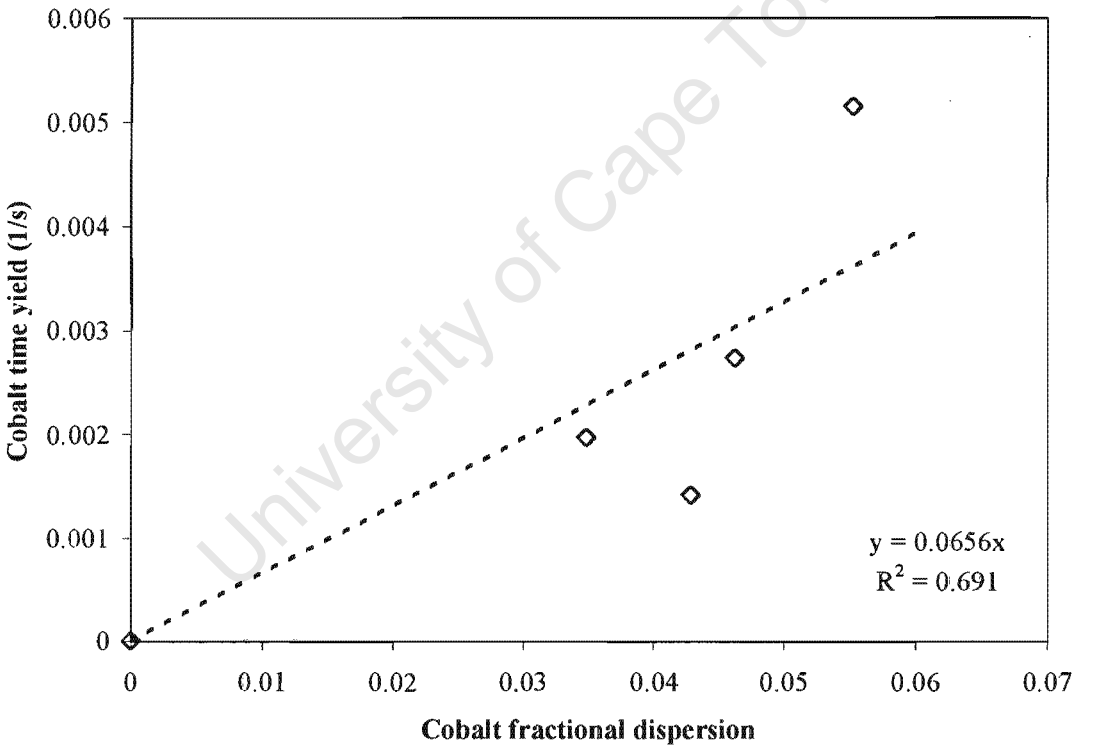

Figure 5-7: The effect of cobalt dispersion (ratio of surface Co to total Co) of the original catalysts on the FTS Co-time yields (mole CO converted/(total g·atom Co·s)). Reaction conditions: 190°C, 5 bar $H_2/CO = 2$ and low CO conversions.

At conditions that favour chain growth (80% > C_5+ selectivity), FTS rates per Co atom should increase linearly with increasing Co dispersion according to Iglesia

(1997), over the experimental dispersion range of 0.02 – 0.12. Figure 5-7 shows that the correlation is not observed in this study. The catalysts were operated at much lower conversions than those that Iglesia (1997) used. Sample calculation of turnover rate can be seen in Appendix X. Crystalline surface structure and orientation should depend to a minor extent on the crystalline diameter over the experimental dispersion range [Iglesia, 1997].

CO hydrogenation activity decreased when the cobalt catalyst underwent high temperature treatment. High temperature treatment resulted in cobalt crystallite agglomeration and thus decreased the number of active sites.

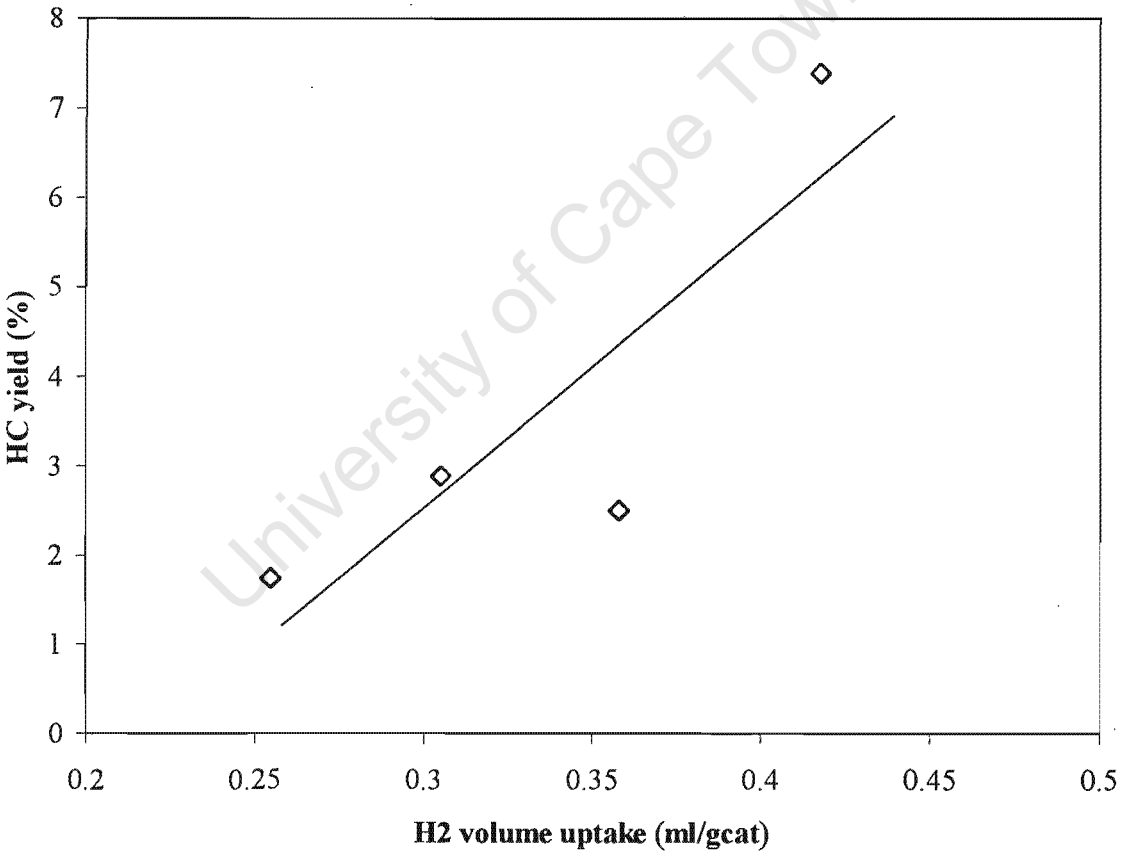

Figure 5-8: The influence of the hydrogen chemisorption volume on the hydrocarbon yield for the original catalysts

Niemelä *et al.* (1997) found a decrease in CO hydrogenation activity of the Co/SiO_2 catalyst with increase in reduction temperature, and this decrease was consistent with

a decrease in H_2 chemisorption uptake. Again the decrease in hydrogen uptake is due to particle agglomeration that leads to the loss in active sites.

5.1.3.1 Olefin Selectivity

The olefin selectivity decreases with carbon number [Schulz *et al.*, 1988] and therefore it is easier to see changes in olefin selectivity in the C13 carbon fraction than in the C8 carbon fraction.

Olefin selectivity is a function of bed and pore residence time [Iglesia *et al.*, 1991]. Readsorption leads to secondary hydrogenation yielding paraffins of the same carbon number, secondary double bond isomerisation yielding β, γ, etc. -olefins, and secondary chain growth. It is therefore expected that the paraffin content in a carbon number fraction increases with increase in pore and bed residence time. The probability for readsorption of the primarily formed products is also enhanced as the site density of cobalt increases.

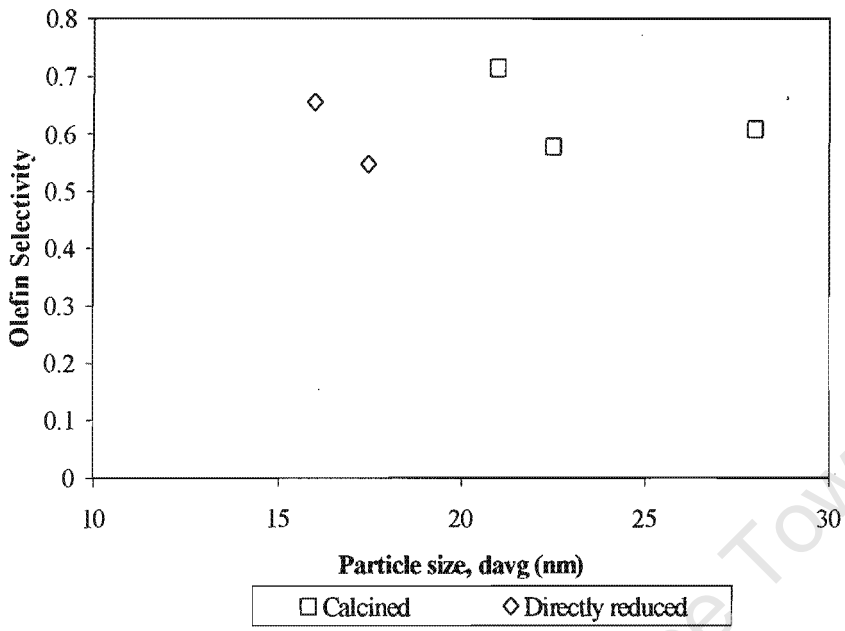

Figure 5-9: Olefin selectivity based on the C8 fraction after 24 hours, vs. average particle size

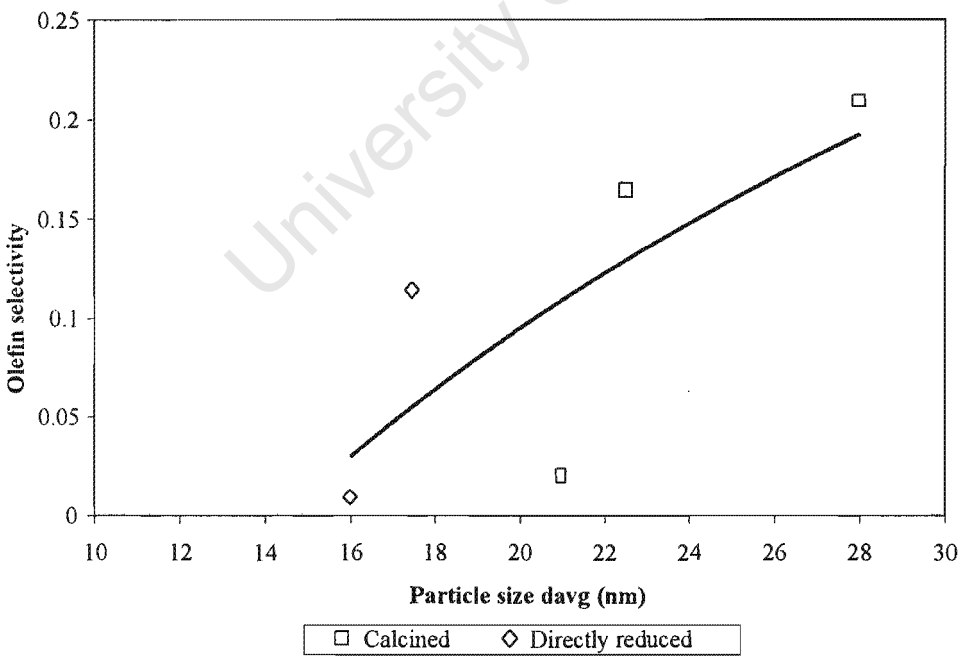

Figure 5-10: Olefin selectivity of the C13 carbon fraction vs. particle size. TOS = 24 hours

The olefin selectivity as a function of the average particle size for the C8 fraction and the C13 fraction are shown in Figure 5-9 and 5-10, respectively. The olefin content in the C8 fraction remained almost constant with particle size. It is not clear from literature whether this is the primary olefin selectivity for C8 under the conditions measured. The olefin selectivity in the C13 fraction increased strongly with increasing particle size. The smaller particles exhibit a higher site density. This leads to a high local concentration of olefins around the active sites and this enhances the readsorption of olefins which leads to a decrease in olefin selectivity.

Figure 5-11 shows the α-olefin selectivity in the fraction of C8-olefins to increase with increase in particle size. α–olefins are thought to be the primary products in the Fischer-Tropsch synthesis. Due to secondary double bond isomerisation, the α-olefin selectivity decreases. The probability for secondary reactions is enhanced if the site density of cobalt is high. A high site density is obtained at with catalysts with small cobalt particle sizes and a low site density is obtained with large cobalt particles. It is thus expected that the α-olefin selectivity would increase with increasing cobalt particle size.

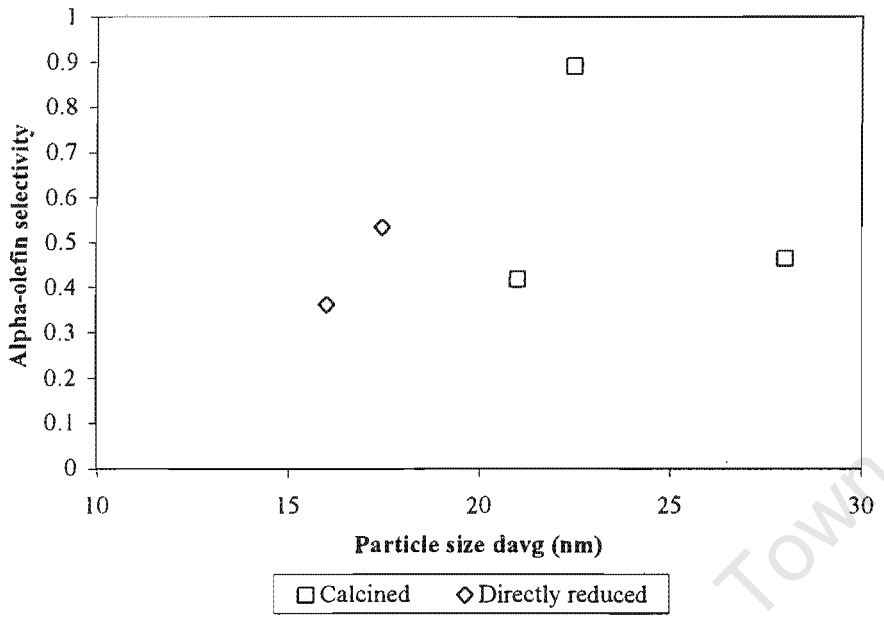

Figure 5-11: Alpha-olefin selectivity based on C8 carbon fraction, after 24 hours.

5.1.3.2 Chain Growth Probability

Figure 5-12 shows the probability for chain growth as a function of the average particle size. A decrease in the probability for chain growth can be observed. The probability for secondary reactions is enhanced if the site density of cobalt is high, i.e. with catalysts with small cobalt particle sizes. Re-adsorption can lead to further chain growth with cobalt based catalysts. It is thus expected that the chain growth probability decrease with increasing cobalt particle size, which is roughly observed. The calcined catalysts exhibit a lower chain growth probability than the directly reduced catalyst.

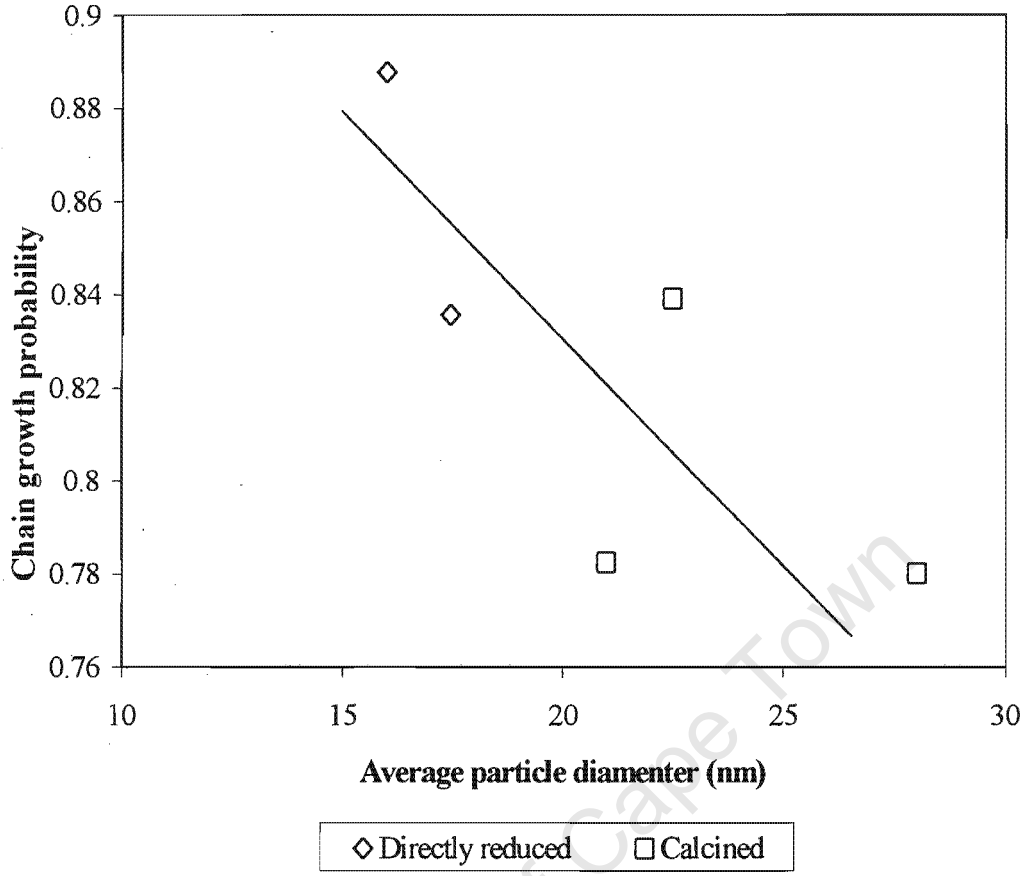

Figure 5-12: The chain growth probability (α) as a function of average particle diameter

Niemelä *et al.* (1997) found a decrease in activity with increase in reduction temperature, but no significant changes in the chain growth probability or product distribution. Fan *et al.* (1997) noticed that a higher calcination temperature (150°C-450°C) favoured carbon chain growth, resulting in a larger growth probability and low conversion. Others have shown that calcination does not affect the chain growth probability when the Co/Al_2O_3 is promoted with Ru [Belambe *et al.*, 1997].

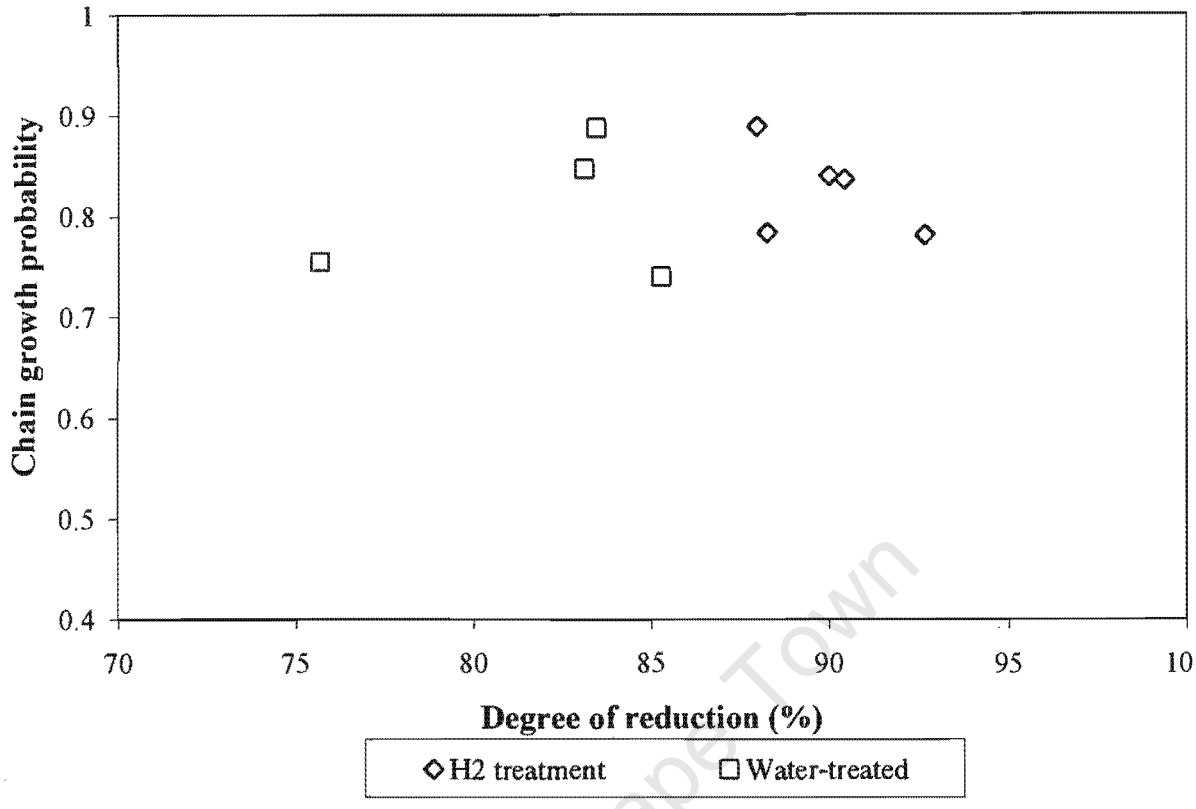

Figure 5-13: Effect of degree of reduction on the chain growth probability

Figure 5-13 shows the effect of the degree of reduction on the chain growth probability. No clear correlation could be ascertained. The water-treated catalysts all have a lower degree of reduction than the original catalysts, but no sharp changes in chain growth probability due to water treatment is visible.

5.1.4 Re-oxidation of Cobalt

The Co/SiO_2 catalysts underwent water treatment prior to reaction using low water partial pressures (0.2 bar) corresponding to H_2/H_2O ratio of 4. The catalyst was first reduced in 60 ml (STP)/min H_2 at 400°C for 16 hours. The catalyst was cooled down to 200°C in H_2 where it was exposed to the water/hydrogen mixture for 24 hours.

5.1.4.1 Validity of Testing Method

There are several ways of studying the effect of water (possible re-oxidation) on the supported cobalt catalyst. Water can be added in different partial pressures to the feed

stream in the Fischer-Tropsch synthesis [Schulz *et al.*, 1995a, Rothaemel *et al.*, 1997, Iglesia, 1997 and Schanke *et al.*, 1995] or the catalyst can undergo hydrothermal treatment, prior to Fischer-Tropsch synthesis [Kogelbauer *et al.*, 1995, Hilmen *et al.*, 1997 and Schanke *et al.*, 1995] to simulate the Fischer-Tropsch reaction conditions.

When water is added to the reactor feed stream, an increase in chain growth and olefin selectivity is observed [Schulz *et al.*, 1995a]. These effects are often reversible with removal of water from the feed stream. Schanke *et al.* (1995) observed a deactivation of the Co/Al_2O_3 that was also reversible upon removal of water from the feed stream.

Changes in the reaction parameters and respective changes of catalyst chemisorbate composition can cause specific inhibition of discrete reaction pathways and will lead to changes in product composition and overall reaction rate [Schulz *et al.*, 1995a]. Secondary hydrogenation is inhibited at high water concentrations [Schulz *et al.*, 1995a] that causes the observed increase in α-olefin content. These observations are related to the kinetic effect that water has on the Fischer-Tropsch reaction pathways, and not necessarily to the effect on catalyst deactivation.

When water is co-fed with the syngas, the effects of water on the catalyst (e.g. decrease in activity) can only be observed after water has been removed from the feed stream. If the observations are made during water treatment under Fischer-Tropsch conditions, kinetic effects of water might be confused with changes in catalyst.

Hydrothermal treatment of the catalyst prior to reaction seems to be the better option. This method has been proved to simulate Fischer-Tropsch conditions adequately: Schanke *et al.* (1995) reported that co-feeding water to the syngas under reaction conditions or pre-treatment of the catalyst with water prior to reaction leads to similar results with respect to catalytic activity after water has been removed from the feed stream.

5.1.4.2 The Observed Deactivation due to Water Treatment

A decrease of reducibility (Table 4-1) and hydrogen uptake during H_2 chemisorption (Table 4-2) was observed.

The deactivation upon water treatment observed can be ascribed to a decrease in reducible metal. Rothaemel *et al.* (1997) ascribed the deactivation caused by water on Co/Al_2O_3 and $Co/Re/Al_2O_3$ as loss in active sites. The intrinsic activity of the catalyst remains the same [Rothaemel *et al.*, 1997]. The decrease in the degree of reduction is accompanied by an increase in metal support compound. The same observations have been made by Hilmen and co-workers (1997), Kogelbauer *et al.* (1995) and Schanke *et al.* (1996).

The formation of a metal support compound when the catalyst is exposed to a H_2/H_2O mixture is thermodynamically feasible (see Figure 2-14.)

5.1.4.3 The Influence of Particle Size on the Re-oxidation of Cobalt

The deactivation of a catalyst concerns the decrease in the concentration of active sites (N_{sites}) of the catalyst [Ertl *et al.*, 1997]. If N_D is expressed as the deactivated sites, then the degree of deactivation can be expressed as

$$\Phi_{sites} = \frac{Number\ of\ deactivated\ sites}{Total\ number\ of\ active\ sites} = \frac{N_D}{N_{sites}}$$

The amount of active sites is determined by the use of hydrogen chemisorption measurements. The volume of hydrogen chemisorbed is related to the active cobalt sites available. Deactivation can thus be expressed in terms of decrease in volume of hydrogen chemisorbed after water treatment:

$$\Phi_{H2\,ads} = 1 - \frac{V_{H2}\ after\ H_2O\ treatment}{V_{H2}\ fresh\ catalyst}$$

where $V_{H2}\,after\ H_2O\ treatment$ indicates the volume of hydrogen chemisorbed on the deactivated catalyst and $V_{H2}\,fresh\ catalyst\ treatment$ indicates the volume of hydrogen chemisorbed on the fresh catalyst.

In Figure 5-14 the degree of deactivation is shown as a function of cobalt particles size. The smaller the particle size, the larger deactivation is observed. According to Iglesia (1997) very small Co particle sizes (5-6 nm) are difficult to achieve during synthesis and they appear to re-oxidise and deactivate rapidly in the presence of water reaction products of typical FTS conditions.

Co/Al_2O_3 promoted by Re exhibited a larger deactivation when treated with He/H_2O as well as H_2/H_2O, than unpromoted Co/Al_2O_3, as investigated by Hilmen *et al.* (1997). Re is a structural promoter of supported Co catalysts and acts by preventing agglomeration of CoO_x particles during calcination treatments [Iglesia, 1997]. Higher cobalt dispersions can be obtained by promoting Co with Re.

Smaller particles undergo a greater degree of deactivation by re-oxidising the cobalt catalyst. This can be explained by the increased surface area of the smaller particles, which leads to a larger thermodynamic driving force for re-oxidation of the cobalt catalyst with water (see Chapter 2).

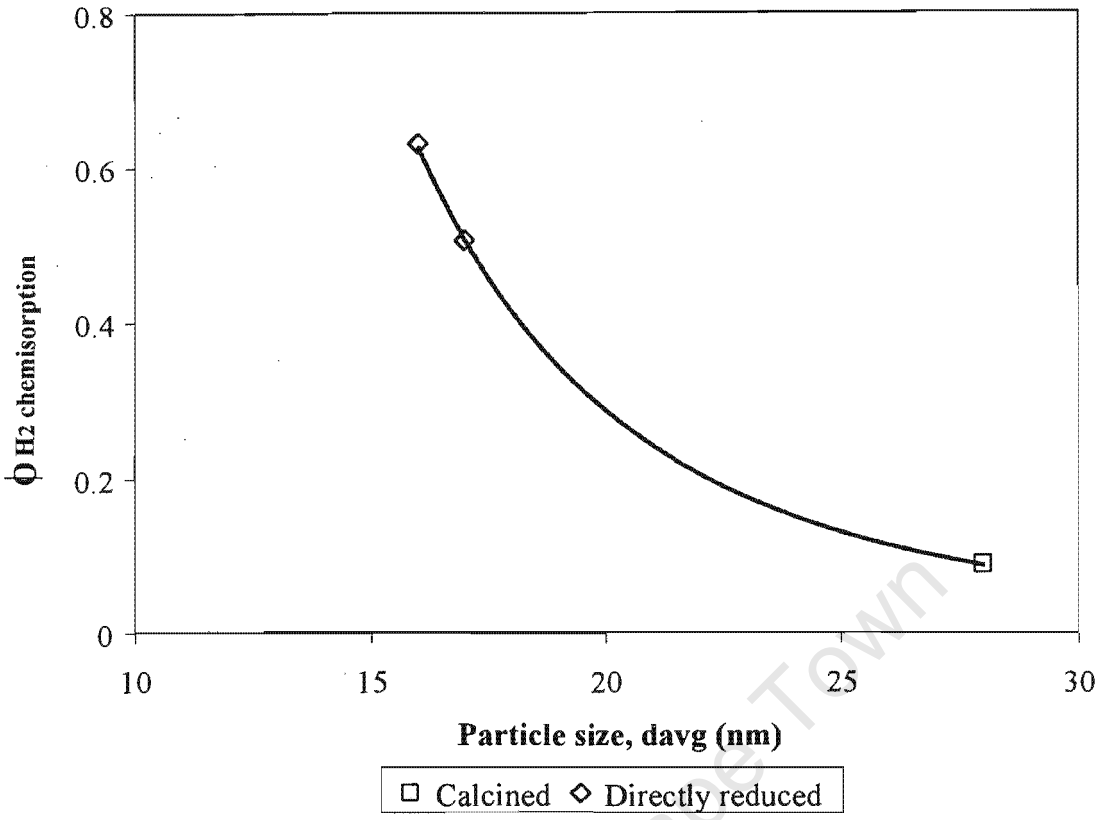

Figure 5-14: The deactivation due to water treatment as a function of the cobalt crystallite size.

Because the oxidation by water is a surface oxidation, more available surface area will lead to a larger deactivation. If the particles are very small (5-6 nm) complete oxidation of the particles will become possible.

Larger surface areas also mean more contact between the metal and the support and thus it is more likely to form an increased amount of metal-support interaction induced by water treatment.

If the catalyst is re-oxidised with water, the oxidised particles are not available for hydrogen chemisorption. Consequently the number of sites available for the Fischer-Tropsch polymerisation reaction is decreased. The decrease in active sites leads to a decrease in hydrocarbon yield.

The degree of deactivation in the Fischer-Tropsch synthesis (Φ_{FT}) can be defined as the decrease in yield of hydrocarbons due to water treatment, relative to the yield of hydrocarbons of the fresh catalyst after 24 hours of reaction:

$$\Phi_{FT} = 1 - \frac{Y_{HC}, water\ treated\ catalyst}{Y_{HC}, fresh\ catalyst}$$

where Y_{HC} is the total yield of hydrocarbons. Figure 5-15 shows the degree of deactivation as a function of average cobalt particle size.

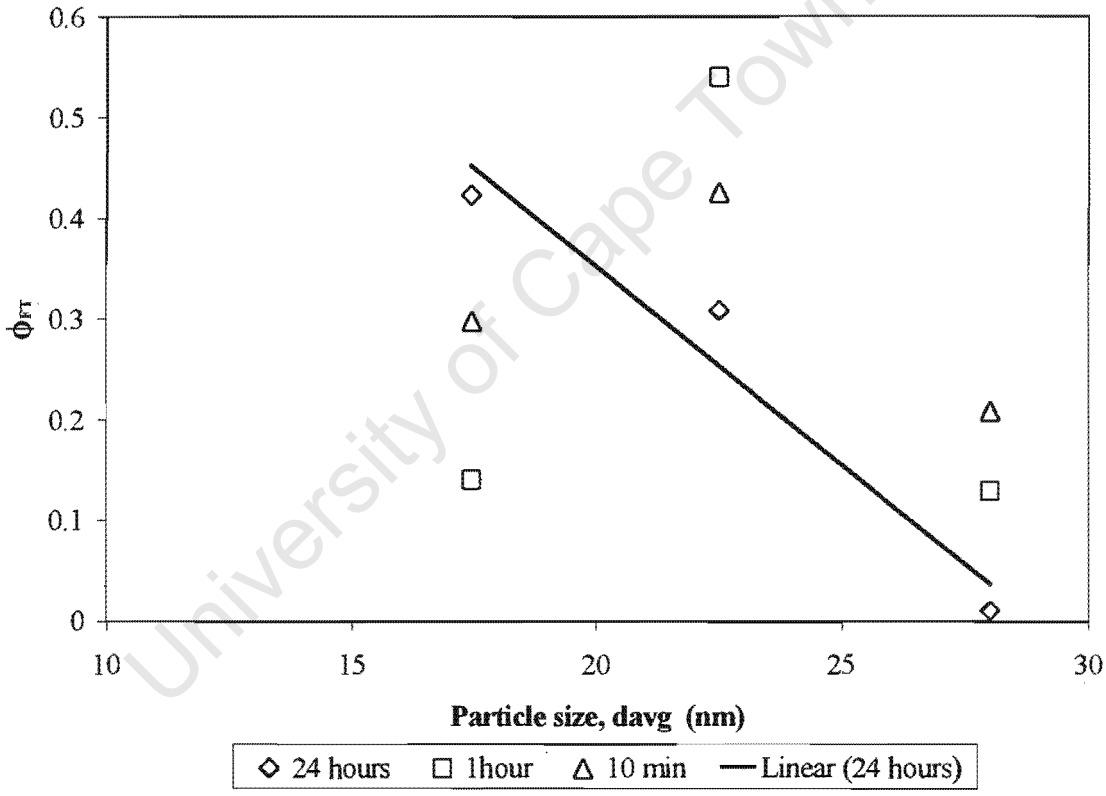

Figure 5-15: The degree of deactivation in the Fischer-Tropsch synthesis as a function of average cobalt particle size

After 24 hours of reaction, the smaller cobalt particles show a larger degree of deactivation in the hydrocarbon yield than the catalyst with larger cobalt particles. The degree of deactivation after 24 hours time on stream, decrease linearly with increase in particle size.

CHAPTER 6

Conclusions

6. CONCLUSIONS

The objective of this study was to investigate the influence of cobalt crystallite size in Co/SiO_2 Fischer-Tropsch catalysts on the re-oxidation of cobalt with product water. For this purpose a number of Co/SiO_2-catalysts with different cobalt crystallite sizes were prepared by varying the preparation variables.

Supported cobalt catalysts do not always have a homogenous particle distribution. The average cobalt particle size was estimated using H_2-chemisorption, which is a reliable method for determining the average crystallite size. The cobalt particle size distribution can be estimated using transmission electron microscopy. However, at least 100 TEM photographs are necessary for an acceptable particle distribution to support the H_2 chemisorption data.

Calcining the Co/SiO_2 catalyst at 400°C resulted in an average cobalt crystallite size of 22 nm. Calcination at 600°C yielded an average cobalt crystallite size of 28 nm. The increase in the average particle size can be attributed to agglomeration of smaller particles at higher temperatures. Even larger cobalt crystallites can be obtained at a metal loading higher than the minimum loading for a monolayer of cobalt on the support. At high temperatures, where cobalt becomes mobile, the particles will agglomerate [Chin and Hercules, 1982]. If a high temperature calcination step is performed at metal loading lower than the loading required for a monolayer, migration of cobalt particles into the support might occur.

Agglomeration of cobalt particles can be avoided by omitting the calcination step and directly reducing the catalyst in hydrogen. NO_x formed as a product of the nitrate precursor decomposition is a strong oxidant. By controlling the NO_x and water partial pressures during the reduction even smaller cobalt particles can be obtained. The control of these partial pressures, and thus the particle size, can be achieved by applying high

flowrates of the reducing gas and slow heating rates. An average cobalt particle size of 16nm was obtained by a slow reduction heating rate (0.5 °C/min). A normal heating rate of 10°C/min yielded an average particle size of 18 nm. It has been reported in literature that cobalt particles as small as 5 nm can be achieved by controlled decomposition of the nitrate precursor and by CVD of cobalt carbonyl [Iglesia, 1997].

The preparation method caused the degree of reduction to vary with cobalt particle size. At high calcination temperatures, high degree of reduction might be achieved but the agglomeration of particles caused a decrease in catalyst activity. The supported cobalt catalyst becomes mobile above the Hüttig temperature (316°C). At very high temperatures excessive sintering takes place. Bulk cobalt becomes mobile at temperatures above the Tamman temperature (611°C). Optimum dispersion has been obtained by reducing the catalyst just above the Hüttig temperature (350°C) [Niemelä *et al.*, 1997].

Activity is directly related to the amount of metal sites available for dissociative hydrogen and carbon monoxide chemisorption. The H_2 uptake at 100°C decreased from 0.418ml/g_{cat} to 0.253ml/g_{cat} with increase in average cobalt particle size from 18nm to 28 nm. This indicates that the agglomeration of cobalt particles results in loss of active sites.

The Fischer-Tropsch synthesis is structure insensitive [Iglesia, 1997]. (Previously, it was reported that the reaction was structure sensitive [Bartholomew and Reuel, 1984], but this can be ascribed to the change in the degree of reduction when modifying the dispersion). The activity should thus increase linearly with increasing dispersion, but a linear dependency was not observed. This might be ascribed to the deactivation of the catalysts with time on stream. Increasing the calcination temperature resulted in a decrease in hydrocarbon yield. This shows again that, upon calcination, active sites are lost due to particle agglomeration.

Olefin selectivity decreases with carbon number [Schulz *et al.*, 1988] due to re-adsorption and secondary hydrogenation. For comparison of the olefin selectivity of the various

catalysts, the carbon number fraction must be chosen in such a way that changes in olefin selectivity can be clearly seen. The C13 carbon fraction showed changes that are more distinct in olefin selectivity where C8 exhibited clear changes in the α-olefin selectivity. Both C13 and C8 fractions were therefore used for comparisons.

Calcination resulted in particle agglomeration and decreased the cobalt site density. This diminishes the probability for re-adsorption of olefins and could be observed by the increase in olefin selectivity and α-olefin selectivity with increasing particle size. The observed decrease in olefin re-adsorption with larger cobalt particle sizes is accompanied by a decrease in chain growth probability.

The re-oxidation of bulk metallic cobalt is thermodynamically not feasible, although surface atoms, which are exposed to a different environment than the atoms in the bulk, might re-oxidise. Iglesia (1997) observed that very small particles, 5-7nm, oxidise easily under Fischer-Tropsch synthesis conditions. The formation of a metal support compound under hydrothermal conditions is feasible (see Chapter 2). Strong metal support interaction is considered to be an irreversible deactivation of the catalyst because cobalt silicates cannot be reduced at the normal reduction temperatures of the catalyst. Deactivation in a water treatment can then be visualised as loss of active sites due to an increase in the formation of the metal-support compound and a small amount of cobalt surface oxidation.

Niemelä and Krause (1996) found that the Co/SiO_2 deactivates at a rate proportional to the extent of dispersion, i.e. the higher dispersion, the higher the rate of deactivation. This can be ascribed to a larger amount of metal support interaction formed due to a greater contact between the metal and the support at higher dispersions

The effect of water during the Fischer-Tropsch synthesis was simulated by passing a hydrogen-water mixture (H_2:H_2O = 4) over the catalyst at 200°C and atmospheric pressure. This hydrothermal treatment was considered to simulate the Fischer-Tropsch

synthesis adequately, since the hydrocarbon yield for the original catalyst after 24 hours was similar to the 24 hour water-treated catalyst at the start of the reaction. Hence, the deactivation caused by 24 hours of water treatment might be similar to the deactivation induced by water as a product in Fischer-Tropsch synthesis after 24 hours of reaction. The average cobalt particle or cluster size (TEM) did not change after treatment of the catalyst with a hydrogen-water mixture.

In temperature programmed reduction (TPR) a shift of the low temperature maximums towards higher temperatures was observed after water treatment. The amount of non-oxidisable cobalt increased after water treatment for each catalyst. This clearly shows that water treatment induces metal-support formation as reflected in a decrease of the degree of reduction. The decrease in the degree of reduction is accompanied by a decrease in H_2-uptake (which can be translated directly into a metal surface area). Since the activity is linked to the metal surface area, the activity of the catalysts (as measured with the yield of hydrocarbons) treated with the hydrogen-water mixture was lower.

The olefin selectivity increased after water treatment. Olefin re-adsorption is enhanced with increasing density of Co-sites. The observed increase in the olefin selectivity can thus be ascribed to the decrease in number of active sites.

It has been reported that there is an increase in chain growth probability when water is co-fed with reactants [Schulz *et al.*, 1995a], due to a kinetic effect of water on the Fischer-Tropsch synthesis. No distinct trends with regard to the chain growth probability could be made after passing a hydrogen-water mixture over the catalyst.

Catalysts with smaller cobalt particles have higher surface areas and more contact between cobalt and the support. For higher dispersions a larger probability exists thus to form more of the metal-support compound. Deactivation can be expected to take place until all cobalt in direct contact with the support is oxidised.

REFERENCES

Adesina A., A., *Appl. Catal. A: General* **138**, 345 (1996). "Hydrocarbon synthesis via Fischer-Tropsch reaction: travails and triumphs."

Anderson, J.R., Academic Press, London, New York, San Francisco (1975). "Structure of Metallic Catalysts"

Anderson, J., R., Pratt, K., C., Academic Press, Sydney, Orlando, San Diego, New York, London, Toronto, Montreal, Tokyo, (1985). "Introduction to Characterisation and Testing of Catalysts."

Anderson, R., B., "The Fischer-Tropsch Synthesis", Academic Press, Inc. Orlando (1984).

Araki, M., Ponec, V., *J. Catal.* **44**, 439, (1976)."Methanation of Carbon Monoxide on Nickel and Nickel-Copper Alloys"

Arnoldy, P. and Moulijn, J.A., *J. of Catal.* **93**, 38 (1985). "Temperature-Programmed Reduction of CoO/Al_2O_3"

Atkins, P.W., "Physical Chemistry", Oxford University Press, Oxford, 4th ed. (1990).

Bartholomew, C.H., and Farrauto, R. J., *J. Catal.* **45**, 41 (1976). "Chemistry of Nickel-Alumina Catalysts."

Belambe, A.R., Oukaci, R., and Goodwin J.G. Jr., *J. Catal.* **166**, 8 (1997). "Effect of Pretreatment on the Activity of a Ru-Promoted Co/Al_2O_3 Fischer -Tropsch Catalyst."

Bonneviot, L., Clause, O., Che, M., Manceau, A. and Dexpert, H., *Catalysis Today* **6**, 39 (1989). "EXAFS characterisation of the adsorption sites of nickel amine and ethylenediamine complexes on a silica surface."

Boskovic, G. and Smith, K., J., *Catalysis Today* **37**, 25 (1997). "Methane homologation and reactivity of carbon species on support Co catalysts."

Brady III, R., C., and Pettit, R., *J.Am.Chem. Soc.* **103**, 1287 (1981). "On the Mechanism of the Fischer-Tropsch Reaction. The Chain Propagation step."

Chin, R. L., and Hercules, D. M., *J. Phys. Chem.* **86**, 360 (1982). "Surface Spectroscopic Characterisation of Cobalt-Alumina Catalysts"

Choi, J., *Catal. Lett.* **35**, 291 (1995). "Reduction of supported cobalt catalysts by hydrogen."

Coulter, K. E. and Sault, A. G., *J. Catal* **154**, 56 (1995). "Effects of Activation on Surface Properties of Silica-Supported Cobalt Catalysts."

Dry, M.E., Springen-Verlag, Berlin, vol. **1**, (Anderson, J. R. and Boudart, M. Eds) p159 (1981), "Catalysis: Science and Technology",

Dry, M. E., *Applied Catalysis A: General* **138**, 319 (1996). "Practical and theoretical aspects of catalytic Fischer-Tropsch process"

Ertl, G., Knözinger, H., Weitkamp, J., (Eds.) vol. **1**, p1-10, 49,50, vol. **2**, p427-464,676-698 (1997). "Handbook of Heterogeneous Catalysis."

Fan, L., Yoshii, Yan, S., Zhou, J., Fujimoto, K., *Catalysis Today*. **36**, 295 (1997). "Supercritical-phase for selective synthesis of wax from syngas: Catalyst and process development"

Fischer, F., Tropsch, H., *Brennstoff-Chem.* **7**, 97, (1926). "Die Erdölsynthese bei gewönlichem Druck aus den Vergasungsprodukten der Kohlen"

Freemantle, M., *C&EN*, August 12, 31 (1996). "New Catalytic Cycle Proposed For Fischer-Tropsch Sythesis"

Geerlings, J.J.C., Zonnevylle, M.C., and de Groot, C.P.M., *Surf. Sci.* **241**, 302 (1991).

Hanssen, K.F., Blekkan, E.A., Schanke, D. and Holmen, A., *Stud. Surf. Sci. Catal.* **109**, 193 (1997). "Transient and Steady-State Studies of the Effect of Water on Cobalt Fischer-Tropsch Catalysts."

Hilmen, A.M., Schanke, D. and Holmen, A., *Catal. Lett.* **38**, 143 (1996). "TPR study of rhenium promotion of alumina-supported cobalt Fischer-Tropsch catalysts."

Hilmen, A.M., Schanke, D. and Holmen, A., in *Natural Gas Conversion IV:* Studies *in Surface Science and Catalysis* **107** (de Pontes, M., Espinoza, R.L., Nicolaides, C.P., Scholz,

J.H. and Scurrell, M.S. Eds.), p237 Elsevier Science B.V. (1997). "Reoxidation of supported cobalt Fischer-Tropsch catalysts"

Iglesia, E., Reyes, S.C. and Madon R.J., *J. Catal.* **129**, 238 (1991). "Transport-Enhanced α-Olefin Readsorption Pathways in Ru-Catalyzed Hydrocarbon Synthesis"

Iglesia, E., Soled, S. L. and Fiato, R., *J. Catal.* **137**, 212 (1992). "Fischer-Tropsch Synthesis on Cobalt and Ruthenium. Metal Dispersion and Support Effects on Reaction Rate and Selectivity."

Iglesia, E., Reyes, S. C, Madon, R.J. and Soled, S.L, Advances in Catalysis. **39**, 221, (1993). "Selectivity Control and Catalyst Design in the Fischer-Tropsch Synthesis: Sites, Pellets and Reactors."

Iglesia, E., Soled, S. L., Baumgartner, J. E., and Reyes, S. C., *J. Catal.* **153**, 108 (1995). "Synthesis and Catalytic Properties of Eggshell Cobalt Catalyst for the Fischer-Tropsch Synthesis "

Iglesia, E., *Appl. Catal. A: General* **161**, 59 (1997). "Design, synthesis, and use of cobalt-based Fischer-Tropsch synthesis catalysts"

Jager, B. and Espinoza, R., *Catal. Today* **23**, 17 (1995). "Advances in low temperature Fischer-Tropsch synthesis"

Jager, B., Kelfkens, R.C., and Steynberg, A.P. in *Natural Gas Conversion II,* (Curry-Hyde, H.E. and Howe, R.F. Eds.), p419 Elsevier Science B.V. (1994). "A Slurry bed reactor for low temperature Fischer-Tropsch"

Johnson, B.G., Batrholomew, C.H., and Goodman W.D., *J. Catal.* **128**, 231 (1991). "The Role of Surface Structure and Dispersion in CO Hydrogenation on Cobalt."

Knacke, O., Kubaschewski, O., Hesselmann, K., "Thermochemical Properties of Inorganic Substances", Springer-Verlag, Berlin, 2nd ed. (1991).

Kogelbauer, A., Weber, J. C. and Goodwin J.G. Jr., *Catal. Lett.* **34**, 259 (1995). "The formation of cobalt silicates on Co/SiO_2 under hydrothermal conditions."

Krishna, K., R. and Bell, A., T., *Catal. Lett.* **14**, 305 (1992). "The role of C_2 intermediates in Fischer-Tropsch synthesis over ruthenium."

Krishna, K., R. and Bell, A., T., New Frontiers in Catalysis, *Stud. Surf. Sci Catal.*. (1993). "Isotopic Tracer Studies of Chain Propagation and termination during Fischer-Tropsch Synthesis over Ru/TiO_2."

Maitlis, P.M, Long, H.C., Quyoum, R., Turner, M.L. and Wang, Z., Chem Commun., pg1 (1996). " Heterogeneous catalysis of C-C bond formation; black art or organometallic science?"

Ming, H., Baker, B.G., *Applied Catal. A: General* **123**, 23 (1995). "Characterisation of cobalt Fischer-Tropsch catalyst I. Unpromoted cobalt-silica gel catalyst."

Moulijn, J.A., van Leeuwen, P. W. N. M. and van Santen, R.A., (Eds) Nederlans Institute for Catalyst Research (1993). "Catalysis: An Integrated Approach to Homogenoues, Heterogeneous and Industrial Catalysis."

Niemelä, M. K., Backman, L., Krause, A.O.I., Vaara, T., *Appl. Catal. A: General* **156**, 319 (1997). "The activity of the Co/SiO_2 catalyst in relation to pretreatment."

Niemelä, M. K. and Krause, A.O.I., *Catal. Lett.* **42**, 161 (1996). "The long-term performance of Co/SiO_2 catalyst in CO hydrogenation."

Nijs, H. H. and Jacobs, P. A., *J. Catal.* **66**, 401 (1980). "New Evidence for the Mechanism of the Fischer-Tropsch Synthesis of Hydrocarbons"

Okamoto, Y., Nagata, K., Adachi, T., Imanaka, T., Inamura, K. and Takyu, T., *J. Phys. Chem.* **95**, 310 (1995). "Preparation and Characterisation of Highly Dispersed Cobalt Oxide and Sulphide Catalyst Supported on SiO_2."

Perego, C., Villa, P., *Catalysis Today* **34**, 281 (1997). "Catalyst preparation methods."

Pichler, H., Schulz, H., *Chem. Ing. Techn.* **42**, 1162, (1970). "Neuere Erkenntnisse auf dem Gebiet der Synthese von Kohlenwasserstoffen aus CO und H_2"

Pines, H., "The Chemistry of Catalytic Hydrocarbon Conversions.", Academic Press, London, (1981).

Puskas, I., Fleisch, T. H., Hall, J. B., Meyers, B. L. and Roginski, R. T., *J. Catal* **134**, 615 (1992). "Metal-support Interactions in Precipitated, Magnesium-Promoted Cobalt-Silica Catalyst"

Quyoum, R., Berdini, V., Turner, M., L., Long, H., C., and Maitlis, P., M., *J. Catal* **173**, 355 (1998). "Mechanistic Studies of Methylene Chain Propagation in the Fischer-Tropsch Synthesis."

Reuel, R. C. and Bartholomew, C. H., *J. Catal.* **85**, 63 (1984). "The Stoichiometries of H_2 and CO Adsorptions on Cobalt: Effects of Support and Preparation."

Riva, J., P., *Congressional Research Service: report for Congress.* http://www.cnie.org/nle/eng-3.htm (1995). "World Oil Production After Year 2000: Business As Usual or Crises?"

Roine, A., Outokumpu Reasearch (1994). "HSC Chemistry for Windows 2.0: Chemical Reaction and Equilibrium Software with extensive Thermochemical Database"

Rosynek, M.P. and Polansky, C.A., *Applied Catalysis* **73**, 97 (1991). "Effect of cobalt source on the reduction properties of silica-supported cobalt catalysts."

Rothaemel, M., Hanssen, K.F., Blekkan, E.A., Schanke, D., Holmen, A., *Catalysis Today* **1065**, 1 (1997). "The effect of water on cobalt Fischer-Tropsch catalyst studied by steady-state isotopic transient kinetic analysis (SSITKA)."

Schanke, D. Hilmen, A.M. Bergene, E., Kinnari, K., Rytter, E., Ådenanes, E. and Holman, A., *Catal. Lett.* **34**, 269 (1995). "Study of the deactivation mechanism of Al_2O_3-supported cobalt Fischer-Tropsch catalyst."

Schanke, D., Hilmen, A.M., Bergene, E., Kinnari, K., Rytter, E., Ådnanes, E. and Holmen, A., *Energy & Fuels* **10** (4), 867 (1996). "Reoxidation and Deactivation of Supported Cobalt Fischer-Tropsch Catalysts."

Schulz, H., Beck, K., Erich, E., *Fuel. Proc Tech.* **18**, 293 (1988). "Kinetics of Fischer-Tropsch Selectivity."

[a]Schulz, H., Claeys, M., and Harms, S., *4th Int. Nat. Gas Conv. Symp.* (Krugerpark SA 1995). "Effect of water partial pressure on steady state Fischer-Tropsch activity and selectivity of a promoted cobalt catalyst."

[b]Schulz, H., van Steen, E., and Claeys, M., *Topics in Catalysis* **2**, 233(1995). "Mechanistic Approach for Describing the Rate of CO-consumption in Fischer-Tropsch CO-Hydrogenation."

Sewell, G.S. PhD Thesis (1996). "The reductive amination of ethanol using supported metal catalyst."

Sewell, G.S., van Steen, E., and O'Connor, C.T., *Catal. Lett.* **37**, 255 (1996). "Use of TPR/TPO for characterisation of supported cobalt catalysts".

Somorjai, G.A., "Introduction to surface chemistry and catalysis", John Wiley & Sons, Inc., New York, (1994)

Storch, H., H., Golumbic, N., and Anderson, R., "The Fischer-Tropsch and related Synthesis, Including a Summary of Theoretical and Applied Contact Catalysis.", John Wiley & Sons, Inc., New York, Chapman & Hall, Limited, London (1951).

van Steen, E., PhD dissertation (1993). "Elementarshritte der Fischer-Tropsch CO-Hydrierung mit Eisen- und Kobaltkatalysatoren."

van Steen, E., Sewell, G.S., Makhote, A., Micklethwaite, C., Manstein, H., de Lange, M., and O'Connor, C.T., *J. Catal* **162**, 220 (1996). "TPR Study on the Preparation of Impregnated Co/SiO_2 Catalysts."

van't Blik, H. F. J. and Niemandsverdriet, J.W. *Appl Catal.* **15**, 155 (1984).

van't Blik, H. F. J. and Prins, R. *J. Catal.* **97**, 188 (1986). "Characterisation of Supported Cobalt and Cobalt-Rhodium Catalysts. I. Temperature-Programmed Reduction (TPR) and Oxidation (TPO) of $Co\text{-}Rh/Al_2O_3$"

Vannice, M. A., *J. Catal.* **37**, 449 (1975). "The Catalytic Synthesis of Hydrocarbons from H_2/CO Mixtures over the Group VIII Metals: I. The Specific Activities and Product Distributions of Supported Metals"

Welz, B., Verlag Chemie, Weinheim, New York (1976). "Atomic Adsorption Spectroscopy"

Wender, I., Synthesis Gas Reactions, Electric Power Research Institute, (EPRI), Report (1995).

Zsoldoz, Z., Garin, F., Hilaire, L., and Guczi, L., *Catal. Lett.* **33**, 39 (1995). " On the development of metallic particles and their intial catalytic properties in the CO + H_2 reaction over Co/Al_2O_3 catalyst."

Appendix I – TPR Calibration and Sample Calculation

Calibration of TPR

The temperature programmed reduction apparatus was calibrated by reducing NiO to metal as a standard. The reduction behaviour of this oxide is characterised by one main hydrogen consumption peak.

The thermal conductivity of 60 ml (STP)/min N_2 is recorded as a baseline for 0% H_2/N_2. Then the stream is switched to a 60 ml (STP)/min 5% H_2/N_2 stream to record the thermal conductivity of the mixture, relative to the reference flow of N_2. The difference between the two streams represents the total hydrogen flow in the reducing gas stream.

The vol. % H_2/N_2 is calibrated by assuming 5% H_2/N_2 mixture. The hydrogen consumption rate can then be determined as a function of elapsed time. The rate of hydrogen consumption/release during TPR can be calculated by using the trapezoidal rule:

$$H_2\ consumption = \sum_n \frac{(t_{n+1} - t_n) \times (f_{n+1} - f_n)}{2}$$

Where f is the rate of hydrogen consumption in mmol/min and t is the time elapsed in minutes.

Integration of the hydrogen uptake peak showed an hydrogen uptake of 0.6066 mmol when assuming a 5% H_2/N_2 reduction gas mixture at 60 ml (STP)/min. This calculated value based on a 5% H_2/N_2 reducing gas mixture, is lower than the amount of NiO added in the TPR reactor (0.6667 mmol). The vol % H_2/N_2 has to be adapted to the actual value, calculated as follow:

$$H_2\ concentration = \frac{0.6667\ mmol}{0.6066\ mmol} \times 5\% = 5.4958\ vol\%\ H_2 / N_2$$

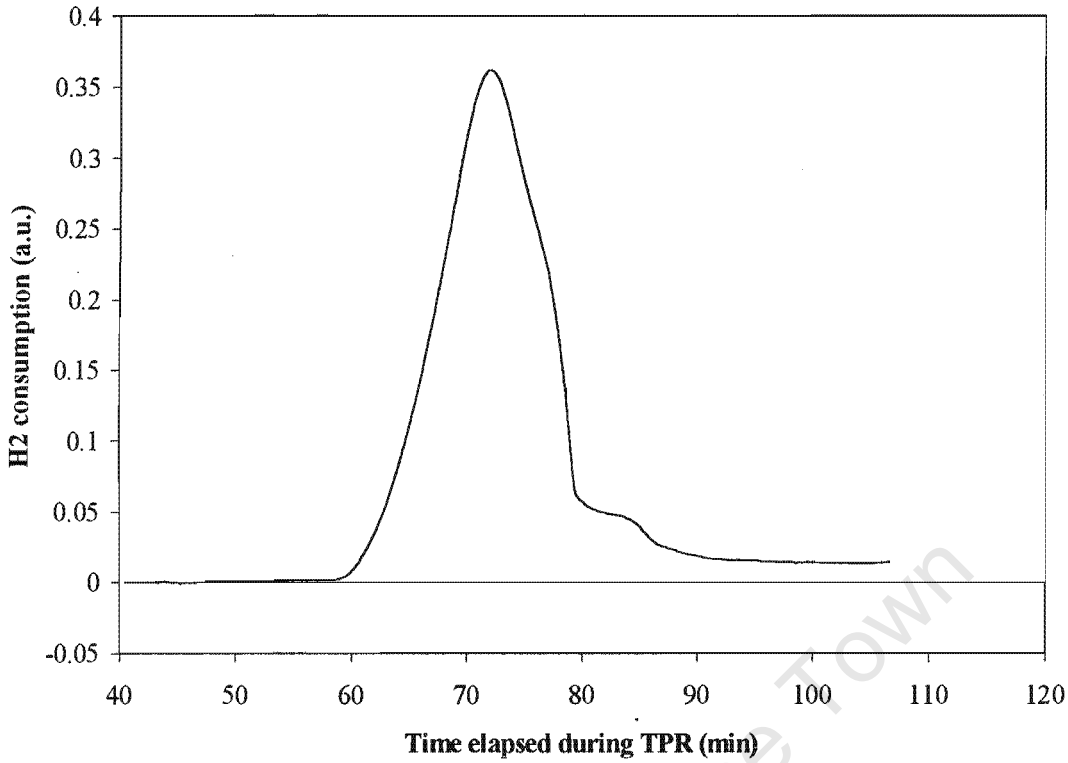

Figure A1-1: Rate of hydrogen consumption of NiO during TPR. (Reducing gas = 60 ml (STP)/min 5% H_2/N_2, temperature programming rate = 10°C/min, $m_{cat} \approx 0.05g$)

Sample Calculation

In the case of silica supported cobalt catalysts, not all the cobalt is completely reduced by hydrogen reduction at 400°C. This incomplete reduction is caused by an interaction between the metal and the support, called cobalt silicates [Puskas *et al*, 1992]. Looking at the TPR spectra for supported cobalt catalyst, the total amount of hydrogen consumed does not always correspond to the total amount of cobalt in the sample. There are two hydrogen consumption peaks visible in the TPR spectra of $Co/SiO_2(N)$-c4 after reduction at 400°C for 16 hours (see Figure A1-2). The first peak is due to a surface oxidation due to exposure to air at ambient conditions. The high temperature peak (> 700 K) is ascribed to metal-support interaction. Metal-support interaction is of importance, because it can only be reduced at temperature higher than where normal reduction (< 698K) takes place. It is thus seen as a permanent deactivation of the catalyst. For the silica supported cobalt catalyst (± 5wt%), ± 0.15g of sample was added to the reactor to give 0.1099 mmol Co. Integration of the high temperature TCD signal shows that a total amount of 0.0184 mmol hydrogen was consumed. The low temperature peak yields a hydrogen consumption of 0.0434 mmol.

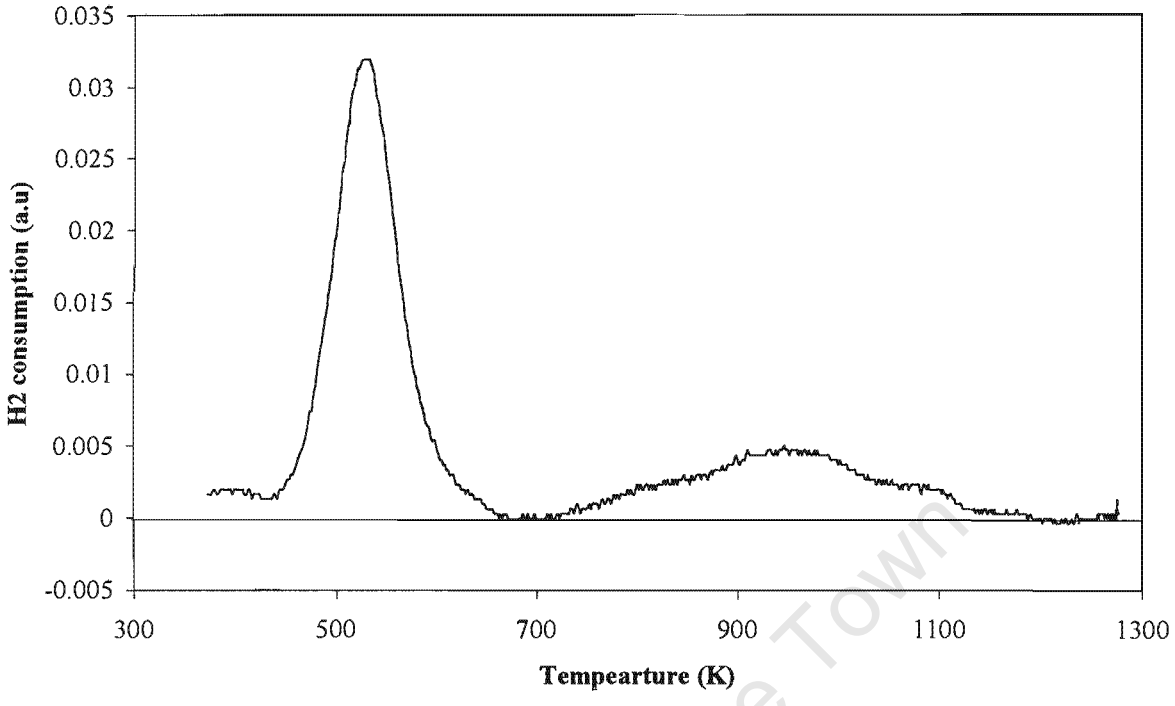

Figure A1-2: The TPR spectrum of $Co/SiO_2(N)$-c4 reduced at 400°C for 16 hours after calcination. TPR reducing gas = 60 ml (STP)/min 5% H_2/N_2, temperature programming rate = 10°C/min, $m_{cat} \approx 0.15g$)

The ratio to the amount of cobalt in the sample is as follow:

$$H_2 : Co\ ratio = \frac{0.0434}{0.1099} = 0.395$$

Table A1-1: Hydrogen consumption during TPR of calcined and subsequently reduced catalyst. Calcination in muffle furnace (static air). Reduction at 400°C for 16 hours with heating rate of 10°C/min.

Catalyst	*H_2: Co ratio Peak below 700K (mole: mole)*	*H_2: Co ratio Peak above 700K (mole: mole)*
$Co/SiO_2(N)$-c4	0.395	0.167

The amount cobalt present as Co^0, Co^{2+} and as cobalt silicate cannot be determined by TPR, due to the unknown complexity of the reduction of Co/SiO_2, and has to be determined by TPO (see Appendix II).

Appendix II – TPO Calibration and Sample Calculation

Calibration of TPO

The temperature programmed oxidation apparatus was calibrated by oxidising reduced cobalt metal as a standard. The oxidation behaviour of cobalt is characterised by two main peaks. The low temperature oxygen consumption peak is the oxidation to form bulk Co_3O_4 (reaction 1). The high temperature oxygen release peak is the thermal reduction of Co_3O_4 to form the form the divalent cobalt oxide CoO (reaction 2), as illustrated in Figure A2-1. The overall stoichiometry of these two reactions are given by the equations below:

$$3\,Co + 2\,O_2 \rightarrow Co_3O_4 \qquad (1)$$

$$Co_3O_4 \rightarrow 3\,CoO + \tfrac{1}{2}\,O_2 \qquad (2)$$

The thermal conductivity of 60 ml (STP)/min He is recorded as a baseline for 0% O_2/He. Then the stream is switched to a 60 ml (STP)/min 2% O_2/He stream to record the thermal conductivity of the mixture, relative to the reference flow of He. The difference between the two streams represents the total oxygen flow in the oxidising gas stream.

When oxygen is used for oxidation of the metal, the thermal conductivity of the stream changes and this is seen as a broad peak, stretching over a low temperature range. Oxygen release is registered as a negative peak, because more oxygen is present than the 2% recorded in the baseline. Since the flowrate of the oxidising gas stream is known, the oxygen consumption can be calculated.

The vol. % O_2/He is calibrated by assuming 2% O_2/He mixture. Oxygen consumption rate can then be determined as a function of elapsed time. The rate of oxygen consumption/release during TPO can be calculated by using the trapezoidal rule:

$$O_2\ consumption = \sum_n \frac{(t_{n+1} - t_n) \times (f_{n+1} - f_n)}{2}$$

Where f is the oxygen consumption rate in mmol/min and t is the time elapsed in minutes.

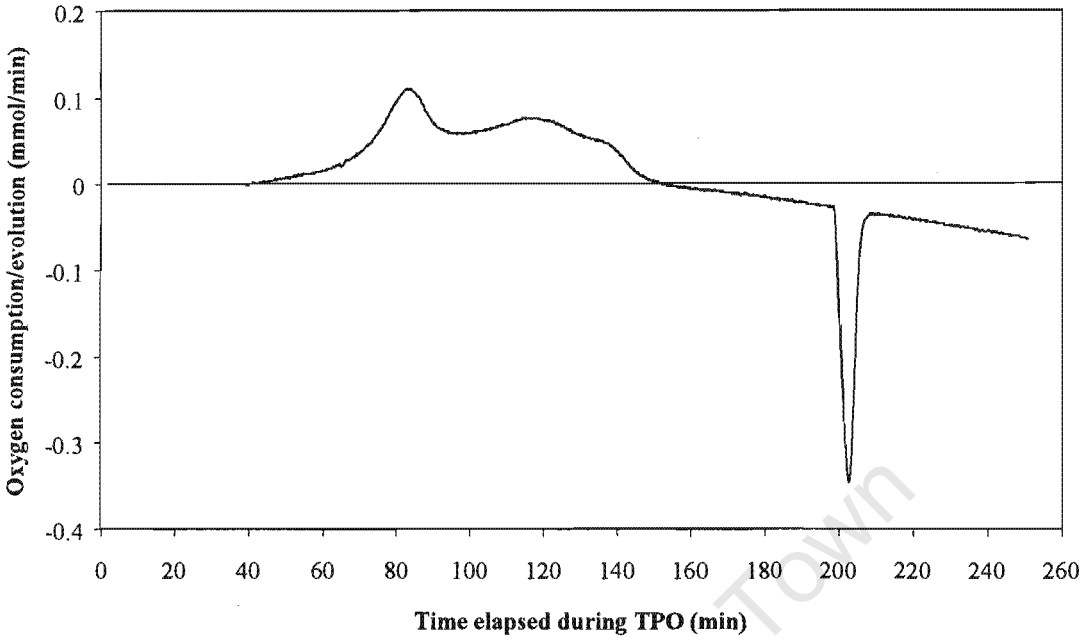

Figure A2-1: Rate of oxygen consumption and release of cobalt during TPO. Oxidising gas = 60 ml (STP)/min 2% O_2/He, temperature programming rate = 10°C/min, $m_{cat} \approx 0.05g$)

Integration of the oxygen uptake peaks occurring at lower temperatures showed an oxygen uptake of 0.4274 mmol when assuming a 2% O_2/He oxidising gas mixture at 60 ml (STP)/min. Since 3 cobalt atoms react with 2 oxygen molecules to form Co_3O_4, the amount of cobalt oxidised is calculated as 0.6411 mmol. This calculated value based on a 2% O_2/He oxidising gas mixture, is lower than the amount of cobalt added in the TPO reactor (0.6886 mmol). The vol. % O_2/He has to be adapted to the actual value, calculated as follow:

$$O_2\ concentration = \frac{0.6886\ mmol}{0.6411\ mmol} \times 2\% = 2.148\ vol\%\ O_2\ /\ He$$

The amount of oxygen release during the thermal reduction of Co_3O_4 should also correspond to amount of cobalt metal added during the TPO. The high temperature oxygen release shows a value of 0.1051mmol oxygen released. The reaction stoichiometry corresponds to 0.6304mmol cobalt. The error, which is an indication of the accuracy of the technique, between the amount of cobalt present as determined

from oxygen release and from oxygen uptake is described by the following expression:

$$Difference = \frac{0.6411 - 0.6304}{0.6411} \times 100\% = 1.7\%$$

Sample Calculation

In the case of silica supported cobalt catalysts, not all the cobalt is completely reduced by hydrogen reduction at 500°C. This incomplete reduction is caused by an interaction between the metal and the support, called cobalt silicates [Puskas *et al*, 1992]. Looking at the TPO spectra for supported cobalt catalyst, the high temperature oxygen release peak does not always correspond to the total amount of cobalt in the sample. Not all of the cobalt present in the sample has been oxidised to trivalent cobalt to a temperature of ± 800°C (where thermal reduction starts occurring). This indicates that this cobalt is most likely present as a stable cobalt silicate.

For the silica supported cobalt catalyst (± 5wt%), ± 0.5g of sample was added to the reactor to give 0.4086 mmol Co. Integration of the high temperature TCD signal shows that a total amount of 0.0474 mmol O_2 oxygen was released during the thermal reduction of Co_3O_4. The amount of Co_3O_4 being thermally reduced can be calculated by reaction stoichiometry as follows:

$$Amount\ Co\ as\ Co_3O_4 = 6 \times 0.0474 = 0.2844\ mmol\ Co$$

The amount of cobalt as in the form of cobalt silicate (non-oxidisable Co^{2+}) is the difference between the experimentally determined amount and theoretical calculated amount of cobalt present as metal.

$$Amount\ Co\ as\ cobalt - support\ compound = 0.4086\text{-}0.2844 = 0.1242\ mmol\ Co$$

Besides the presence of cobalt species as non-oxidisable cobalt-silicate, there can be divalent oxidisable Co^{2+} species left over after reduction. These Co^{2+} species will attribute to the first oxygen uptake peak.

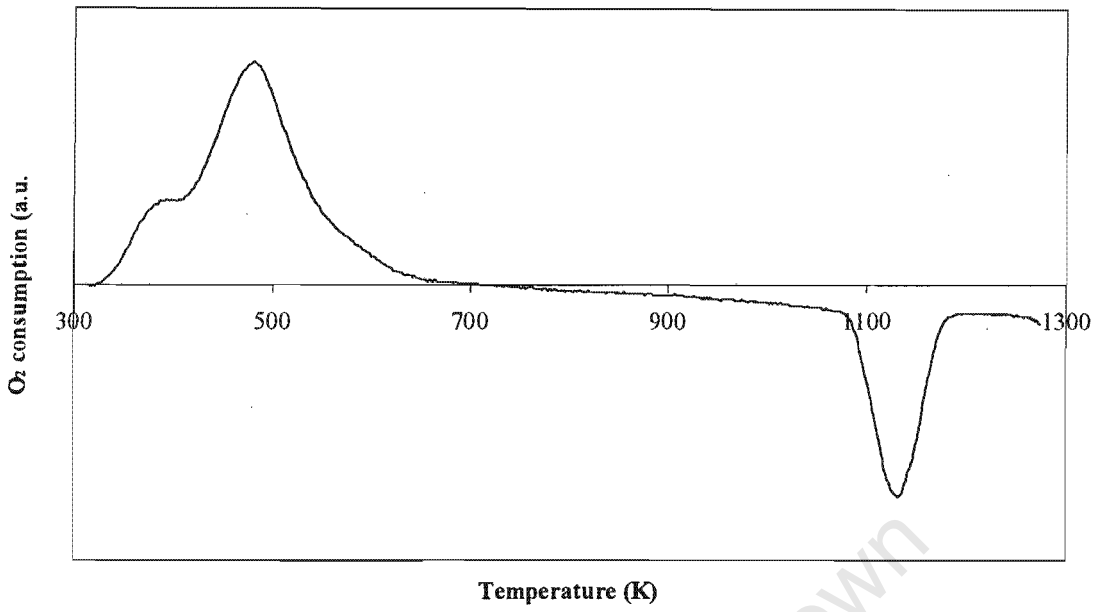

Figure A2-2: A TPO spectrum of the reduced Co/SiO_2(N) catalysts re-reduced at 200°C (10°C/min) for 4½ hours prior to TPO. Oxidising gas = 60 ml (STP)/min 2% O_2/He, temperature programming rate = 10°C/min, $m_{cat} \approx 0.5$g)

Two types of oxidation reactions can therefore be responsible for the low temperature oxygen uptake peak in the TPO spectra:

$$3\ Co + 2\ O_2 \rightarrow Co_3O_4 \qquad (3)$$

$$3\ CoO + \tfrac{1}{2}\ O_2 \rightarrow Co_3O_4 \qquad (4)$$

If all the cobalt oxide were reduced to cobalt metal during the activated hydrogen reduction, then only the first reaction would attribute to the low temperature oxygen consumption peak. The ratio in area corresponding to the oxygen uptake and oxygen release peak will be 4. If none of the cobalt was reduced to metal, and only the second reaction occurs, then the ratio will be 1. In practise, the value lies between 1 and 4. The oxygen uptake for the silica supported cobalt catalyst was 0.1797 mmol, with a relative peak ratio of 3.79.

By assuming x mmol Co_3O_4 are formed through reaction 3 and y mmol Co_3O_4 are formed via reaction 4, an oxygen balance results in the following equations:

$2x + ½y = oxygen \quad uptake \quad = 0.1797\ mmol$

$½x + ½y = oxygen \quad release \quad = 0.0474\ mmol$

Solving these equations simultaneously shows that x = 0.0882 mmol Co_3O_4 and y = 0.0066 mmol Co_3O_4.

Therefore, the amount of cobalt present as a zerovalent metal after reduction is 3 × 0.0882 = 0.2646 mmol. The amount of cobalt present as an oxidisable divalent species is 3 × 0.0066 = 0.0198 mmol.

Table A2-1: Composition of cobalt for Co/SiO_2(N) determined by TPO

Composition	*Mole*	*Mole %*
Co as zerovalent	0.2646	64.76
Co as oxidisable Co^{2+}	0.0198	4.84
Co as Non-oxidisable Co^{2+}	0.1797	30.4

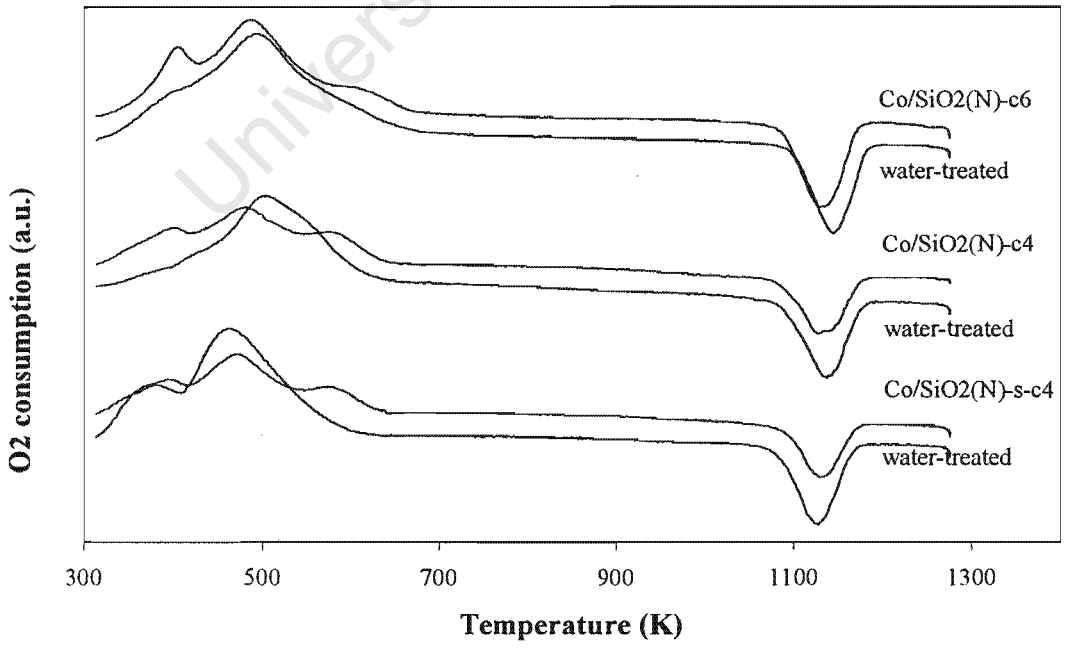

Figure A2-3: The temperature programmed oxidation spectra of the catalysts calcined at different temperatures and their water-treated counterparts

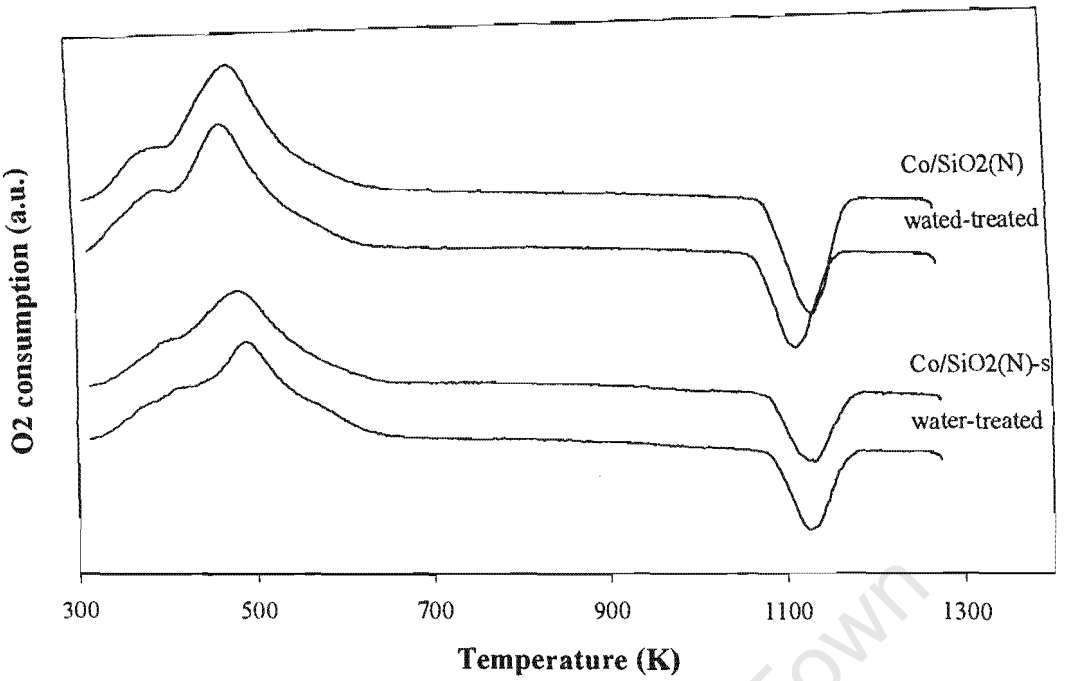

Figure A2-4: The temperature programmed oxidation spectra of the directly reduced catalysts and their water-treated counterparts

Appendix III – Particle Size Determination from H_2 Chemisorption Data

Hydrogen chemisorption was used to measure the total hydrogen uptake. From the saturation volume, the total number of exposed metal atoms can be calculated. The sample was evacuated and then exposed to hydrogen. Hydrogen chemisorbs dissociatively on the cobalt metal surface. This process was left for 270 s to reach equilibrium.

The free gas and the adsorbed gas are in dynamic equilibrium.

$$A_{(g)} + M_{(surface)} \leftrightarrow AM$$

The fractional coverage of the surface θ depends on the pressure of the overlaying gas. This dependence at a set temperature is called the adsorption isotherm. The fractional surface coverage θ is described as:

$$\theta = \frac{number\ of\ adsorption\ sites\ occupied}{number\ of\ adsorption\ sites\ available}$$

The Langmuir isotherm is based on the assumptions that every adsorption site is equivalent and that the ability of a particle to bind there is independent of whether or not nearby sites are occupied.

The rate of change of surface coverage due to adsorption is proportional to pressure P of A and the number of vacant sites $N_{sites}(1-\theta)$, where N_{sites} is the total number of sites:

$$\dot{\theta} = k_a P N_{sites}(1-\theta)$$

with k_a, the rate constant for adsorption.

The rate of change of surface coverage due to desorption is proportional to the number of adsorbed species, $N_{sites}\theta$:

$$\dot{\theta} = k_d N_{sites}\theta$$

with k_d the rate constant for desorption.

At equilibrium, the two rates are equal. Solving for θ results in the Langmuir isotherm:

$$\theta = \frac{KP}{1+KP}$$

with

$$K = \frac{k_a}{k_d}$$

For dissociative adsorption, the rate of adsorption is proportional to the pressure and the probability that both atoms will find sites:

$$\dot{\theta} = k_a P\{N_{sites}(1-\theta)\}^2$$

The rate of desorption is proportional to the frequency of encounters of atoms on the surface:

$$\ddot{\theta} = k_d (N_{sites}\theta)^2$$

When the rates are equal, θ can be solved by:

$$\theta = \frac{(KP)^{1/2}}{1+(KP)^{1/2}}$$

Then follows:

$$\theta + \theta(KP)^{1/2} = (KP)^{1/2}$$

and:

$$\theta = \frac{V}{V_m}$$

then:

$$\frac{V}{V_m} + \frac{V(KP)^{½}}{V_m} = (KP)^{½}$$

and:

$$\frac{P^{½}}{V} = \frac{1}{K^{½}V_m} + \frac{P^{½}}{V_m}$$

The Langmuir isotherm predicts a straight line when $P^{½}/V$ is plotted vs $P^{½}$ and gives the saturation volume V_m as 1/slope.

When $P^{½}/V$ vs. $P^{½}$ is plotted a straight line with the equation :

$y = 1.5879x + 5.7165$

is obtained.

Table A3-1: The H_2 chemisorption equilibrium data for $Co/SiO_2(N)$-s

Pressure mmHg	*Volume adsorbed* cm^3 *(STP)/*g_{cat}
52.28	0.431
119.26	0.467
178.50	0.487
242.46	0.510
308.14	0.530

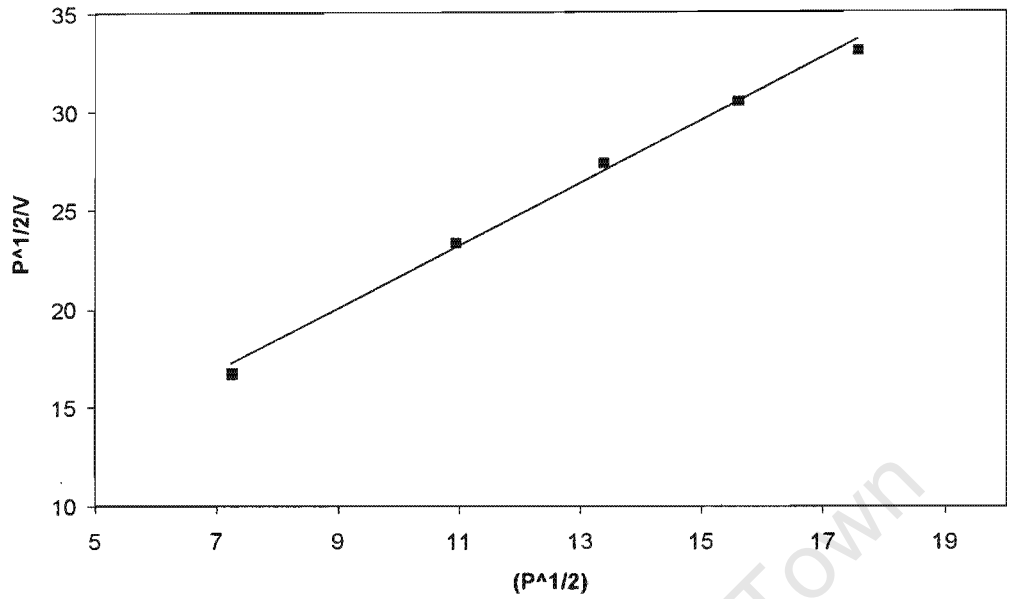

Figure A3-1: Hydrogen adsorption isotherm for Co/SiO_2 plotted in the linear form of the Langmuir isotherm

R^2 for the line is 0.9955, indicating a good fit. The slope of the line is 1.5879:

$$V_m = \frac{1}{1.5879}$$

Thus V_m = 0.6298 cm^3/g_{cat}

The total number of exposed atoms can be calculated from the following relationship:

$$N_{CO} = \frac{0.6298\ cm^3 H_2/g_{cat}}{22414\ cm^3 H_2/mol\ H_2} \cdot \frac{2\ mol\ CO}{mol\ H_2} \cdot N_A = 3.384 \times 10^{19}\ atoms\ Co/g_{cat}$$

The site density of fcc cobalt is 14.6 atoms/nm^2 [Sewell, 1996]. The metallic surface area can be determined as follows:

$$Surfacearea = \frac{3.384 \times 10^{19}\ atoms}{14.6\ atoms/nm^2} \cdot 10^{-18}\ m^2/nm^2 = 2.318\ m^2/g_{cat}$$

1.325g of catalyst was used in H_2 chemisorption analysis. The surface area of the catalyst is then:

$$Surface\ area = 2.318\ m^2/g_{cat} \times 1.325\ g_{cat} = 3.07\ m^2$$

The metallic dispersion is the number of metal atoms exposed, relative to the total amount of zerovalent metal present in the catalyst sample. The number of reduced metal atoms can be determined by multiplying the total number of metal atoms in the catalyst sample by the extent of reduction.

$$Dispersion = \frac{3.384 \times 10^{19}\ exposed\ Co\ atoms}{4.719 \times 10^{20} reduced\ Co\ atoms} \cdot 100\% = 6.4\%$$

To determine the average diameter of the metal particles, all particles are assumed to be spherical. From the volume to surface relationship of a sphere, the particle diameter can be calculated. The volume of reduced cobalt present on the reduced Co/SiO_2 catalyst is determined by using the following relationship, with density of 8.9 g/cm^3 [Sewell, 1996].

$$Volume = \frac{4.719 \times 10^{20} atoms}{6.023 \times 10^{23} atoms/mol} \cdot \frac{58.93 g/mol}{8.9 g/cm^3} \cdot 10^{-6}\ m^3/cm^3 = 5.188 \times 10^{-9} m^3$$

The average particle diameter follows then from the volume surface relationship as:

$$Average\ diameter = 6 \cdot \frac{5.188 \times 10^{-9}\ m^3}{3.07\ m^2} \cdot 10^9 nm/m = 16\ nm$$

Appendix IV – Sample Calculation for Co wt.% from Atomic Adsorption Spectroscopy

The cobalt content of the catalyst was determined by Atomic Absorption Spectroscopy (AAS). 0.2507g of the reduced Co/SiO2(N) catalyst was weighed and wetted with a few drops of deionised water. After digestion with 4 ml of cold 40% HF, the solution was diluted to 100 ml with deionised water. The Varian Spectra AA-30 spectrometer with optimum range of 1-200 µg/ml was used to analyse for the cobalt concentration of the solution.

Calibration was done with cobalt nitrate in solution with and without adding HF. Standards were made up to 50 m/l, 80 mg/l, 100 mg/l and 150 mg/l.

99.883µg/ml Co was found to be present in the solution.

$$\frac{99.883\,\mu g/m\ell \times 100 m\ell}{1000000} = 0.0099883\,g\ Co\ in\ solution$$

Since 0.2507 g of catalyst was used, the Co wt.% of the catalyst was calculated to be:

$$\frac{0.0099883}{0.2507} \times 100 = 3.98\%\ (wt)\ Co\ on\ silica$$

Appendix V – Calibration of Mass Flow Controllers

The mass flow controllers were calibrated by measuring the flowrate of the gas at several setpoints.

Nitrogen flow to the cyclohexane saturator was controlled by a Brooks mass flow controller, with a maximum flowrate of 13 ml (STP)/min. The equation of the linear fit to the data enables the calculation of the exact setpoint for a desired flowrate, example: the calibration equation for N_2 MFC:

$$Y = 0.131X - 0.0502$$

where Y is the flowrate (ml (STP)/min) and X is the setpoint (%). To obtain a flowrate of 5 ml/min a setpoint of X = 38.55 % is needed.

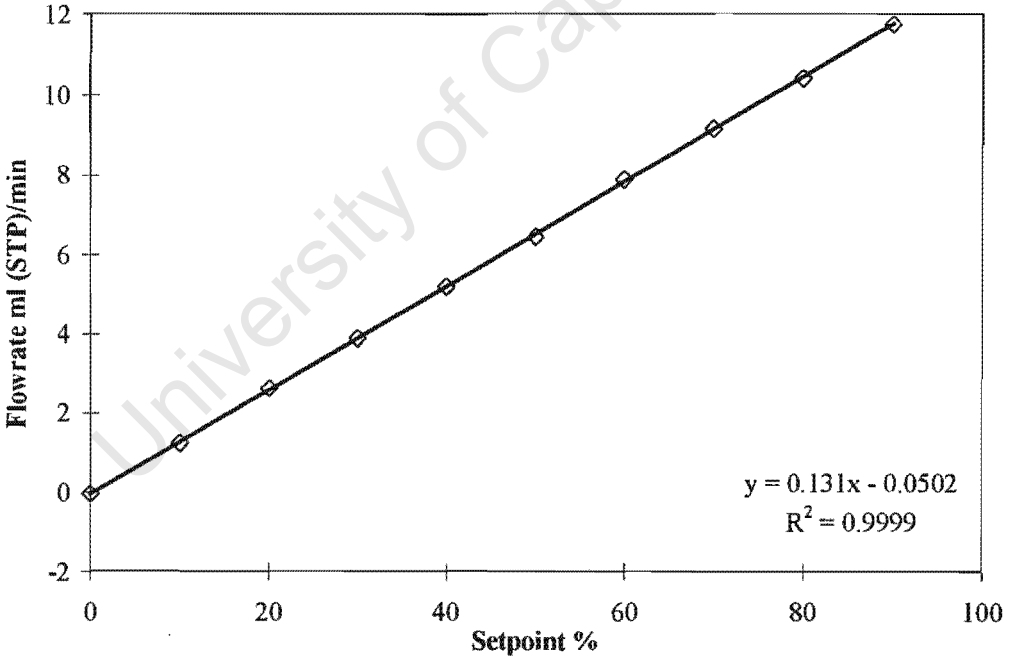

Figure A5-1: Calibration of N_2 mass flow controller

The CO and H_2 flow were controlled with Unit Instrument Mass Flow Controllers. H_2 and CO was fed in the ratio of 2:1. A total flow of 10.5 ml (STP)/min was used, which resulted in a flowrate of 7 ml (STP)/min H_2 (X= 7.2 %) and 3.5 ml (STP)/min CO (X= 8.7 %).

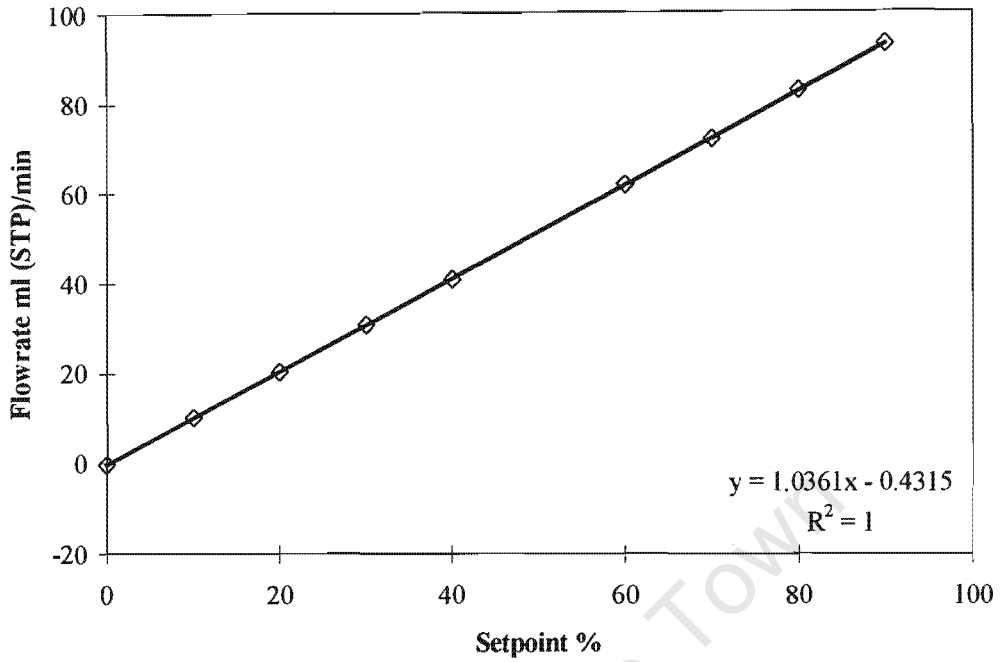

Figure A5-2: Calibration of H_2 mass flow controller

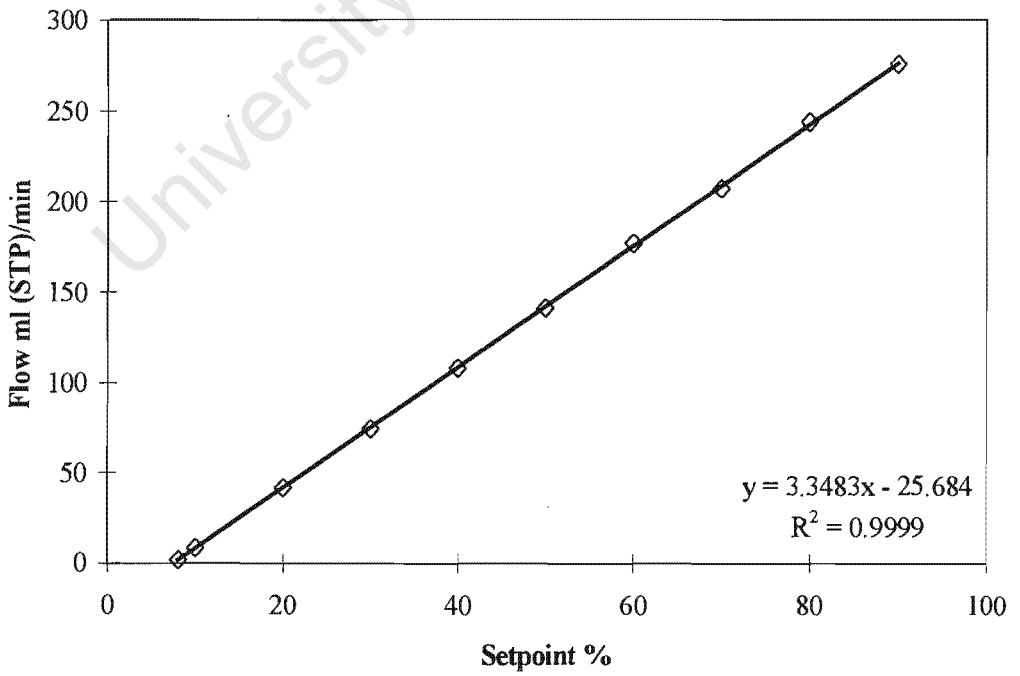

Figure A5-3: The calibration of CO mass flow controller

Appendix VI – Δ Gibbs free energy (kcal) for different reactions as calculated by HSC Chemistry for Windows

Table A6-1: The Δ Gibbs free energy (kcal) for reactions of cobalt with water and silica at 200°C.

Reaction	Temperature	ΔGibbs free energy
	°C	kcal
$Co + H_2O\ (g) \rightarrow CoO + H_{2\ (g)}$	0	4.665
	100	4.018
	200	4.665
	300	5.023
	400	5.677
	500	6.101
	600	6.485
	700	6.837
	800	7.167
	900	7.484
	1000	7.794
$CoO + SiO_2 \rightarrow 2CoO*SiO_2$	0	-6.004
	100	-6.239
	200	-6.383
	300	-6.476
	400	-6.533
	500	-6.556
	600	-6.538
	700	-6.485
	800	-6.420
	900	-6.302
	1000	-6.170

Appendix VII – Sample Calculation for Weight Hourly Space Velocity

The H_2:CO flow was fed in a ratio of 2:1. The flowrate of H_2 was 7ml (STP)/min and CO was 3.5ml (STP)/min, to give a total flow of 10.5ml (STP)/min, which was 630ml (STP)/hr. The syngas was passed over 1g of catalyst that had a bed length of 4.5cm. and bed volume of 321ml.

The weight hourly space velocity was then calculated as follow:

$$WHSV = \frac{entrance\ flow\ (ml/hr)}{volume\ of\ bed\ (ml)}$$

wich gave:

$$WHSV = \frac{630\ ml/hr}{321ml} = 196\ hr^{-1}$$

Appendix VIII – Transmission Electron Microscopy Photographs

The catalyst samples were crushed and wetted with a few drops of distilled water. Copper grids with a thin film of carbon acting as a support for the specimen were floated on the droplets of the sample. Excess sample was blotted with filter paper and the sample was allowed to dry.

The samples were viewed in bright field mode in a JEOL 200CX transmission electron microscope using an acceleration voltage of 200kV.

The cobalt particles were visible as darker units on the silica grains. The magnification used was from 20 000 times to 100 000 depending on the cobalt particle size on the catalyst sample.

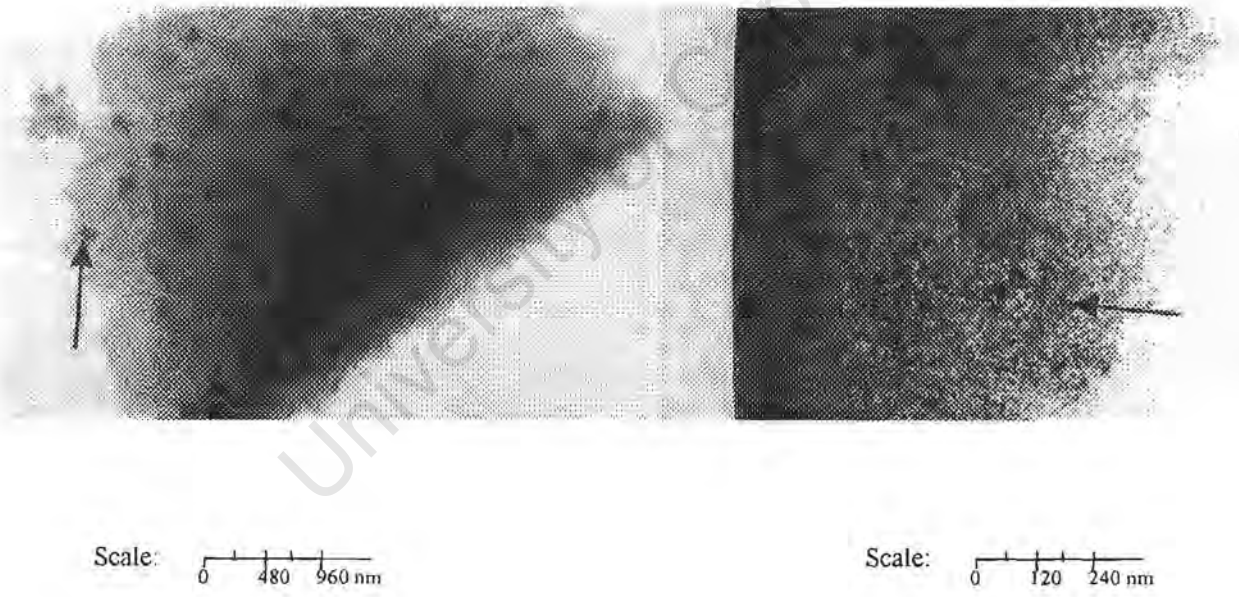

Figure A8-1: TEM photographs of the calcined catalyst. Left: catalyst calcined at 400°C, magnification 20 000 times. Right: catalyst calcined at 600°C, magnification 73 000 times.

The catalyst calcined at 400°C has a larger particle size (120 nm) than the catalyst calcined at 600°C (see Figure A8-1).

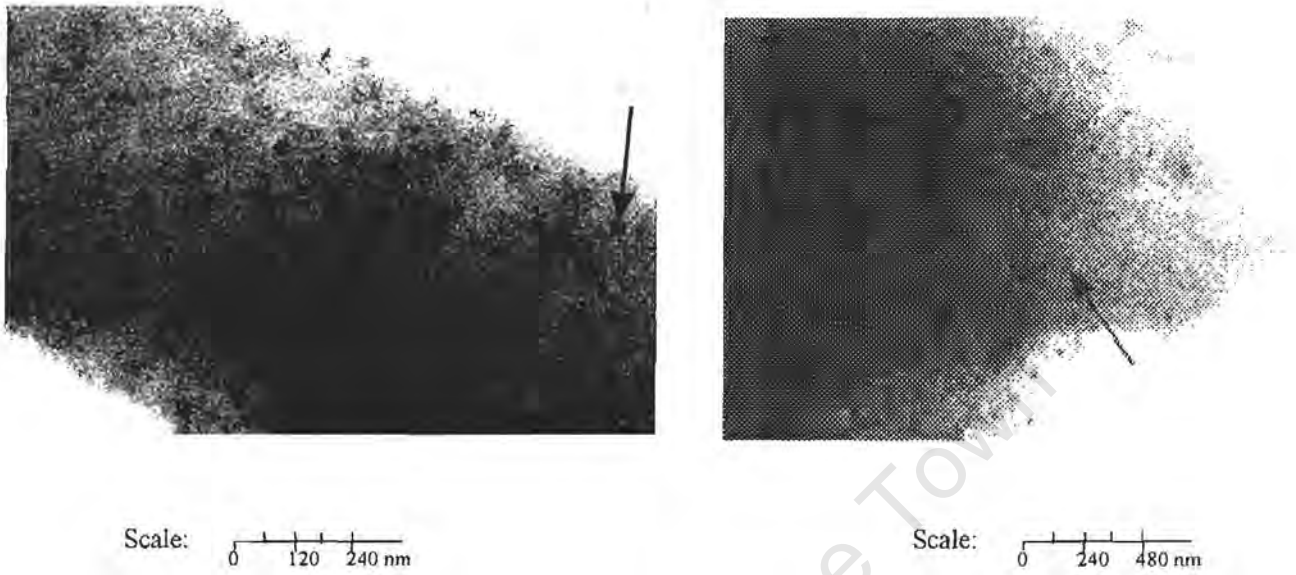

Figure A8-2: TEM pictures of directly reduced catalysts with different heating rates. Left: Normal heating rate (10°C/min), magnification: 37 000 times. Right: Slow heating rate (0.5°C/min), magnification: 50 000 times.

The particles formed during a normal reduction heating rate (10°C/min) are about 50 nm, on the catalyst sample. When the reduction heating rate was slowed down to 0.5°C/min, smaller particles were formed (30 nm) (See Figure A8-2).

Figure A8-3: TEM photographs of $Co/SiO_2(N)$ before and after water treatment. Left: $Co/SiO_2(N)$, magnification: 37 000 times. Right $Co/SiO_2(N)$-w, magnification: 59 000 times.

Water treatment does not change the particle size of he cobalt. In Figure A8-3 it can be seen that the particle size of $Co/SiO_2(N)$ remains constant (50 nm) after water treatment.

Cobalt supported on silica does not have one homogeneous particle size but a particle size distribution. It must be borne in mind that with TEM only a few Co particles were measured. At least 100 TEM photographs have to be taken to obtain a meaningful particle distribution. The darker units that are visible as cobalt can be clusters of small cobalt particles and is not necessarily representative of the true cobalt crystallite size.

Appendix IX– Experimental Results of Fischer-Tropsch Synthesis

Table A9-1: Fischer-Tropsch reaction settings

$T_{Reactor}$	190°C	Cyclohexane flowrate	0.1 ml (STP)/min
$P_{Reactor}$	5 bar	N_2 flowrate	1.5 ml (STP)/min
H_2 flowrate	7.0ml (STP)/min	$T_{saturator}$	10°C
CO flowrate	3.5ml (STP)/min	WHSV	200 hr^{-1}

Table A9-2: The data obtained form the GC spectrum for the Co/SiO_2(N) catalyst

Catalyst	5%Co/SiO2(N)				
Mr (CO)	28	g/gmole			
Mr(C6H12)	84.16	g/gmole			
Flowrate of CO	3.5	ml (STP)/min			
	0.000156	mol/min			
Flowrate of mol c.hx	0.105	ml (STP)/min			
	4.69E-06				
Flowrate of c.hx (ml (STP)/min)	2.82E-05	2.82E-05	2.82E-05	2.82E-05	8.05E-05
sample time	0:11:25	0:31:57	1:01:19	2:00:00	24:01:11
Fco/Fc.hx	5.536	5.536	5.536	5.536	1.940
Total area	28391502	28308314	25449307	27354523	54135876
Int. area	23203519	21194782	19841583	20118395	47357143
(Afid-Aint)/Aint	0.224	0.336	0.283	0.360	0.143
Organic Yield	0.040	0.060	0.051	0.064	0.074
%	4.0	6.0	5.1	6.5	7.4
GC trace					
sample time	0:11:25	0:31:57	1:01:19	2:00:00	24:01:11
Area C8	411300	419900	335135	497170	456915
AC8/8	51412.5	52487.5	41891.9	62146.3	57114.4
Area C9	371652	407863	313547	436551	416877
AC9/9	41294.7	45318.1	34838.6	48505.7	46319.7
Area C10	301759	456210	312417	451825	437531
AC10/10	30175.9	45621.0	31241.7	45182.5	43753.1
Area C11	167860	394735	268550	388434	349954
AC11/11	15260.0	35885.0	24413.6	35312.2	31814.0

Area C12	94570	379165	261744	330789	300896
AC12/12	7880.8	31597.1	21812.0	27565.8	25074.7
Area C13	52615	352042	254580	292813	256001
AC13/13	4047.4	27080.2	19583.1	22524.1	19692.4
Area C14	21754	285080	250508	275376	240466
AC14/14	1553.9	20362.9	17893.4	19669.7	17176.1
Area C15		177191	235906	247281	214644
AC15/15	0	11812.7	15727.1	16485.4	14309.6
Area C16		103042	186323	223771	193865
AC16/16	0	6440.1	11645.2	13985.7	12116.6
Area C17		57007	122269	206870	184133
AC17/17	0	3353.4	7192.3	12168.8	10831.4
Area C18		28333	75505	150525	169824
AC18/18	0	1574.1	4194.7	8362.5	9434.7
Area C19			38803	150525	149541
AC19/19	0	0	2042.3	7922.4	7870.6
Area C20			15069	33294	119312
AC20/20	0	0	753.5	1664.7	5965.6
Area C21			5209	10672	79037
AC21/21	0	0	248.1	508. 2	3763. 7
Area C22					36052
AC22/22	0	0	0	0	1638.7

OLEFIN SELECTIVITY	**Co/SiO2(N)**				
sample time	0:11:25	0:31:57	1:01:19	2:00:00	24:01:11
Area olefin C8	70964	119121	145572	244751	247654
Selectivity	0.177	0.287	0.436	0.498	0.547
Area olefin C13	936	4575	19811	26616	28934
Selectivity	0.019	0.013	0.079	0.092	0.114

Alpha-olefin selectivity	**Co/SiO2(N)**				
Sample time	0:11:25	0:31:57	1:01:19	2:00:00	24:01:11
Area alpha-olefin C8	21570	59262	73378	110246	132030
Selectivity	0.304	0.497	0.504	0.450	0.533

Table A9-3: The data obtained form the GC spectrum for the water-treated $Co/SiO_2(N)$ catalyst

Catalyst	**Co/SiO2(N)-w**				
Flowrate of CO	3.5	ml/ (STP)min			
mol flowrate	0.000156	mol C/min			
Flowrate of c.hx	0.108	Ml (STP)/min			
	2.9E-05	mol C /min			
Flowrate of c.hx (ml (STP)/min)	2.90E-05	2.90E-05	2.90E-05	2.90E-05	2.98E-05
sample time	0:10:21	0:10:25	0:30:22	1:01:42	24:10:41
Fco/Fc.hx	5.388	5.388	5.388	5.388	5.245
Total area	19170515	21549186	24135591	20901413	15955029
int area	16190805	18566729	19089948	16593012	13390496
(Afid-Aint)/Aint	0.184	0.160	0.264	0.260	0.192
Organic Yield	0.034	0.030	0.049	0.048	0.037
%	3.4	3.0	5.0	4.8	3.7
GC trace					
sample time	0:10:21	0:10:25	0:30:22	1:01:42	24:10:41
Area C8	201183	184163	322556	249839	110119
AC8/8	25147.9	23020.3	40319.5	31229.9	13764.9
Area C9	130471	130850	263163	237208	143625
AC9/9	14496. 8	14538.9	29240.3	26356. 4	15958. 3
Area C10	81163	91287	274808	212623	143228
AC10/10	8116.3	9128.7	27480.8	21262.3	14322.8
Area C11	40162	43572	255993	203871	111125
AC11/11	3651.1	3961. 1	23272.1	18533.7	10102.3
Area C12	15742	19485	230829	193743	111744
AC12/12	1311.8	1623.8	19235.8	16145.3	9312.0
Area C13			209012	173715	105128
AC13/13	0	0	16077.8	13362.7	8086.8
Area C14			146235	175863	96731
AC14/14	0	0	10445.4	12561.6	6909.4
Area C15			75908	158126	88555
AC15/15	0	0	5060.5	10541.7	5903.7

Area C16			45211	121228	85217
AC16/16	0	0	2825.7	7576.8	5326.1
Area C17			23185	74847	87442
AC17/17	0	0	1363.8	4402.8	5143.6
Area C18			8299	37868	82921
AC18/18	0	0	461.1	2103.8	4606.7
Area C19				14523	67868
AC19/19	0	0	0	764.4	3572.0
Area C20				3252	52101
AC20/20	0	0	0	162.6	2605.1

OLEFIN SELECTIVITY	**Co/SiO2(N)-w**				
sample time	0:10:21	0:10:25	0:30:22	1:01:42	24:10:41
Area olefin C8					
Selectivity	55548	40013	109810	92495	48879
	0.283	0.223	0.353	0.391	0.447
Area olefin C13					
Selectivity			6721	12248	21624
			0.033	0.071	0.209

Alpha-olefin selectivity	**Co/SiO2(N)-w**				
Sample time	0:10:21	0:10:25	0:30:22	1:01:42	24:10:41
Area alpha-olefin C8	6669	8172	45569	48318	44016
Selectivity	0.120	0.204	0.415	0.522	0.901

Table A9-4: The data obtained form the GC spectrum for the $Co/SiO_2(N)$ -s catalyst

Catalyst	**Co/SiO2(N)-s**		
Flowrate of CO	3.5	ml/ (STP)min	
N CO	0.000156	mol C/min	
Flowrate of c.hx	0.012	ml (STP)/min	
N C (c.hx)	3.07E-06	mol C /min	
N C (c.hx)	3.07E-06	3.07E-06	3.19E-06
sample time	2:00:59	24:02:30	24:07:00
Fco/Fc.hx	304.836	304.836	48.949
GC trace			
Total area	15144743	1387150	2206212
int area		56601	7578
(Afid-Aint)/Aint		23.508	290.134
Organic Yield		0.077	5.927
		7.711	
PLOT			
sample time	2:00:59		24:07:00
Area C8	170770		84019
AC8/8	21346.3		10502.4
Area C9	166992		116246
AC9/9	18554.7		12916. 2
Area C10	158440		197797
AC10/10	15844.0		19779.7
Area C11	137566		94512
AC11/11	12506.0		8592.0
Area C12	133146		128030
AC12/12	11095.5		10669.2
Area C13	124584		93332
AC13/13	9583.4		7179.4
Area C14	122151		86771
AC14/14	8725.1		6197.9
Area C15	117514		79276
AC15/15	7834.3		5285.1
Area C16	113281		73384

AC16/16	7080.1		4586.5
Area C17	105690		75559
AC17/17	6217.1		4444.6
Area C18	71715		72480
AC18/18	3984.2		4026.7
Area C19	37722		64670
AC19/19	1985.4		3403.7
Area C20	12010		47915
AC20/20	600.5		2395.8

OLEFIN SELECTIVITY	**Co/SiO2(N)-s**		
sample time	2:00:59		24:07:00
Area olefin C8	98108		87752
Selectivity	0.577		0.655
Area olefin C13	4583		859
Selectivity	0.038		0.009

Alpha-olefin selectivity			
Sample time	2:00:59		24:07:00
Area alpha-olefin C8	45724		31714
Selectivity	0.466		0.361

Table A9-5: The data obtained form the GC spectrum for the water-treated $Co/SiO_2(N)$-s catalyst

Catalyst	**Co/SiO2(N)-s-w**				
Flowrate of CO	3.5	ml/ (STP)min			
N CO	0.000156	mol C/min			
Flowrate of c.hx	0.108	ml (STP)/min			
N C (c.hx)	2.90E-05	mol C /min			
N C (c.hx)	2.89E-05	2.90E-05	2.90E-05	2.90E-05	2.98E-05
sample time	0:10:29	0:29:44	1:02:09	2:02:46	24:00:30
Fco/Fc.hx	5.389	5.389	5.389	5.389	5.245
Total area	25631977	23831906	13584503	16356404	22661804
int area	22013148	19602743	11296557	13617784	19387323
(Afid-Aint)/Aint	0.164	0.216	0.203	0.201	0.169
Organic Yield	0.030	0.040	0.038	0.037	0.032
%	3.1	4.0	3.8	3.7	3.2
PLOT					
sample time	0:10:29	0:29:44	1:02:09	2:02:46	24:00:30
Area C8	283421	298629	129143	141981	179285
AC8/8	35427.6	37328.6	16142.9	17747.6	22410.6
Area C9	74146	235105	110154	127363	156736
AC9/9	8238. 4	26122.8	12239.3	14151.4	17415.1
Area C10	89822	357834	143853	172643	217431
AC10/10	8982.2	35783.4	14385.3	17264.3	21743.1
Area C11	22874	187896	96757	95118	136102
AC11/11	2079.5	17081.5	8796.1	8647.1	12372.9
Area C12	24413	202789	99629	135095	128009
AC12/12	2034.4	16899.1	8302.4	11257.9	10667.4
Area C13	10824	139338	86478	101510	114757
AC13/13	832.6	10718.3	6652.2	7808.5	8827.5
Area C14	9775	87183	89607	94454	107947
AC14/14	698.2	6227.4	6400.5	6746.7	7710.5
Area C15		39753	77930	87993	101496
AC15/15	0	2650.2	5195.3	5866.2	6766.4

Area C16		12496	53074	85031	95305
AC16/16	0	781.0	3317.1	5314.4	5956.6
Area C17			30053	87710	80388
AC17/17	0	0	1767.8	5159.4	4728.7
Area C18			13346	69921	68744
AC18/18	0	0	741.4	3884.5	3819.1
Area C19			6235	48297	51753
AC19/19	0	0	328.2	2541.9	2723.8
Area C20				18284	32300
AC20/20	0	0	0	914.2	1615.0

OLEFIN SELECTIVITY	**Co/SiO2(N)-s-w**				
sample time	0:10:29	0:29:44	1:02:09	2:02:46	24:00:30
Area olefin C8	163810	160381	71010	79824	112812
Selectivity	0.592	0.543	0.558	0.569	0.635
Area olefin C13	1729	3014	3144	724	11544
Selectivity	0.299	0.024	0.035	0.007	0.103

Alpha-olefin selectivity					
Sample time	0:10:29	0:29:44	1:02:09	2:02:46	24:00:30
Area alpha-olefin C8	3449	52216	28262	37007	63176
Selectivity	0.021	0.326	0.398	0.464	0.560

Table A9-6: The data obtained form the GC spectrum for the $Co/SiO_2(N)$-c4 catalyst

Catalyst	**Co/SiO2(N)-c4**				
Flowrate of CO	3.5	ml/ (STP)min			
Mol flowrate	0.000156	mol C/min			
Flowrate of c.hx	0.111	ml (STP)/min			
Mol C Flowrate	2.97E-05	mol C /min			
mol Flwrt of C (chx)	2.98E-05	2.98E-05	2.98E-05	2.98E-05	2.98E-05
sample time	0:10:20	0:31:14	1:00:37	02:01:52	24:00:00
Nco/Nc.hx	5.245	5.245	5.245	5.245	5.245
Total area	20200040	14005696	21834500	19116265	18798766
int area	17177502	11604609	18068637	16121838	16817975
(Afid-Aint)/Aint	0.176	0.207	0.208	0.186	0.118
Organic Yield	0.034	0.040	0.040	0.040	0.022
%	3.4	3.9	4.0	3.5	2.2
GC trace					
sample time	0:10:20	0:31:14	1:00:37	02:01:52	24:00:00
Area C8	245895	162357	225004	170532	115552
AC8/8	30736.9	20294.6	28125.5	21316.5	14444.0
Area C9	213743	124481	177705	152514	96623
AC9/9	23749.2	13831.2	19745.0	16946.0	10735.9
Area C10	201308	151166	226920	204620	153130
AC10/10	20130.8	15116.6	22692.0	20462.0	15313.0
Area C11	93843	126066	175631	136389	92213
AC11/11	8531.2	11460.6	15966.5	12399.0	8383.0
Area C12	51040	131959	167469	118096	87776
AC12/12	4253.3	10996.6	13955.8	9841.3	7314.7
Area C13	35897	124929	160454	118947	76366
AC13/13	2761.3	9609.9	12342.6	9149.8	5874.3
Area C14	21501	104228	183550	127437	72583
AC14/14	1535.8	7444.9	13110.7	9102.6	5184.5
Area C15	12936	62234	152823	110635	65317
AC15/15	862.4	4148.9	10188.2	7375. 7	4354.5
Area C16	7032	34575	126406	98697	51319

AC16/16	439.5	2160.9	7900.4	6168.6	3207.4
Area C17	9109	20756	77531	106521	54598
AC17/17	535.8	1220.9	4560.6	6265.9	3211.6
Area C18	8645	10145	41255	79430	43044
AC18/18	480.3	563.6	2291.9	4412.8	2391.3
Area C19		3765	18511	42921	36207
AC19/19	0	198.2	974.3	2259.0	1905.6
Area C20		1242	7334	21735	27815
AC20/20	0	62.1	366.7	1086.8	1390.8

OLEFIN SELECTIVITY	**Co/SiO2(N)-c4**				
sample time	0:10:20	0:31:14	1:00:37	02:01:52	24:00:00
Area olefin C8	103305	82046	131237	107617	54118
Selectivity	0.428	0.522	0.591	0.631	0.576
Area olefin C13	4738	4817	15138	13428	12290
Selectivity	0.174	0.038	0.096	0.115	0.164

Alpha-olefin selectivity	**Co/SiO2(N)-c4**				
Sample time	0:10:20	0:31:14	1:00:37	02:01:52	24:00:00
Area alpha-olefin C8	24026	40522	80478	65748	48241
Selectivity	0.232	0.493	0.613	0.610	0.891

Table A9-7: The data obtained form the GC spectrum for the water-treated $Co/SiO_2(N)$-c4 catalyst

Catalyst	**Co/SiO2(N)-c4-w**				
Flowrate of CO	3.5	ml/ (STP)min			
N CO	0.000156	mol C/min			
Flowrate of c.hx	0.108	ml (STP)/min			
N C (c.hx)	2.90E-05	mol C /min			
Flowrate of c.hx	2.90E-05	2.90E-05	2.9E-05	2.90E-05	1.50E-05
sample time	0:11:30	0:30:00	1:03:54	2:01:31	24:00;00
Nco/N C (c.hx)	5.389	5.389	5.389	5.389	10.404
Total area	26387993	29505961	25542502	22681909	16026240
int area	23331857	26963664	22465781	20165399	13619370
(Afid-Aint)/Aint	0.131	0.094	0.137	0.125	0.177
Organic Yield	0.024	0.017	0.025	0.023	0.017
%	2.4	1.7	2.5	2.3	1.7
GC trace					
sample time	0:11:30	0:30:00	1:03:54	2:01:31	24:00;00
Area C8	96620	106694	246570	172142	206477
AC8/8	12077.5	13336.8	30821.3	21517.8	25809.6
Area C9	117659	98738	112735	94244	72232
AC9/9	13073.2	10970.9	12526.1	10471.6	8025.8
Area C10	117258	82177	181058	133374	148796
AC10/10	11725.8	8217.7	18105.8	13337.4	14879.6
Area C11	162276	86925	94826	79573	67338
AC11/11	14752.4	7902.3	8620.5	7233.9	6121.6
Area C12	177231	86617	81916	77482	61135
AC12/12	14769.2	7218.1	6826.3	6456.8	5094.6
Area C13	166104	74084	90578	65963	48499
AC13/13	12777.2	5698.8	6967.5	5074.1	3730.7
Area C14	126542	68654	81390	69033	46785
AC14/14	9038.7	4903.9	5813.6	4930.9	3341.8
Area C15	79012	51671	68975	56169	44915
AC15/15	5267.5	3444.7	4598.3	3744.6	2994.3
Area C16	44386	32066	53964	51776	29412

AC16/16	2774.1	2004.1	3372.8	3236.0	1838.3
Area C17	32488		36493	48343	34635
AC17/17	1911.1	0	2146.6	2843.7	2037.4
Area C18	27260		24592	29920	20541
AC18/18	1514.4	0	1366.2	1662.2	1141.2
Area C19			9913	14884	16411
AC19/19	0	0	521.7	783.4	863.7
Area C20			14373		9819
AC20/20	0	0	718.7	0	491.0

OLEFIN SELECTIVITY					
sample time	0:11:30	0:30:00	1:03:54	2:01:31	24:00;00
Area olefin C8	41645	13938	174220	59062	150928
Selectivity	0.338	0.132	0.719	0.527	0.780
Area olefin C13	11449	629	2971	8773	7635
Selectivity	0.069	0.008	0.039	0.140	0.164

Alpha-olefin selectivity	**Co/SiO2(N)-c4-w**				
Sample time	0:11:30	0:30:00	1:03:54	2:01:31	24:00;00
Area alpha-olefin C8	11606	13938	39415	33188	31417
Selectivity	0.279	1.000	0.226	0.562	0.208

Table A9-8: The data obtained form the GC spectrum for the Co/SiO_2(N)-s-c4 catalyst

Catalyst	**5%Co/SiO2(N)-s-c4**				
Flowrate of CO	3.5	ml/ (STP)min			
Nco	0.000156	mol C/min			
Flowrate of c.hx	0.111	ml (STP)/min			
Nc (c.hx)	2.98E-05	mol C /min			
Nc (c.hx)	2.98E-05	2.98E-05	2.98E-05	2.98E-05	3.14E-05
sample time	0:10:14		1:02:00	2:00:16	24:01:40
Fco/Fc.hx	5.245	5.245	5.245	5.245	4.970
Total area	16220626		14861658	13408071	20619309
int area	13768414		12116069	11194648	18054580
(Afid-Aint)/Aint	0.178		0.227	0.198	0.142
Organic Yield	0.034		0.043	0.038	0.029
%	3.4		4.3	3.8	2.9
GC trace					
sample time	0:10:14		1:02:00	2:00:16	24:01:40
Area C8	191017		162540	96788	170516
AC8/8	23877.1		20317.5	12098.5	21314.5
Area C9	81826		140639	115095	141675
AC9/9	9091.8		15626.6	12788.3	15741.7
Area C10	56049		182112	178349	231977
AC10/10	5604.9		18211.2	17834.9	23197.7
Area C11	14728		116841	93207	80276
AC11/11	1338.9		10621.9	8473.4	7297.8
Area C12			118092	89058	122488
AC12/12	0		9841.0	7421.5	10207.3
Area C13			109048	83051	71003
AC13/13	0		8388.3	6388.5	5461.8
Area C14			112602	77087	60020
AC14/14	0		8043.0	5506.2	4287.1
Area C15			99946	72642	53444
AC15/15	0		6663.1	4842.8	3562.9

Area C16			66604	70645	47649
AC16/16	0		4162.8	4415.3	2978.1
Area C17			33206	60280	52628
AC17/17	0		1953.3	3545.9	3095.8
Area C18			16083	37808	52024
AC18/18	0		893.5	2100.4	2890.2
Area C19				19361	56592
AC19/19	0		0	1019.0	2978.5
Area C20					24015
AC20/20	0		0	0	1200.8

OLEFIN SELECTIVITY	**Co/SiO2(N)-s-c4**			
sample time	0:10:14	1:02:00	2:00:16	24:01:40
Area olefin C8	52867	57338	37188	121190
Selectivity	0.289	0.433	0.4145	0.714
Area olefin C13		2903	2334	1385
Selectivity		0.027	0.028	0.020

Alpha-olefin selectivity	**Co/SiO2(N)-s-c4**			
Sample time	0:10:14	1:02:00	2:00:16	24:01:40
Area alpha-olefin C8	4170	26658	26087	50753
Selectivity	0.079	0.465	0.701	0.419

Table A9-9: The data obtained form the GC spectrum for the Co/SiO_2(N)-c6 catalyst

Catalyst	Co/SiO2(N)-c6				
Flowrate of CO ml (STP)/min	3.5	ml/ (STP)min			
N CO mol C/ min	0.000156	mol C/min			
Flowrate of c.hx ml (STP)/min	0.097	ml/ (STP)min			0.063
N C (c.hx)	2.58E-05	2.58E-05	2.58E-05	2.58E-05	1.68E-05
Flowrate of c.hx	2.589E-05	2.58E-05	2.58E-05	2.58E-05	1.68E-05
sample time	0:13:21	:0:30:00	1:01:06	2:00:00	25:01:22
Fco/Fc.hx	6.0428	6.042	6.042	6.042	9.270
Total area	17023100	9747404	7833299	19476916	14738309
int area	14328114	8257018	6546331	16731789	13111427
(Afid-Aint)/Aint	0.188	0.180	0.197	0.164	0.124
Organic Yield	0.031128549	0.029872	0.032536	0.027153	0.013385
%	3.1	3.0	3.3	2.7	1.3
GC trace					
sample time	0:13:21	:0:30:00	1:01:06	2:00:00	25:01:22
Area C8	171628	72673	57456	120463	69145
AC8/8	21453.5	9084.1	7182.0	15057.9	8643.1
Area C9	128575	67305	70092	109529	67202
AC9/9	14286.1	7478.3	7788.0	12169.9	7466.9
Area C10	81950	78643	116240	124019	105298
AC10/10	8195.0	7864.3	11624.0	12401.9	10529.8
Area C11	39710	75826	62762	94322	54881
AC11/11	3610.0	6893.3	5705.6	8574.7	4989.2
Area C12	31488	61781	53813	91338	39346
AC12/12	2624.0	5148.4	4484.4	7611.5	3278.8
Area C13	33766	38249	48040	79889	64192
AC13/13	2597.4	2942.2	3695.4	6145.3	4937.8
Area C14	36486	23925	55427	81082	87326
AC14/14	2606.1	1708.9	3959.1	5791.6	6237.6
Area C15	32937	12851	34409	75516	33924
AC15/15	2195.8	856.7	2293.9	5034.4	2261.6
Area C16	32261	8744	19935	67123	31366
AC16/16	2016.3	546.5	1245.9	4195.2	1960.4

Area C17	25548	6990	12709	49135	41590
AC17/17	1502.8	411.2	747.6	2890.3	2446.5
Area C18	15098	5477	6719	22121	37168
AC18/18	838. 8	304.3	373.3	1228.9	2064.9
Area C19		3009	3528	12393	61903
AC19/19	0	158.4	185.7	652.3	3258.1
Area C20		1898	2380		18755
AC20/20	0	94.9	119.0	0	937.8

OLEFIN SELECTIVITY	**Co/SiO2(N)-c6**				
sample time	0:13:21	:0:30:00	1:01:06	2:00:00	25:01:22
Area olefin C8	56394	26813	27154	57700	42054
Selectivity	0.415	0.380	0.503	0.514	0.608
Area olefin C13	2071	2431	7875	4546	7619
Selectivity	0.078	0.067	0.178	0.057	0.209

Alpha-olefin selectivity	**Co/SiO2(N)-c6**				
Sample time	0:13:21	:0:30:00	1:01:06	2:00:00	25:01:22
Area alpha-olefin C8	25999	26225	24299	37087	19471
Selectivity	0.461	0.979	0.895	0.643	0.463

Table A9-10: The data obtained form the GC spectrum for the water-treated $Co/SiO_2(N)$-c6 catalyst

Catalyst	**Co/SiO2(N)-c6-w**				
Flowrate of CO	3.5	ml/ (STP)min			
Nco	0.000156	mol C/min			
Flowrate of c.hx	0.111	ml (STP)/min			
N C (c.hx)	2.98E-05	mol C /min			
Flowrate of c.hx	2.98E-05	2.98E-05	2.98E-05	2.98E-05	2.98E-05
sample time	0:11:04	0:30:51	1:01:47	2:01:16	25:05:00
Fco/Fc.hx	5.245	5.245	5.245	5.245	5.245
Total area	13125019	46136319	12918275	11890911	14146459
int area	11668392	24206249	11319378	10294164	12766772
(Afid-Aint)/Aint	0.125	0.906	0.141	0.155	0.108
Organic Yield	0.024	0.173	0.027	0.030	0.021
%	2.4	17.3	2.7	3.0	2.1
GC trace					
sample time	0:11:04	0:30:51	1:01:47	2:01:16	25:05:00
Area C8		230462	96773	45265	104097
AC8/8		28807.8	12096.6	5658.1	13012.1
Area C9		528213	37540	27496	39724
AC9/9		58690.3	4171.1	3055.1	4413.8
Area C10		386353	29188	72992	54443
AC10/10		38635.3	2918.8	7299.2	5444.3
Area C11		596014	38731	33692	44803
AC11/11		54183.1	3521.0	3062.9	4073.0
Area C12		1113037	27723	28929	54510
AC12/12		92753.1	2310.3	2410.8	4542.5
Area C13		1000375	32599	22846	32349
AC13/13		76951.9	2507.6	1757.4	2488.4
Area C14		2164960	31401	17247	20853
AC14/14		154640.0	2242.9	1231.9	1489.5
Area C15		1599511	24859	115770	17868
AC15/15		106634.1	1657.3	7718.0	1191.2

Area C16		1283127	14165	18269	16148
AC16/16		80195.4	885.3	1141.8	1009.3
Area C17				11053	17078
AC17/17		0	0	650.2	1004.6
Area C18					9270
AC18/18		0	0	0	515.0

OLEFIN SELECTIVITY	**Co/SiO2(N)-c6**			
sample time	0:30:51	1:01:47	2:01:16	25:05:00
Area olefin C8	181097	21842	9342	17384
Selectivity	0.817	0.474	0.228	0.178
Area olefin C13	218597	1940	1174	977
Selectivity	0.283	0.060	0.056	0.058

Alpha-olefin selectivity	**Co/SiO2(N)-c6**			
Sample time	0:30:51	1:01:47	2:01:16	25:05:00
Area alpha-olefin C8	17467	21842	8625	13921
Selectivity	0.096	1.000	0.923	0.801

Appendix X – Sample Calculation of Turnover Rate

The turnover rate is the Fischer-Tropsch reaction rate per surface Co atom. At chain growth favoring conditions, FTS turnover rates are not influenced by dispersion and support effects [Iglesia, 1997].

The turnover rate can be calculated as follow:

$$Turnover\ rate = \frac{number\ of\ CO\ converted}{Active\ sites}$$

with

$$number\ of\ CO\ converted = F_{inlet,CO} \times X \times t$$

where $F_{inlet, CO}$ is the inlet flowrate of CO, X is conversion and t is time in seconds. The inletflow of CO was 3.5ml (STP)/min for all the catalyst. After 24 hours, the % HC yield of the $Co/SiO_2(N)$ catalyst was 7.4%.

$$number\ of\ Co\ converted = \frac{3.5 \times 7.4\%}{60} = 0.0043\ ml$$

0.4177ml/g_{cat} H_2 was chemisorbed on the $Co/SiO_2(N)$ catalyst. The stochiometry of disociative hydrogen chemisorption on cobalt is 2:1. The number of active sites is thus:

$$active\ sites = 2 \times V_{H\,2,chemisorbed}$$

therefore,

$$active\ sites = 2 * 0.4177 = 0.8354\ ml$$

The turnover rate for $Co/SiO_2(N)$ after 24 hours is then:

$$Turnover\ rate = \frac{0.004317}{0.8354} = 0.00516$$